Design and Characterization of a Miniaturized Fluorescence Analysis System for Measurement of Cell-Free DNA

Design and Characterization of a Miniaturized Fluorescence Analysis System for Measurement of Cell-Free DNA

By

PARKER BONDI, B. ENG.

B. ENG (University of Guelph)

A Thesis

School of Graduate Studies

In Fulfilment of the Requirements

For the Degree

Master of Applied Science

McMaster University

MASTERS OF APPLIED SCIENCE (2018) McMaster University

(Biomedical Engineering) Hamilton, Ontario, Canada

TITLE DESIGN AND CHARACTERIZATION OF A MINIATURIZED FLUORESCENCE ANALYSIS SYSTEM FOR MEASUREMENT OF CELL-FREE DNA

AUTHOR PARKER BONDI, B.Eng.

SUPERVISOR Professor P. R. Selvaganapathy
Department of Mechanical Engineering

NUMBER OF PAGES XV, 109

Abstract

Sepsis is a dysregulated systemic response to infection and is one of the leading causes of in-hospital mortality in Canada. Accurate distinction between survivors and non-survivors of sepsis has recently been demonstrated through quantification of cell-free DNA (cfDNA) concentration in blood. In an analysis of 80 septic patients, non-survivors of sepsis had significantly higher cfDNA concentration levels than that of survivors or healthy patients. Real time separation of cfDNA from contaminants in blood has also been done using a cross channel microfluidic device. Current methods for DNA quantification utilize time consuming and complicated laboratory equipment and therefore are not suitable for bedside real-time testing. Thus a handheld cfDNA fluorescence device coined the *Sepsis Check* was designed that can perform DNA characterization in a reservoir device and DNA detection in a microfluidic cross channel device. The goal is to use this system along with the cross channel devices to set apart survivors or healthy donors from non-survivors in patients with sepsis.

The design consists of a $470nm$ light emitting diode (LED) with $170mW$ of optical power (LED470L – *ThorLabs*), an aspherical uncoated lens with a focal length of $15mm$ (LA1540-ML – *ThorLabs*), a $488nm$ bandpass filter with a $3nm$ full width at half maximum (FWHM) (FL05488-3 – *ThorLabs*), an aspherical uncoated lens with a focal length of $25mm$ (LA1560-ML – *ThorLabs*), an aspherical uncoated lens with a focal length of $35mm$ (LA1027-ML – *ThorLabs*), a $525nm$ longpass filter with an optical density > 4.0 (F84744 – *Edmund Optics*), and a Raspberry Pi Camera V2 (*Raspberry Pi Foundation*). The Sepsis Check is made to excite the dsDNA specific PicoGreen fluorophore which has a peak absorbance at $502nm$ and a peak emission at $523nm$. In summary, the Sepsis Check in this thesis is capable of calibrating dsDNA concentration from $1\mu g/mL$ to $10\mu g/mL$ and detect DNA accumulation of $5\mu g/mL$ and $10\mu g/mL$ in the cross channel device. This tool can be a valuable addition to the ICU to rapidly assess the severity of sepsis for informed decision making.

Acknowledgements

First, I would like to acknowledge my supervisor Professor Ponnambalam Ravi Selvaganapathy for his trust and support through this thesis and the past two years. He encouraged me to pursue a large multi-year project with real intentions to bring the final product to the Hamilton General Hospital for clinical trials. He allowed me to explore the field and invest time into my own ideas and supported me with his expertise and guidance.

I want to thank Dr. Alison Fox-Robichaud and the team at TaARI for supporting my research and allowing me to utilize plasma, blood, and isolated DNA samples from non-septic and septic patients from the clinical sepsis study to boost the significance of my work. My appreciation also goes to Dr. Fang and his team. They assisted me with the analysis of the optical elements.

I thank my fellow lab-mates in the Center for Advanced Micro-Electro-Fluidics: Aditya Aryasomayajula, Reza Ghaemi, Jun Yang, Ali Shahid, Rana Attalla, Aliakbar Mohammadzadeh, Mohammadhossein Dabaghi, Alireza Shahin-Shamsabadi, Sreekant Damodara, Celine Ling, Devon Jones, and Nidhi Jain. They are all very nice friends who gave me great advice and help with this research and my graduate education in general.

I want to thank Steve Rulo and Lulu Faidi for helping me with the lengthy experimental procedures that were required for the calibration experiments. Without them my quality of work would have been reduced as we double checked each other's work and improved the consistency of the experimental procedure.

I want to specifically thank my friend Sreekant Damodara and Aditya Aryasomayajula. They helped me throughout my thesis with manufacturing of the microfluidic devices, troubleshooting my results, development of the electrical amplification circuit, analysis of my optics, and the statistical analysis of my results.

Last but not least, I have to thank my girlfriend Sabrina Oddi who has spent countless hours helping me organize and plan my work, sifting through new ideas, and providing constructive criticism and questions to better my design. She has supported me and acted as my foundation through many tough and difficult times. Her accompaniment has made my life in these 2 years memorable and beautiful. My sincere gratitude also goes to my parents who supported my decision to pursue my masters when I finished my undergraduate studies.

Table of Contents

List of Figures

List of Tables

List of Abbreviations

SIRS	Systemic Inflammatory Response Syndrome
ICU	Intensive Care Unit
cfDNA	Cell-Free DNA
MODS	Multiple Organ Dysfunction Score
APACHE	Acute Physiology And Chronic Health Evaluation
dsDNA	Double Stranded DNA
PoC	Point of Care
TE buffer	Tris-EDTA buffer
LED	Light Emitting Diode
PDMS	Polydimethylsiloxane $CH_3[Si(CH_3)O]_nSi(CH_3)_3$
MEMS	Micro-Electro-Mechanical Systems
UV	Ultraviolet
TAE buffer	Tris Base, Acetic Acid, and EDTA
ABS	Acrylonitrile Butadiene Styrene Plastic
FWHM	Full Width at Half Maximum
DC	Direct Current
OD	Optical Density
I/O	Input / Output
LCD	Liquid Crystal Display
MP	Megapixel
PG	PicoGreen
LoD	Limit of Detection
μTAS	Micro Total Analysis Systems

Nomenclature

$\lambda - DNA$	Lambda DNA Standard
$R(\lambda)$	Resistivity
λ	Wavelength
I_{PD}	Generated Photocurrent
P	Optical Intensity
C_{PG}	Concentration of PicoGreen
A	Amount of light absorbed at a particular wavelength
ε	Molar Extinction Coefficient
l	Distance that light travels through the sample
c	Concentration of the solution
ϕ	Quantum Yield

Chapter 1.

1 Motivation and Organization

1.1 Motivation

Sepsis is when there is a dysregulated host response to infection that results in life-threatening organ dysfunction [1]. Sepsis is one of the leading causes of in-hospital mortality in Canada. According to an observational study of 12 Canadian community and teaching hospital critical care units, the crude mortality for all patients with sepsis was 30.5% in 2008-2009 [2]. More specifically, the mortality rate for patients with severe sepsis was 45.2% and patients whose sepsis did not progress to severe had a mortality rate of 20.9% [2]. With such a high mortality rate, the discriminative power of testing procedures must be improved to better avoid mortality as a result of sepsis.

In addition to the high mortality rate, the median length of an ICU stay for patients with sepsis was 6.3 days – about four days longer than the median ICU stay of patients admitted for other reasons [2]. Moreover, the median stay of patients with severe sepsis was an additional six days longer than patients whose sepsis did not progress to severe [2]. As a result of lengthy ICU stays, sepsis patients are amongst the most ICU resource exhaustive patients.

The advancement to severe sepsis can quickly lead to organ failure and is particularly potent in mortality, length of time in the ICU, and resource exhaustive in the ICU. As such, there is a need for a predictive tool system to quantify sepsis severity prior to acute organ dysfunction. Scoring systems and biomarker technology have been studied and developed for decades as potential systems to fill this void. In general, current scoring systems focus mainly on physiological variables and do not have sufficient discriminative power [3]. Biomarkers such as C-reactive protein, procalcitonin, serum amyloid A, mannan and IFN-γ-inducible protein 10 are being investigated, however none of them have been accepted as highly reliable clinical outcome predictors of severe sepsis [4] and thus lack the ability to provide discriminative capabilities.

Recently, cell-free DNA (cfDNA) in plasma was found to have higher prognostic utility than the Multiple Organ Dysfunction Score (MODS), the Acute Physiology And Chronic Health Evaluation II (APACHE II) score, or other biomarkers measured [5]. In an analysis of 80 severely septic patients, the mean cfDNA levels in survivors ($1.16 \pm 0.13 \mu g/mL; n = 46$) was similar to healthy volunteers ($0.93 \pm 0.76 \mu g/mL;\ n = 14$)

($P = 0.426$), while that of non-survivors ($4.65 \pm 0.48 \mu g/mL; n = 34$) was notably higher ($P < 0.001$) [5].

Current methods for quantification of cfDNA are time consuming and require multiple preparation steps. For instance, the Nanodrop 2000 is capable of linear quantification of dsDNA, however this system is laboratory based, requires sample processing, and requires expertise to use. A point of care (PoC) system that is capable of processing whole blood, provide rapid results by the bedside, and does not require laboratory expertise could greatly enhance the clinical value of the tool.

As part of an effort to develop a PoC system for such quantification, a technique was developed to rapidly quantify cfDNA in plasma on a microfluidic chip [6]. This device allows for rapid separation of cfDNA from contaminants in the plasma while maintaining the ability to discriminate between survivors and non-survivors. Although it is a powerful proof of concept and demonstrates rapid quantification using a small volume of blood, it still uses a laboratory fluorescence microscope to quantify the cfDNA concentration [6]. Therefore a PoC system that can accommodate this microfluidic chip to quantify cfDNA by the bedside would be optimal.

1.2 Organization of the Chapters

Chapter 2 provides a comprehensive background review on the thesis. Sepsis is defined, the mortality rate associated with it is reported, and its impact on the ICU is discussed. Current scoring systems used and the gold standard for sepsis assessment is briefly described. The importance of biomarkers is discussed and the limitations are presented. cfDNA is introduced and the significance of quantification in plasma is emphasized for sepsis prognosis before organ failure. Current commonly used DNA quantification approaches are summarized as laboratory equipment, μTAS's, and miniaturized fluorescence systems. The cross channel microfluidic device is discussed. As such, Chapter 2 provides a strong reference for developing the prototypes in this thesis.

Chapter 3 presents the materials used in the device and the prototyping design process. Materials include consumable reagents, electrical systems that were used, purchased optical components, and supporting equipment in the lab. The design process is initiated with the introduction of the performance criteria. The design process justifies the materials used and the various prototypes that were designed.

Chapter 4 presents results that support the prototype development. A proof of concept result shows that the prototype is capable of linear characterization of DNA concentration in TE buffer and healthy patient blood plasma. A second proof of concept result is presented when the prototype demonstrates the ability

to detect DNA accumulation on the cross channel devices. Both of these were necessary results for the progress of the project.

Chapter 5 highlights the conclusion of the results and the contribution towards the device. Future work is alluded to and introduced at the end.

Chapter 2.

2 Introduction

2.1 Sepsis

Sepsis is when there is a dysregulated host response to infection that results in life-threatening organ dysfunction [1]. The signs and symptoms of sepsis vary drastically because it is involved in many complex pathophysiological processes. The infection can originate from bacterial, fungal, or parasitic infections [7]. Even factors such as the method of entry or the time at which the patient is evaluated can drastically change the condition of the patient [7]. Even if the signs and symptoms of sepsis are correctly defined, the severity of the symptoms are not always correlative to the state of sepsis [7]. This complexity results in a high mortality among patients with sepsis. For these reasons prognostication of sepsis has been focused on for many years beginning with physiological scoring systems and biomarker quantification.

2.2 Sepsis and Mortality Rate among Patients

The hospitalization and mortality rate of sepsis patients is remarkably high in Canada. According to the Surviving Sepsis Campaign in 2008, the mortality rate associated with sepsis was 30-50% [2]. Patients who were diagnosed as severely septic had a mortality rate slightly above 38% based on a prospective observational study of 12 Canadian community and teaching hospital critical care units [2].

Another aspect of sepsis is the large resource consumption and high costs of social resources in the intensive care unit [2]. Due to the reasons mentioned above, mortality prediction of sepsis patients and evaluation of their severity is of great importance. It can assist with clinical decision making and better allocation of the hospital's resources. With a precise assessment of the risk for mortality, a more comprehensive and timely treatment could be implemented for a patient. Therefore, intense efforts to decrease the risk of mortality for septic patients has a big impact on the survivability of the condition as well as the hospital's resources.

2.3 Current Methods to Evaluate Organ Dysfunction: Scoring Systems

For years, the standard protocol for evaluating sepsis severity has been utilizing clinical scoring systems. These scoring systems have been widely accepted and, if observed by an expert, can provide insightful knowledge on the state of the patient. The rationale for using scoring systems is to provide an immediate evaluation and description of the septic case and organ dysfunction. Ensuring consistency between healthcare providers is of utmost importance for the continued success of this method and is dependent

on the education of the practitioner [8]. ICU scoring systems can be grouped into two categories: general risk prognostication scores (severity of illness scores) and organ dysfunction (failure) scores [3]. These systems have a number of limitations and should not be used for clinical or prognostication purposes without in-depth knowledge of the science of severity scoring [3].

2.3.1 General Risk Prognostication Scoring Systems

General scoring systems take the assumption that the severity of an acute disease is in some way correlative with the degree of abnormality of one or many general physiologic variables [3]. General scoring systems are quick to access and much of the information for these systems, such as blood pressure or swelling have been noted throughout the standard triage procedure. The APACHE II scoring system is one of the earliest implemented general scoring systems and remains as one of the most accepted and validated strategies for the evaluation of sepsis [3]. The performance of general scoring systems with sepsis is poor due to the variability in the symptoms from patients with distinct individual conditions and as a result have weak discriminative power and predictive ability [3].

2.3.2 Organ Dysfunction Scoring Systems

Organ dysfunction scoring systems quantify abnormalities according to clinical findings, laboratory data, or therapeutic interventions [1]. The predominant scoring system currently in use is the Sequential Organ Failure Assessment (SOFA) (originally the *Sepsis-Related Organ Failure Assessment*) which uses routinely collected data such as respiration pressure, platelet count, bilirubin concentration, the Glasgow Coma Scale score, and creatinine to asses for organ dysfunction [1]. A grade between 0 & 4 is provided for each variable and summated for a score for each organ [1], [3]. An example SOFA table used to assess organ dysfunction is shown below in Figure 2.1.

	Score				
System	0	1	2	3	4
Respiration					
Pao_2/Fio_2, mm Hg (kPa)	≥400 (53.3)	<400 (53.3)	<300 (40)	<200 (26.7) with respiratory support	<100 (13.3) with respiratory support
Coagulation					
Platelets, $\times 10^3/\mu L$	≥150	<150	<100	<50	<20
Liver					
Bilirubin, mg/dL (μmol/L)	<1.2 (20)	1.2-1.9 (20-32)	2.0-5.9 (33-101)	6.0-11.9 (102-204)	>12.0 (204)
Cardiovascular	MAP ≥70 mm Hg	MAP <70 mm Hg	Dopamine <5 or dobutamine (any dose)[b]	Dopamine 5.1-15 or epinephrine ≤0.1 or norepinephrine ≤0.1[b]	Dopamine >15 or epinephrine >0.1 or norepinephrine >0.1[b]
Central nervous system					
Glasgow Coma Scale score[c]	15	13-14	10-12	6-9	<6
Renal					
Creatinine, mg/dL (μmol/L)	<1.2 (110)	1.2-1.9 (110-170)	2.0-3.4 (171-299)	3.5-4.9 (300-440)	>5.0 (440)
Urine output, mL/d				<500	<200

Abbreviations: Fio_2, fraction of inspired oxygen; MAP, mean arterial pressure; Pao_2, partial pressure of oxygen.

[a] Adapted from Vincent et al.[27]

[b] Catecholamine doses are given as μg/kg/min for at least 1 hour.

[c] Glasgow Coma Scale scores range from 3-15; higher score indicates better neurological function.

Figure 2.1: Example of a SOFA scoring table used to asses organ dysfunction and quantify risk of mortality [1].

A few high risk factors (Respiration <200) or many low risk factors (Platelets <150) may result in a cumulative SOFA score of 2 points or more which is associated with an in-hospital mortality greater than 10% [1]. One benefit to these scoring systems is that scores to quantify single-organ failure or a specific disease are often caught before the patient enters the ICU [3]. This knowledge is valuable if the case becomes more life-threatening. Unfortunately, in many septic cases organ failure and the presentation of high risk factors are typically one of the final stages of sepsis. Therefore, these scoring systems are often too late for severely septic patients.

The Multiple Organ Dysfunction Score (MODS) looks at multiple organs of the patient independently [3]. These systems can provide better specificity to sepsis where a score is assigned based on the severity of multiple organ failure. In these systems, each crucial organ gets scored independently, and multi-scores from different organs are considered comprehensively. These systems by their very definition analyze one aspect of a patient's condition which is organ dysfunction. Therefore extrapolation to a comprehensive evaluation of the patient's condition is difficult [3]. Organ dysfunction scoring systems often miss major physiological aspects that could be significant to the discrimination between a survivor and non-survivor.

In general, severity scoring systems have filled a necessary void in both quality control and management of the ICU. Existing severity scores have been shown to give valuable information when used on ICU groups [3]. The use of severity scoring systems requires standardization and education across the field.

Although these have been developed and are well documented, several pitfalls such as interpretation of the results, non-specificity to sepsis, a lack of a comprehensive evaluation of the patient's condition, and late detection of the symptoms all lead to the need for a more accurate and time sensitive sepsis prognostic tool.

2.4 Biomarkers for Severe Sepsis Prognostication

As discussed above, a more accurate sepsis quantification method is needed. Hence, alternative approaches are required to provide detailed and accurate evaluation of sepsis severity in patients. A wide variety of biomarkers have been considered as a replacement or addition.

2.4.1 Sepsis Biomarker

A biomarker is generally defined as an objectively measured indicator of certain biological processes, pathogenic processes, or pharmacologic response to a therapeutic intervention [4]. Compared to the scoring systems, biomarkers have some obvious benefits: 1) they have an indicative and unbiased ability to tell the absence or presence of a potentially correlative species in a sample; 2) certain biomarkers can lead to the source of infection (bacterial, viral, or fungal infection, etc.) of sepsis which helps in formulating treatment [4]; 3) biomarker monitoring can be an easy and continuous process, thus providing an option to evaluate the real time response of a patient to therapy [9].

2.4.2 Current State of Sepsis Biomarkers Development

According to review work in 2010, a total of 178 biomarkers have been associated with the sepsis process [9]. For comparison just 8 biomarkers have been associated with Alzheimer's disease [9]. The reliability of these biomarkers in clinical application for sepsis prognostication has not been established [9]. Despite this, numerous microfluidic devices have been developed to analyze sepsis related biomarkers.

One microfluidic device performed sequence-specific capture of target DNA related to the *Klebsiella pneumoniae* carbapenemase (KPC) gene by utilizing monolithic columns modified with oligonucleotides [10]. While this could be useful for septic cases that resulted from the expression of the KPC gene, it is one of many causes of sepsis and thus falls short when trying to quantify sepsis under other conditions. As will be discussed shortly, sepsis is related to NETosis which is the release of neutrophil extracellular traps [11]. A related response of neutrophils specifically to bacterial infection is the increased expression of CD64 [12]. Therefore a microfluidic device was designed to capture neutrophils that had increased CD64 expression by utilizing a herringbone cell capture channel coated with anti-CD64 antibodies [12]. However, sepsis is not solely cause from bacterial infections and thus sepsis from viral causes [9], [12]. A

third microfluidic device quantified the Soluble Triggering Receptor Expressed on Myeloid Cells 1 (sTREM-1 cells) as an attempt to quantify sepsis [13]. sTREM-1 is an innate inflammatory transmembrane receptor that is enhanced in many ICU cases including sepsis and therefore would not suffice as a complete sepsis quantification biomarker [9]. In fact, the research on seeking a highly discriminative biomarker is extremely challenging for sepsis mainly due to two factors:

1. The pathophysiology of sepsis is a complex process involving multiple mechanisms. A large number of mediators, such as cytokines, cell-surface markers, acute phase proteins, coagulation factors and apoptosis mediators, participate in the septic process, all of which can be studied as potential biomarkers [9]. However, most of the mediators do not participate in the whole septic process; thus they can hardly reflect an overview of the pathological development in septic patients. Instead, most of the biomarkers are relevant for only one aspect of sepsis. For example, some biomarkers were shown to be effective in distinguishing septic patients with non-septic patients, some were identified to be useful in early diagnosis of sepsis; and most of the biomarkers were analyzed to distinguish patients who were likely to survive (survivors) with those who have high probability to die (non-survivors) [9].
2. It is extremely difficult to build up an experimental model for sepsis biomarker studies, thus current ways to find a reliable biomarker is through clinical practice or animal trials, which have high cost and long duration [9]. As mentioned above, the pathological process of sepsis is complicated and the factors may vary among patients, hence biomarkers research based on an accurate sepsis model is extremely difficult. Most of the results from current studies are validated by comparing with the methods used in everyday clinical practice [9].

In summary, numerous biomarkers have been investigated as diagnostic indicators of sepsis and its various processes. However, none of them have demonstrated suitable accuracy or sensitivity to be used as a prognostic tool in clinical practice. It has been proposed that a combination of several biomarkers could be used for sepsis prognostication, however there is insufficient data and a lack of consensus to validate this approach [9]. Based on review and analysis, it is unlikely to get a single ideal predictor that can be used for sepsis diagnosis due to the complex pathophysiology of sepsis and the consistency of the experimental model in sepsis biomarker studies. Biomarkers as a whole could be useful in improving sepsis prognostication because they provide discriminative and unbiased severity assessment which is the major disadvantage of scoring systems.

These biomarkers and devices have focused on sepsis detection, diagnosis, or quantification. An increase in circulating cfDNA in blood as a result from activated neutrophils extruding neutrophil extracellular traps (NETs), cell necrosis, and cell apoptosis has recently been investigated as a potential biomarker for cancer, trauma, stroke, and sepsis prognostication [5], [11], [14]. Prognostication is different from diagnosis as it pertains to the probability of developing a given outcome. Until now the relationship between cfDNA concentration and sepsis severity has not been defined.

2.4.3 Circulating Cell-Free DNA (cfDNA)

Circulating cfDNA broadly refers to extracellular DNA present in blood. It was first discovered in 1948 [15], and since 2000, has been increasingly investigated for application in disease diagnosis and prognosis [16]. An increased level of cfDNA reflects some pathological processes that may or may not include tumor development, the beginning of the inflammatory response, trauma, sepsis, or other [15], [5]. However, higher levels of cfDNA can also be detected in certain non-related pathological results such as intense exercise [11]. Thus, cfDNA always exists in the blood of healthy individuals at a relatively low level around $1\mu g/mL$. These characteristics combine to suggest that cfDNA has the potential to be a valuable biomarker of sepsis.

The sources of cfDNA in blood and the mechanism by which its concentration increases are numerous and vary by degree. The most recent study suggest that the majority of cfDNA concentration is a result of activated neutrophils extruding neutrophil extracellular traps (NETs) [14]. The NETs are comprised of cfDNA that traps pathogens and provides a stimulus for clot formation in a process coined NETosis [14] as shown in Figure 2.2.

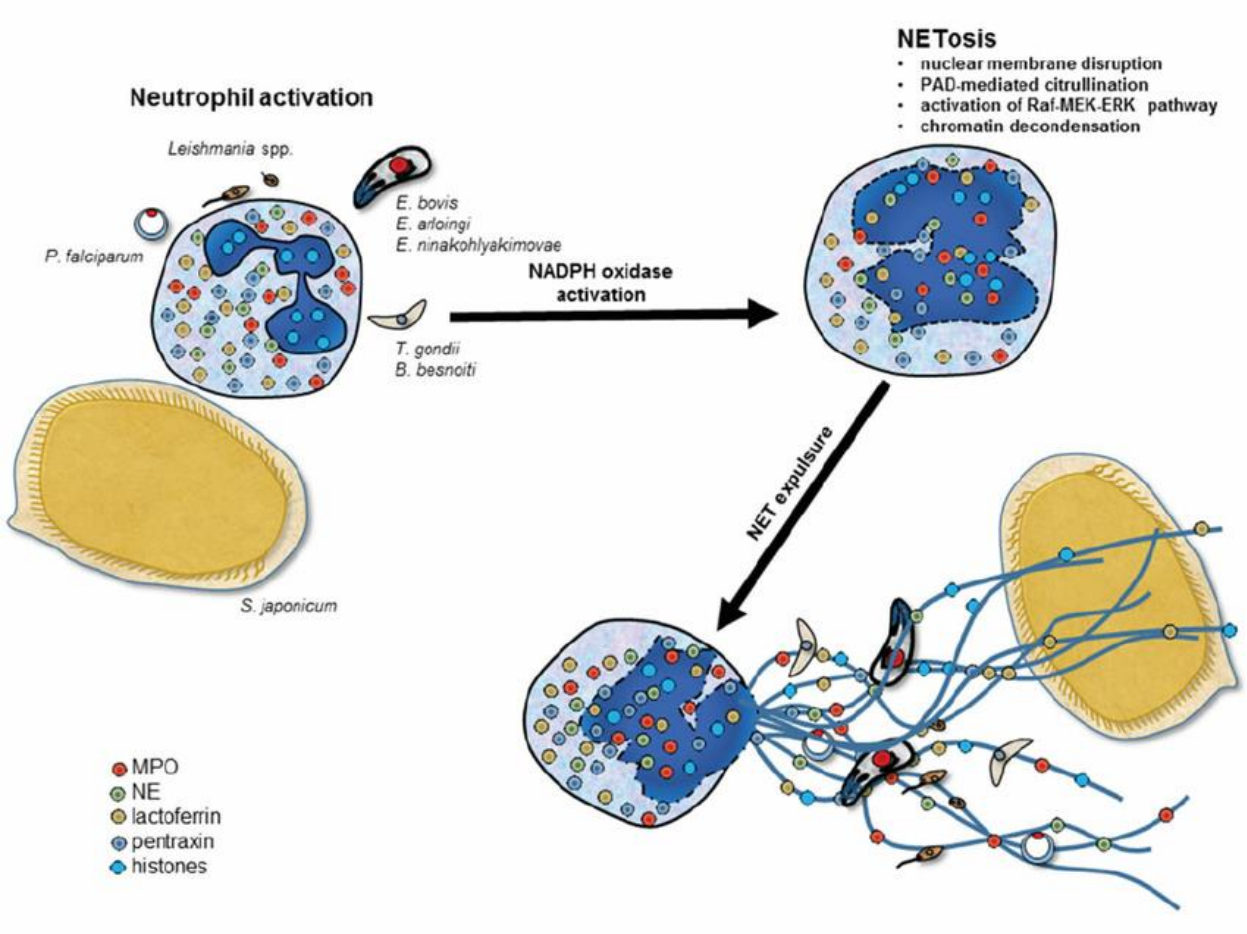

Figure 2.2: The mechanism of NETosis [11], [14] *and the release of cfDNA into the bloodstream as a response to pathogenic infection.*

cfDNA is usually efficiently mobilized out of the circulatory system by the liver and kidney [17]. Thus cfDNA spikes are short lived (lasting several hours at most) [17]. However, when cfDNA cannot be efficiently mobilized out of the blood by the kidney, it can become a highly thrombogenic material in the blood causing blood clot formation inside the circulatory system [14]. This blocks nutrient and oxygen delivery to vital organs and thus can quickly lead to organ failure [14]. In a healthy patient, the primary source of cfDNA is cell death (apoptosis), cellular necrosis, or secretion [17], [15] as shown in Figure 2.3.

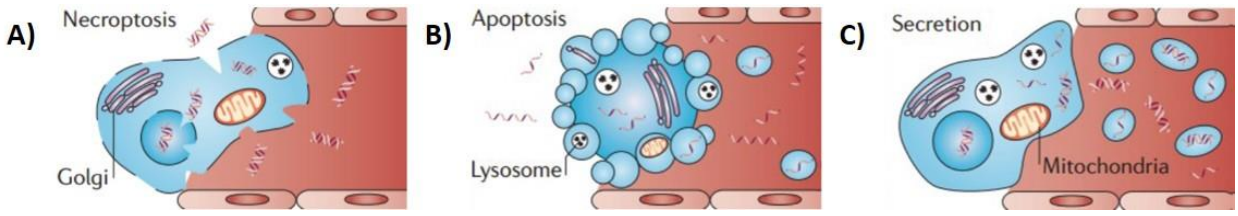

Figure 2.3: The mechanism of DNA release [15]. *A) Production of cfDNA by Necroptosis. B) Production of cfDNA by Apoptosis. C) Production of cfDNA by Secretion*

In all of the above processes, the DNA remains undamaged and thus cfDNA is primarily double stranded DNA (dsDNA) [16]. A recent study has made a major breakthrough by quantifying the correlation between the concentration of dsDNA in whole blood and sepsis prognostication.

2.4.4 Cell-Free DNA for Severe Sepsis Prognostication

Regardless of the method by which cfDNA concentration is increased, it recently has been found to be a reliable indicator for predicting mortality in ICU patients. In combination with current scoring systems (e.g. MODS) and some other sepsis biomarkers (e.g. Protein C), cfDNA levels can potentially have stronger predictive powers than any other conventional method [5], [17]. The study concludes that cfDNA concentration in blood is much higher in patients who died in the ICU (non-survivors) compared with those who survived (survivors) based on the data collected from 80 severely septic patients. The mean cfDNA level in survivors ($1.16 \pm 0.13 \mu g/mL$) was similar to that of healthy volunteers ($0.93 \pm 0.76 \mu g/mL$) ($P = 0.426$), while that of non-survivors ($4.65 \pm 0.48 \mu g/mL$) was notably higher ($P < 0.01$) [5] in Figure 2.4.

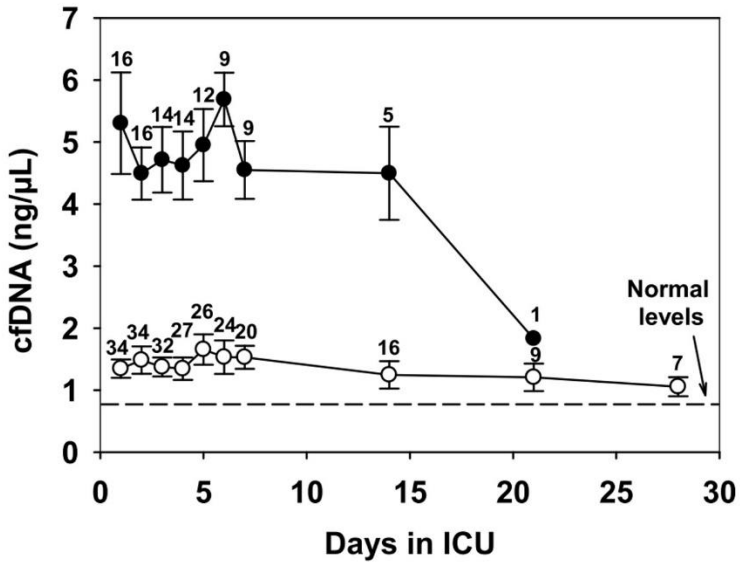

Figure 2.4: Temporal changes in levels of cfDNA in 50 patients with sepsis [5]. *Survivors are shown by white circles (○), and non-survivors are shown by black circles (●). The number of patients at each time point is indicated above each circle. The mean levels of cfDNA in healthy volunteers ($n = 14$) is shown as a dashed line indicated with an arrow. Error bars represent standard error of mean (SEM).*

The cfDNA concentrations in blood of a number of non-survivors were found to be much higher than $5 \mu g/mL$ [5]. The dsDNA concentration difference between survivors and non-survivors (approximately $1 \mu g/mL$ versus $5 \mu g/mL$) in ICU could be used to select out patients with much higher risk of death (non-survivors).

Therefore, rapid quantification of cfDNA in severe septic patients in ICU could be of great help in mortality prediction and disease prognosis.

2.4.5 Current Methods for dsDNA Quantification

The two overarching methods for dsDNA quantification are techniques using ultraviolet absorbance and fluorescence measurements with PicoGreen. Both methods have their advantages and disadvantages and will be discussed with the final goal of cfDNA quantification in whole blood as the focus.

DsDNA and nucleic acids absorb UV light. Molecules can absorb and emit light according to the Jablonski Energy Diagram shown in Figure 2.5.

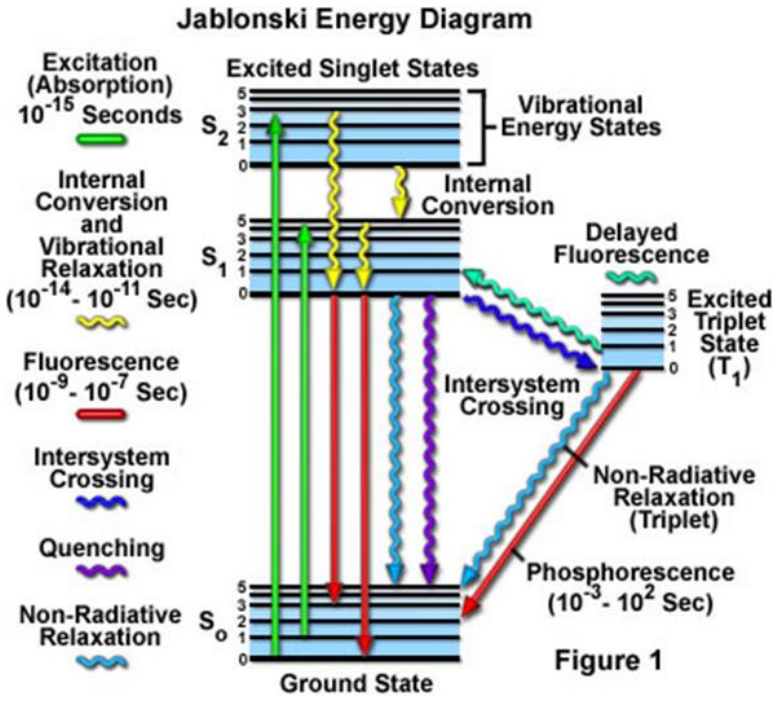

Figure 2.5: Jablonski Energy Diagram showing the difference between Absorbance, Fluorescence, and Phosphorescence. Diagram courtesy of [18].

The energy in a photon is inversely related with the wavelength of that photon [18]. A higher energy photon will have a shorter wavelength and vice versa. A molecule will absorb a photon if the energy of that photon is equal to or slightly greater than the amount of energy it takes to excite an electron from its ground state to an excited state [18]. Molecules hold electrons at their ground states with different bond strengths and thus, different molecules absorb different wavelengths of light. In Figure 2.5 absorbance of UV light by an electron in a dsDNA molecule moves the electron from the ground state to the excited state (following the green lines). This happens at a consistent rate for each molecule according to the molar absorptivity constant (ε). This constant is a fundamental molecular property that, at a

particular temperature, pressure, and wavelength, describes the amount of light that is absorbed by a specific species. The amount of UV light absorbed by the sample can be correlated to the concentration of DNA and the path length by following the Beer-Lambert Law [19] in Equation 2.1.

$$A = log_{10}\left(\frac{I_0}{I}\right) = \varepsilon c l \tag{2.1}$$

Where A is the measured absorbance (in Absorbance Units (AU)), I_0 is the intensity of the incident light at a given wavelength, I is the transmitted intensity, l is the path length through the sample, and c is the concentration of the absorbing species. In the case of DNA absorbing UV light, the electron jumps to the excited state and returns to the ground state via internal conversion and vibrational relaxation (shown as the wavy lines going from the excited state to the ground state in Figure 2.5).

2.4.5.1 UV Absorbance

UV absorbance was one of the methods used to determine the concentration of dsDNA in the cfDNA study discussed earlier. It was found that a cfDNA concentration of $5\mu g/mL$ in whole blood indicates a patient is not likely to survive their septic condition. With the current technology such as the Nanodrop 2000 spectrophotometer quantification of dsDNA down to $2\mu g/mL$ can be done with confidence in volumes as small as $0.5\mu L$ in under 5 minutes [20]. However, dsDNA, RNA, ssDNA, and other nucleic acids all absorb UV photons at $260nm$ [19]. Therefore, the UV absorbance measurement can be contaminated and result in an overestimation of the dsDNA concentration [19]. DsDNA concentration measurements with UV absorbance at $260nm$ should not be relied upon unless the quality and condition of the sample is extremely well controlled [21]. Solution homogeneity, delay time, sample volume, and cross contamination all need to be carefully controlled to ensure accurate quantification [20]. Isolation of dsDNA with laboratory procedures that include centrifugation, separation on silica columns, and other time consuming steps are employed to ensure the quality of the sample for accurate quantification. Additionally, DNA purity by UV spectroscopy can be analyzed by the ratio of the absorbance at $260nm$ and $280nm$ (A_{260}/A_{280}). Good quality dsDNA with minimal contaminants will have a ratio of 1.7-2.0 [19]. Therefore, despite exceptional dsDNA quantification with micro-liter volumes, UV absorbance suffers from contamination issues that require multi-step and time consuming laboratory procedures to mitigate. As a result UV absorbance is not a suitable detection method for this purpose.

2.4.5.2 Fluorescence

Luminescence is the emission of light from any substance and occurs from electronically excited states [18]. It is the defining feature between a fluorescent molecule (a fluorophore), and a non-fluorescent

molecule. A fluorescent molecule will absorb a photon shown as the green arrows in the Jablonski diagram in Figure 2.5 but instead of releasing the energy by vibrational relaxation (wavy arrows), a fluorescent molecule will release the energy via luminescence (red arrows). DsDNA and lipids are essentially devoid of the ability to fluorescence on their own and thus are not considered fluorophores [18]. In the case of dsDNA instead of fluorescing, the excited electrons of DNA return to the ground state via vibrational relaxation [18]. Contrary two this, PicoGreen (a dsDNA specific fluorophore) is a molecule that is capable of absorbing a photon of light and re-emitting a photon with great efficiency only when it is bound with dsDNA. When bound to dsDNA PicoGreen will absorb and emit light according to the spectra shown in Figure 2.6.

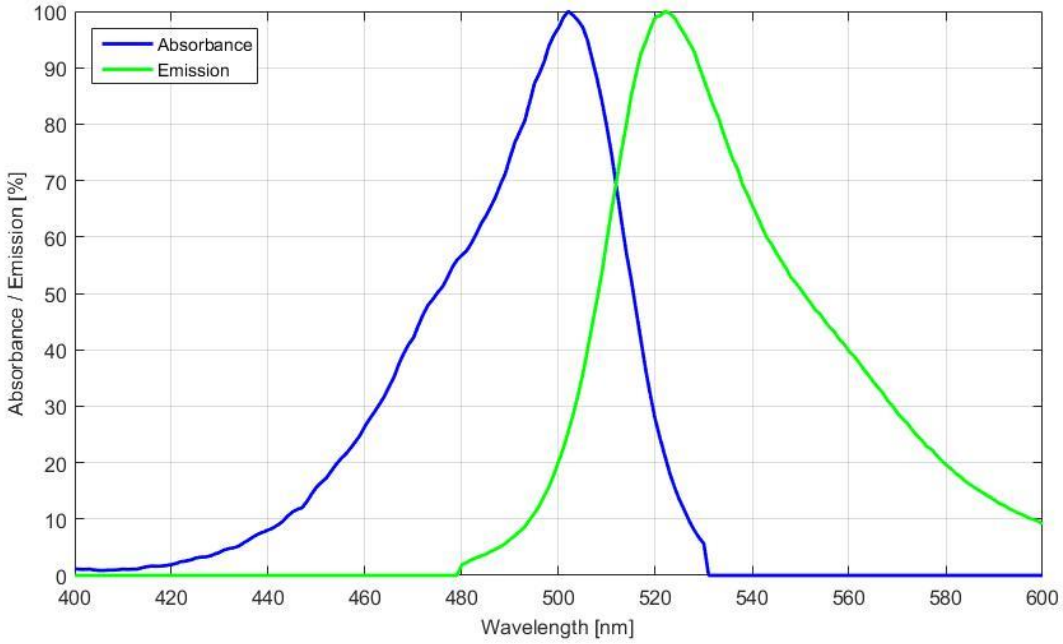

Figure 2.6: Absorption and emission profiles of PicoGreen showing a very small stokes shift from the peak of the absorbance profile at $502nm$ to the peak of the emission profile at $523nm$.

Because of the method by which PicoGreen only becomes fluorescently active when it is bound to dsDNA, proteins and other nucleic acids including ssDNA do not interfere with the resultant measurements thus making PicoGreen a highly specific fluorophore to dsDNA [22].

The most reliable and readily available device in the lab that is based on fluorescence is the Qubit Flurometer. The Qubit Fluorometer can provide linear quantification of dsDNA down to $0.2\mu g/mL$ with the high sensitivity kit [23]. In order to detect these small concentrations of dsDNA the device utilizes $200\mu L$ assay tubes which is much larger than a droplet of blood that would be available in a PoC setting.

Therefore, the limitations of the Qubit deem it unsuitable for a one-step dsDNA quantification device in whole blood at the PoC. DNA detection in smaller volumes and a single step have been presented in a category of microfluidic devices called Micro-Total Analysis Systems (μTAS's). However, these systems still have limitations that will be discussed below.

2.4.5.3 Micro Total Analysis Fluorescent Systems for DNA Detection and Quantification

The laboratory based DNA quantification equipment described above provide linear and quantified DNA concentration detection down to very low concentrations. For most applications, this is sufficient as these systems are multi-functional and can provide accurate measurements. However, quantification of dsDNA in whole blood introduces additional complications such as sample preparation, centrifugation, and isolation steps that make the total procedure to quantify dsDNA ineffective. Furthermore, quantification of dsDNA in whole blood was not needed until now as DNA is typically cleared from blood quickly. However, with the correlation between sepsis prognostication and the concentration of dsDNA, accurate and rapid quantification in whole blood becomes of utmost importance.

The field of μTAS's has been expanding since the early 2000's due to the increased availability of miniaturized manufacturing and the demand for cheap analytical devices [24]. The μTAS's described in the following section provide a solution to the limitations of UV absorbance and laboratory fluorescence devices such as the Qubit fluorometer. They can quantify dsDNA in a single step, and utilize smaller volumes that conventional fluorometers. As will be discussed, two challenges that significantly hinder the sensitivity of μTAS's is poor signal to noise ratios and alignment of the sample with the optical elements [24]. The PIN photodiode is the leading product used in most μTAS's due to very low dark current and detection limits in the range of nano-watts of optical power on the sensor's surface [25], [26]. The devices discussed below use photodiodes to convert optical fluorescence into an electrical current signal that is on the order of $1 - 10nA$ [27]. Field of view and alignment is typically an issue with μTAS's that utilize sample loading systems that are disconnected to the optical setup.

The gold standard μTAS device consists of a microfluidic system that performs PCR and gel electrophoresis to detect DNA [28]. This device could detect fluorescence at DNA concentrations as low as $10\mu g/mL$ in volumes less than $1\mu L$ [28]. The team noted that the device suffered from poor photodiode sensitivity which results in a poor LoD and implemented a secondary device. They changed the structure of the photodiode detector by making a shallow PINN diode structure which gave the device the capability to linearly correlate DNA concentration from $80\mu g/mL$ down to $0.9\mu g/mL$ [29]. In both devices excitation light was provided by an external light source and the photodiode was integrated into a disposable sample

loading chip [28], [29]. A multiple layer dielectric interference filter was utilized to attenuate the excitation light from the fluorescence so that a broadband photodiode which was embedded below the gel electrophoresis channel could detect the fluorescence and correlate it to a signal from $3 - 6nA$ depending on the DNA concentration [29]. The electrical signal from the photodiode is received by an external data acquisition system that is sensitive enough to detect the very small current signals [24], [28], [29].

In summary, the devices designed by this group have been devices that utilize PCR to amplify the DNA product and detect the presence of a DNA fluorophore with an integrated photodiode detector under the gel electrophoresis channels [28], [29], [27]. As with other fluorescence systems, there was three optical elements in this device: the excitation source, the sample, and the photo detector. By integrating the photodiode into the sample loading chip the sample will always be aligned with the photodetector. However the team utilized a macro scale excitation light source that is disconnected from the sample chip which introduces alignment inconsistencies. Also the geometry of these devices are such that the excitation source is directed towards the photodiode with the sample in the middle. This geometry will be discussed in more depth in the following section but in general is highly susceptible to having a poor signal to noise ratio with broad spectrum photo sensitive detectors such as the photodiodes used in these designs.

The device designed in this thesis has been the Sepsis Check and the design characteristics are described in Chapter 3. Some improvements that intend to be developed throughout the design of the Sepsis Check is to decrease the sensitivity of the photo detection system to the excitation light and to separate the sample from a functional excitation and detection system.

The geometry of the device and the optical elements of the device could be used to decrease the sensitivity of the photo detection system to the excitation light. The photodiode detectors in most μTAS's are non-specific light sensitive detectors and thus are paired with a longpass filter to attenuate excitation light in the range of the fluorophores emission spectrum [24]. In the case of PicoGreen this would mean that the longpass filter would have a cut-on wavelength near $523nm$. However, despite utilizing high quality filters with optical densities >4.0, the photodiode can still be saturated from the optical output of the excitation beam and overpower the fluorescence from the sample, especially at low target concentrations. Therefore, the addition of an excitation filter with a cut-off frequency below $523nm$ will further attenuate the excitation beam intensity above $523nm$.

The second drawback from μTAS's is that they suffer from poor alignment between the excitation beam and the sample/detector. A major requirement for fluorescence quantification devices is the demonstration of a consistent background measurement [24]. With a disconnected excitation system from the photo detection system this is not the case for the gold standard devices discussed. A connected excitation and emission system and a separate sample loading chip would be better suited for consistent quantification results.

2.4.5.4 Miniaturized Fluorescence Systems

The addition of excitation filters and a reusable emission collection system that was not present with the μTAS's have been implemented for other applications such as tracing of Ca^{2+} concentration spikes in mice neurons, somatic cell counting, and nucleic acid detection. These systems have focused on the miniaturization of the microscope for PoC and in field detection of fluorescence. The analysis of these systems focuses on the geometry of the optical elements as this is the origin of the unique advantages and disadvantages of each system.

Miniaturized fluorescence systems can be categorized in two main geometrical configurations: transmission configuration and epifluorescence configuration. Both designs are shown below in Figure 2.7.

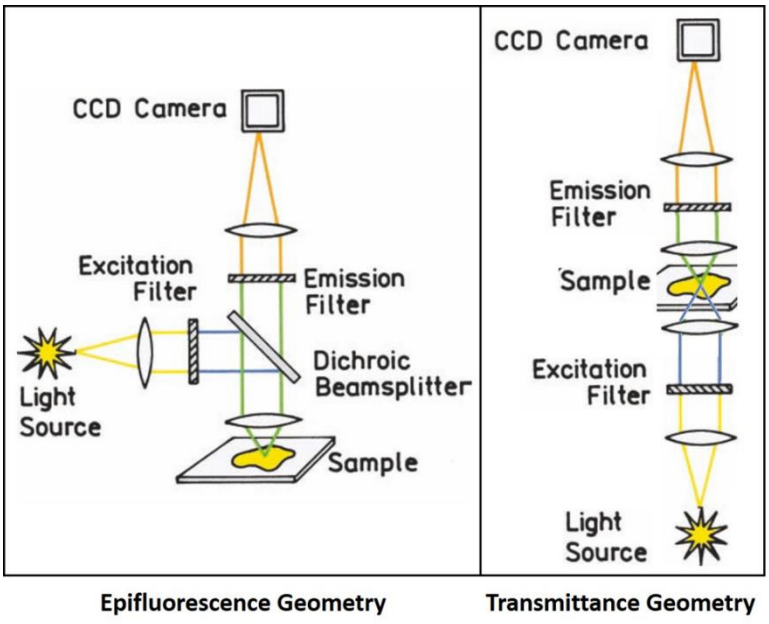

Figure 2.7: Comparison of a transmission configuration and an epifluorescence configuration for miniaturized fluorescence microscopes

Systems that utilize a transmission based approach are where the excitation beam is directed towards the detector and the sample is obstructing the beam path. Transmission configurations are less common than epifluorescence configurations and can be found in many scenarios where the design requires a probe type configuration with a long active length but a very narrow cross sectional area, or with μTAS's. An epifluorescence configuration is much more common and is defined as a system in which the excitation and emission beams pass through the same objective lens between the sample and the rest of the device.

2.4.5.4.1 Transmission Miniature Fluorescence Microscopes

Transmission configuration systems are good for simplification of the beam paths. Transmission configurations can also be commonly found in other fields such as lensless images or other macro-vision systems. Miniaturized transmission systems have been designed for use in cell counting and sorting devices [30], [31]. As with μTAS's, the general consensus on transmission based geometries is that they suffer from high background excitation noise because the photodetector is directly in line with the excitation source [30], [31]. This is sufficient for using contrast to outline boundaries and features as in cell counting, however not sufficiently sensitive for calibration and quantification of fluorescence.

2.4.5.4.2 Epifluorescence Miniature Fluorescence Microscopes

The major advantage to an optical device that utilizes an epifluorescence configuration is that the fluorescence emission is separated from the excitation beam by utilizing optical elements such as dichroic mirrors or diffraction gratings [32]. Current designs available have low optical power in the range of $170 - 600\mu W$ [32] which results in a weak fluorescence emission that is difficult to detect with macro imaging systems. Highly light sensitive photodiodes again are commonly used due to their low dark current, however are not well suited for the intended application due to alignment limitations.

2.4.5.4.3 Parallel Ray Fluorescence Geometry

An additional system that is similar to epifluorescence without the objective lens is where the excitation source and fluorescence detector are both directly above the sample and the excitation and emission beams of interest are parallel. This miniaturizes the device as the emission and collection beams are located along the same path and there is no dichroic mirror that adds displacement from the sample. Parallel ray fluorescence geometry has been made portable and handheld in the past via the use of fiber optics. The combination of two fiber optic cables to emit excitation light and collect emitted fluorescence relay the optical information to desktop equipment. Analog continuous optical signals in fiber optics perform with high consistency however suffer from increased absorption and leakage that is proportional to the fiber length [32], [33]. Although a high powered desktop excitation source could be used to

generate sufficient fluorescence from the sample, the use of a fiber optic cable limits the field of view and cannot transmit spatial information that would be possible with an image acquisition system.

With this in mind, a miniaturized and reusable fluorescence design that does not rely on desktop equipment, captures wide field of view images, that utilizes optimized optical elements for the quantification of cfDNA in whole blood with the cross channel device is in demand.

Chapter 3.

3 Materials and Design Methodology

This chapter identifies and describes the materials used in the design process, the devices themselves, and the methods used to advance the prototypes. The total device including optical components, electronic components, and housing unit comprise the Sepsis Check. This chapter also describes the method used to develop the design from the initial photodiode design to the final imager design.

3.1 Materials

The materials include consumable reagents, materials utilized to construct the microfluidic devices, materials that were purchased including optical elements, and materials used to build the 3D printed prototypes.

3.1.1 Consumable Reagents

These materials are utilized in the quantification of DNA in every sample. These materials interact with the sample inside the microfluidic devices.

3.1.1.1 Quant-iT™ PicoGreen dsDNA Nucleic Acid Stain

The Quant-iT™ PicoGreen dsDNA Nucleic Acid Stain Reagent Kit was purchased from *Invitrogen™ Life Technologies*. The kit includes standard lambda DNA ($\lambda - DNA$) solution, PicoGreen fluorescent probe solution, and buffer designed for DNA quantification [34], [35]. The specific details about the three components in the kit are detailed below in Table 3.1.

Table 3.1: Quant-iT™ PicoGreen dsDNA Nucleic Acid Stain Reagent Kit component details

MATERIAL	AMOUNT	COMPOSITION
QUANT-IT™ PICOGREEN DSDNA REAGENT	$100\mu L$ in 10 Vials	200 Fold concentration in DMSO
20X TE (TRIS + EDTA) BUFFER	$25mL$	$200mM$ Tris-HCL, $20mM$ EDTA, pH 7.5
$\lambda - DNA$ STANDARD	$1mL$	$100\mu g/mL$ in TE buffer

1) Component 1: Lambda DNA Standard ($\lambda - DNA$)

   Studies have shown that cfDNA is mostly double stranded DNA (dsDNA) [16] with a molecular size ranging from $\sim 150bps$ to over $\sim 10kpbs$ [5]. The $\lambda - DNA$ standard provided in this kit is linear

double-stranded DNA with a molecular size ranging from $125\ bps$ to $23.1\ kpbs$ [34]. It is prepared from $\lambda - DNA$ (clindlts875 Sam7) that has been digested to completion with Hind III [36]. Therefore this $\lambda - DNA$ sample is a reasonable substitute for cfDNA in clinical blood samples.

2) Component 2: Quant-iT™ PicoGreen®

   PicoGreen is a fluorescent nucleic acid stain for quantitating dsDNA in solution [34]. PicoGreen has shown a linear relationship between dsDNA concentration and fluorescence intensity over four orders of magnitude in DNA concentration [37]. This linearity is maintained in the presence of several compounds that commonly contaminate nucleic acid preparations, including salts, urea, ethanol, chloroform, detergents, proteins and agarose [37]. PicoGreen nucleic acid stain is ideal for the quantification of cfDNA in clinical blood samples because of this specificity to dsDNA and it's resilience against contaminants that could potentially be found in whole blood samples.

3) Component 3: TE (Tris + EDTA) Buffer

   TE buffer is a commonly used buffer solution for procedures involving DNA. TE buffer is the combination of pH buffer (Tris) and EDTA, a molecule that chelates cations. It has been shown that DNA extracted from formalin fixed tissues was not degraded when EDTA was added to the buffered formaldehyde [38]. Therefore, TE buffer is appropriate for testing with plasma, clinical isolated DNA, and whole blood because of the ability of TE to maintain the quality of DNA in solution.

Other DNA dyes have been utilized for DNA quantification in the past such as SybrGreen or Hoechst 33258 [37] however PicoGreen is an optimal fluorophore to use when trying to quantitate dsDNA concentration because of its high sensitivity to the molecule. The combination of a quantum yield of ~ 0.5 when bound with dsDNA and very low quantum yield when it is not bound with dsDNA as well as the large molar extinction coefficient ($\sim 70000 cm^{-1}M^{-1}$) result in PicoGreen surpassing the sensitivity of Hoechst 33258 by 400-fold [22].

3.1.1.2 Sample Preparation

A typical sample preparation procedure would be as follows. The original $100\mu g/mL\ \lambda - DNA$ sample was diluted to $10\mu g/mL$ with TE buffer by combining $2\mu L$ of $100\mu g/mL\ \lambda - DNA$ with $18\mu L$ of TE buffer. Serial dilutions of this $10\mu g/mL$ sample ranged from 0.008 to $10\mu g/mL$. Concentrations down to $2\mu g/mL$ were verified by measuring with the *Eppendorf BioPhotometer Plus* spectrophotometer available in the lab. A 20-fold dilution of the PicoGreen reagent from the kit was also prepared using TE buffer. A one to one volume ratio of $\lambda - DNA$ to 20x dilution PicoGreen was mixed for each sample. As an example,

a $2\mu g/mL$ sample would contain $1\mu L$ of $10\mu g/mL\ \lambda - DNA$ mixed with $4\mu L$ of TE buffer to make $5\mu L$ of $2\mu g/mL$. This was mixed with $5\mu L$ of 20-fold diluted PicoGreen dye to make a final sample with a volume of $10\mu L$. This is the equivalent substitute for a $2\mu g/mL$ septic patient sample because the patient sample would be mixed in the same method ($5\mu L$ of whole blood at a cfDNA concentration of $2\mu g/mL$ and $5\mu L$ of 20x diluted PicoGreen).

The reagents were mixed thoroughly by repeatedly pumping the pipette five times before letting the sample sit for 10 minutes prior to measuring in the Sepsis Check. This ensured that the DNA and PicoGreen were thoroughly intercalated. The sample would then be loaded into the Sepsis Check, the light emitting diode turned on to maximum optical power, and a sample measurement taken.

3.1.1.3 Agarose Gel

Agarose gel (1%; Type III-A, high EEO) was purchased from *Bioshop Life Science Products®*. Agarose gel has been widely applied in DNA electrophoresis due to its conductivity [39]. A gel concentration of 1% was prepared for the microfluidic device. A 1% concentration was chosen because previous electrophoresis experiments using 2% gel resulted in no migration of DNA above $300\ bps$, which is a principal size for cfDNA in blood [5] into the gel. Therefore the gel concentration was decreased to allow for accumulation of the longer cfDNA strands while still blocking other whole blood contaminants like proteins and cells.

3.1.2 Microfluidic Devices

The microfluidic devices are used to hold each sample for quantification. Two designs were constructed: the reservoir device and the cross channel device. Both were made of Polydimethylsiloxane (PDMS). The reservoir device was made from a 3D printed mold and the cross channel device was made from a silicon wafer mold.

3.1.2.1 Polydimethylsiloxane (PDMS)

PDMS is a commercially available and widely used silicone rubber. The chemical formula is $CH_3[Si(CH_3)O]_nSi(CH_3)_3$. It has several desirable properties such as: being transparent from $235nm$ to $800nm$, hydrophobic, non-toxic, biocompatible, an ability to replicate submicron features, easy bonding to itself or glass, and low cost [40], [41]. To make PDMS elastomer, *Slygard® 184 Elastomer Kit* was purchased from *Dow Corning Corp.* in the USA. The kit contains two liquid components: a base and a curing agent. After thoroughly mixing the base and curing agent with a weight ratio of 10:1, the mixture solidifies into a flexible elastomer with 30 minute polymerization time at $80℃$ [42].

3.1.2.2 Manufacturing the Microfluidic Devices

3.1.2.2.1 Silicon Wafer

A silicon wafer served as a substrate upon which the mold for the cross channel device was fabricated using the photolithography process. Silicon wafers bond well with a negative photoresist SU-8 at a low temperature [43], which increases the lifetime of the mold. In this process, a 3-inch silicon wafer from *University Wafers, MA, USA* was utilized.

3.1.2.2.2 SU-8 Photoresist

SU-8 Photoresist is an epoxy based negative photoresist commonly used in micromachining and other micro-electro-mechanical systems (MEMS) applications. With a single coating process it can be spun into thicknesses ranging from $1\mu m$ to $200\mu m$ [44]. After exposure to near UV light ($350 - 400nm$), SU-8 photoresist becomes polymerized and has highly stable thermal, chemical, and mechanical properties. It has been widely used in fabrication of micro-structured molds even with high aspect ratios. In this process SU-8 2000 series products from *MicroChem Corp.* are used to fabricate the PDMS molds on the silicon wafer.

3.1.2.2.3 Fabrication of the Cross Channel Device

The fabrication of the cross channel device was a three step process: the master mold fabrication, the microchannel casting, and the device bonding. Fabrication of the cross channel device was optimized by using glass slides and petri dishes to minimize debris and ensure a clean environment during the bonding steps. The process is shown below in Figure 3.1.

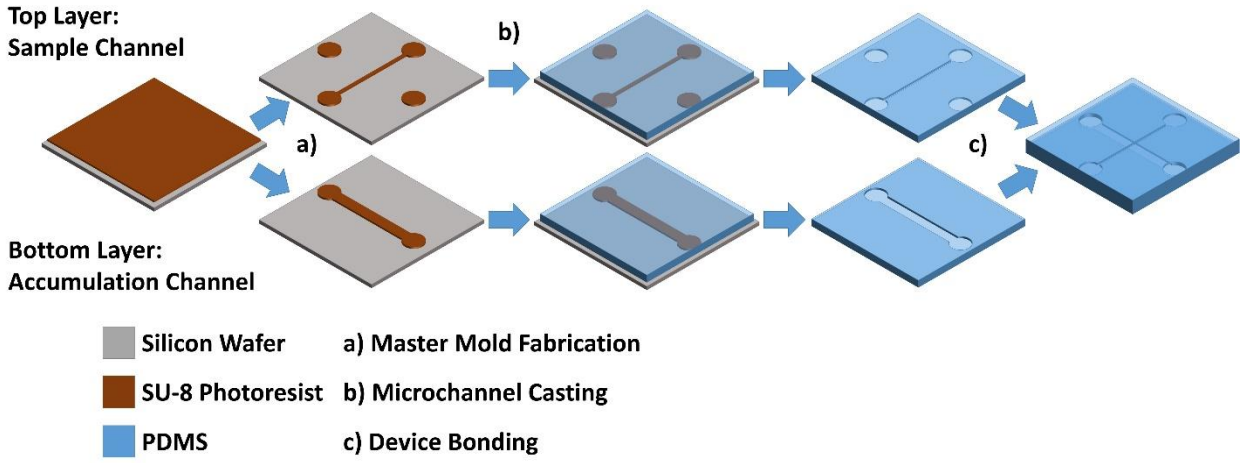

Figure 3.1: Schematic of the cross channel fabrication process

a) Fabrication of the master mold (Figure 3.1 a).

The molds of the cross channels were casted using the photolithography method. Photomasks with desired channel dimensions were designed on AutoCAD. From there the files were sent to *CAD/Art Services Inc.* for ultra-high-resolution printing on transparency sheet.

b) Microchannel Casting (Figure 3.1 b).

The PDMS microchannel casting process was to be conducted in a clean environment and always protected from debris. First, 5 grams of PDMS was prepared in a 10:1 weight ratio of base to curing agent and poured onto the silicon microchannel molds. The molds were placed in the desiccator to remove air bubbles and then moved to the oven at $80℃$ for 30 minutes.

c) Device Bonding (Figure 3.1 c).

The now solidified PDMS channels are placed face up on glass slides and exposed to air plasma generated with 100W of power for 20s with the plasma machine from *Harrick Plasma, NY, USA*. After which they were aligned face-to-face and bonded as shown in Figure 3.1 c). Plasma bonding seals the channels and the wells that are necessary for generating the electric fields inside the device as well as providing a point of entry for the liquid reagents. Post bonding, the cross channels were put on a hot plate at $70℃$ for 20 minutes to strengthen the bonding.

3.1.2.2.4 Filling of the Cross Channel Device

Once the device had been fabricated the accumulation channel was loaded with 1% agarose gel in preparation for loading the DNA sample into the sample channel. The filling process is shown below in Figure 3.2.

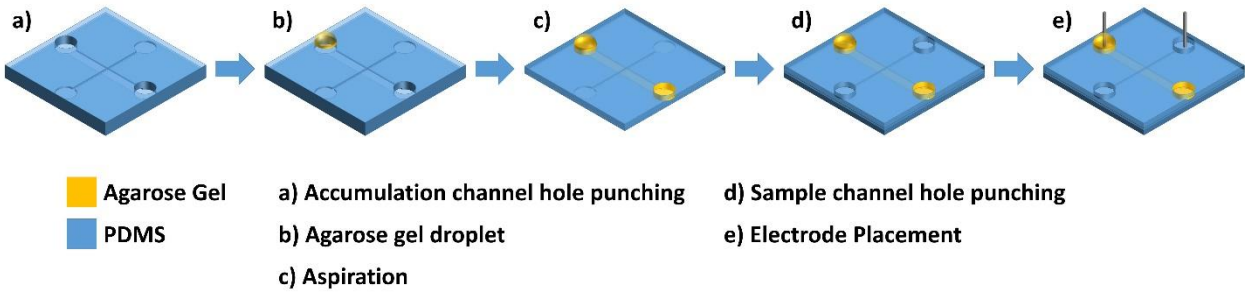

Figure 3.2: Schematic of the cross channel gel filling process

a) Accumulation Channel Hole Punching (Figure 3.2 a).

Two holes were punched to give access to the accumulation channel. Punching of these holes was conducted with caution as to not punch through the entire device. The holes were punched through only the top layer of PDMS which contained the sample channel.

b) Agarose Gel Droplet (Figure 3.2 b).

1% Agarose Gel was prepared by mixing $10mL$ of TAE buffer with 0.1 grams of Agarose Gel powder in the microwave for two minutes at low power. A droplet of this heated liquid gel was quickly placed on one of the holes for the accumulation channel creating a seal around the well.

c) Aspiration (Figure 3.2 c).

The pipette that was used to place the droplet of liquid Agarose Gel on the inlet of the accumulation channel was quickly inserted into the outlet hole at the other end of the accumulation channel. A seal was set and the pipette was used to pull the gel into the channel until uniform filling was achieved. After aspiration the gel was left to sit for 20 minutes to solidify.

d) Sample Channel Hole Punching (Figure 3.2 d).

Holes were again carefully punched through only the top layer of PDMS to connect to the sample channel. The holes were punched post accumulation channel filling because the aspiration of the gel would not have worked. The sample channel is now ready for sample loading.

e) Electrode Placement (Figure 3.2 e).

The positive electrode was placed in the accumulation channel and the negative electrode was placed in the sample channel. These electrodes will generate a small electrical field in the channels to perform gel electrophoresis inside the microfluidic device.

3.1.2.3 Manufacturing the Reservoir Microfluidic Device

The reservoir fabrication method was much simpler than the cross channel devices which allowed for rapid testing of the prototypes while still providing valuable information as to the capabilities of the prototype to quantify dsDNA concentration. The 3D printed molds for the reservoir devices were printed out of *EasyABS Filament* from *PRUSA Research* extrusion printer. ABS was used because it has a higher melting point, thus making these molds suitable for baking PDMS in the oven at $80℃$. A picture of the mold is shown in Figure 3.3 and Figure 3.4.

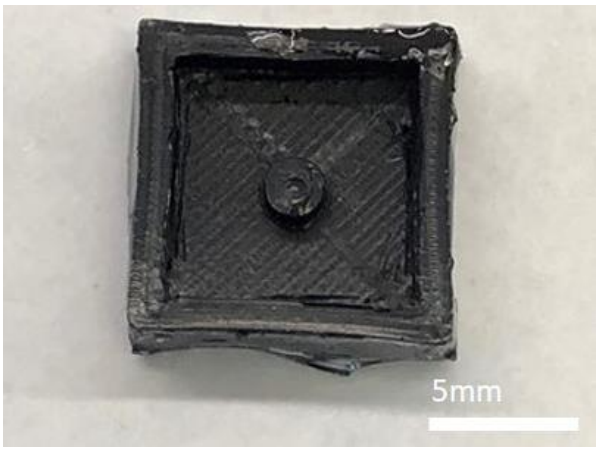

Figure 3.3: Picture of the reservoir molds used for rapid prototype testing and analysis.

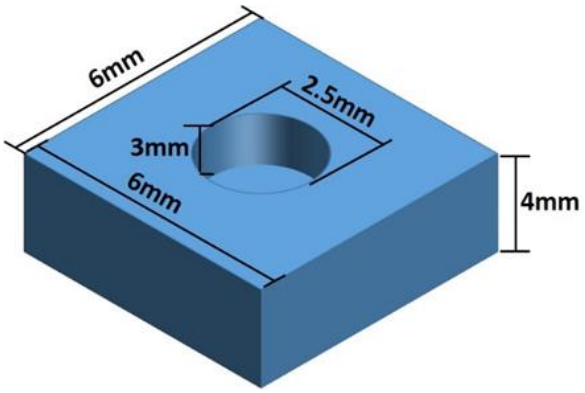

Figure 3.4: Reservoir device when it is removed from the 3D printed mold.

The reservoir device is a PDMS reservoir with a $2.5mm \emptyset \, x \, 3mm$ deep reservoir in the center. This device was used in many of the experiments as it could hold a small sample of $10\mu L$ and provided dependable results.

3.1.3 Optical Housing Unit

The optical elements in the various Sepsis Check prototypes were encapsulated in a 3D printed housing unit. This unit acted as an optical table that aligned and spaced the optical elements appropriately. The housing unit also isolated the optical excitation and fluorescence from external light sources. The 3D printed housing unit was printed out of *EasyABS Filament* from *PRUSA Research*. Off-white colored ABS as well as black ABS were both used in different Prototypes to make the housing unit.

3.1.4 Optical Elements

The optical elements in the various Sepsis Check prototypes were focused on the excitation and emission profiles of the PicoGreen dsDNA fluorescent tag. The optical elements described here were combined in various geometries to optimize the performance in relation to the excitation and emission profiles of PicoGreen.

3.1.4.1 Light Emitting Diodes (LEDs)

Light emitting diodes (LEDs) are compact, energy efficient light sources that can emit light in a narrow band of wavelengths. An integrated LED and lens module was purchased from *ThorLabs* that has a glass lens, a $470nm$ center wavelength, and a peak optical power of $170mW$ at peak power consumption [45]. The center wavelength is $470 \pm 5nm$ with a full width at half maximum (FWHM) of $22nm$ [45]. As a result, the optical output of the LED is characterized by the optical power spectrum shown in Figure 3.5.

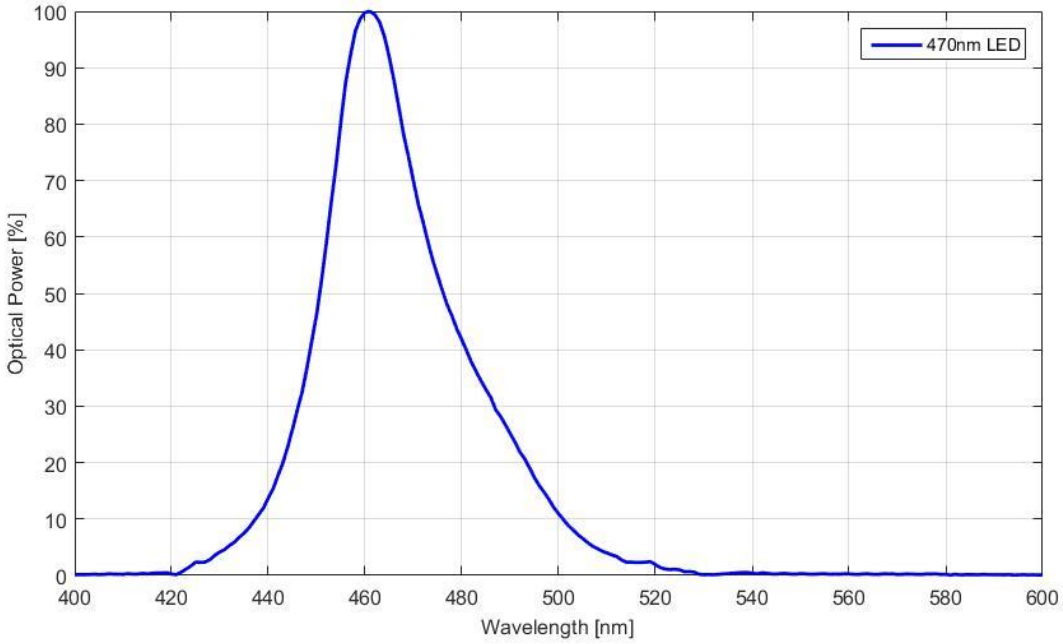

Figure 3.5: Output of the LED470L as a percentage of the optical power. Provided by Thorlabs [45].

The optical power ($170mW$) of the $470nm$ LED is distributed across the entire spectrum of wavelengths. In order to compare spectra in this thesis, the optical power of the LED in Figure 3.5 was normalized. The integral of the spectrum represents the optical power of the spectrum. Mathematically, this can be approximated by the summation of the values in the spectrum across a range of wavelengths. For example, to determine the amount of optical power that is emitted between $500nm$ and $505nm$ the percentage intensity values are added (0.51) and compared to the sum of the percent intensity values in the entire spectrum (32.14). The sum between $500nm$ and $505nm$ was 1.60% of the area of the total spectrum $(0.51/32.14) = 0.016$ therefore, $2.72mW$ of optical power is emitted between $500nm$ and $505nm$ $(170 * 0.016 = 2.72mW)$. Manipulation of this spectrum and others is used in the design section of this thesis to validate the prototype improvements.

3.1.4.1.1 LED Power Supply Circuit

The LED can be powered by a voltage source that is capable of providing $3.8V$ and $300mA$. At these values, the LED will be near it's maximal optical power of $170mW$. To provide this power a DC circuit was designed as shown below in Figure 3.6.

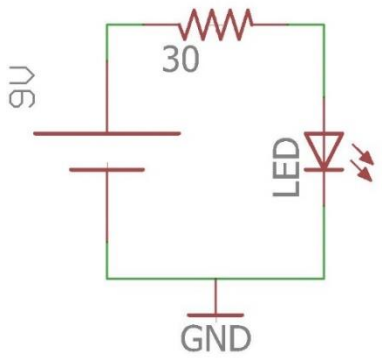

Figure 3.6: Schematic of the principle circuit for the LED power control system

The 30Ω resistor controls the current that is flowing through the LED by Ohms law in Equation 3.1 [18].

$$\begin{aligned} V &= IR \\ 9V &= I(30\Omega) \\ \frac{9V}{30\Omega} &= 300mA \end{aligned} \tag{3.1}$$

A transistor was added to the circuit to allow for control by an electrical input instead of turning on the power supply. Transistors are components that allow for control of high current and high voltage power sources from a low current output device [46]. By applying voltage to the middle pin of a transistor (the gate) it completes the circuit between two additional pins (the source and drain), creating a unidirectional short circuit from the source pin to drain. A transistor was incorporated as shown in Figure 3.7.

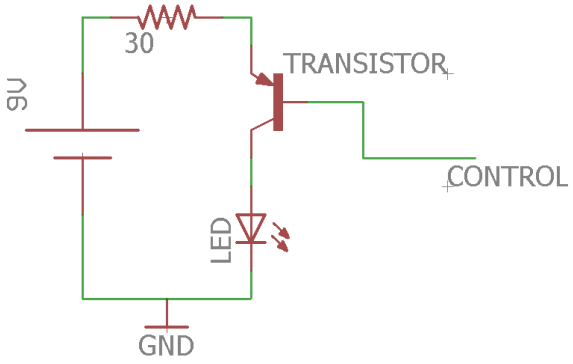

Figure 3.7: Schematic of the LED power circuit with the ability to control the state of the LED with electrical input through a transistor

When there is no voltage applied to the middle of the transistor it acts as an open circuit and the power from the $9V$ battery will not flow through the LED. Thus, the LED will remain off. Once sufficient voltage is applied to the transistor, the circuit is completed and power can flow through the LED turning it on. This way the entire system can be powered by the $9V$ supply, but the LED can be turned on and off separately.

3.1.4.2 Optical Filters

The passive optical filters used in the various Sepsis Check prototypes are highly effective at isolating regions of a spectrum [47], [18]. The filters used are dichroic filters that work by reflecting unwanted wavelengths and transmitting desired wavelengths [48]. Numerous optical filters were purchased from *ThorLabs* and *Edmund Optics* throughout the prototyping stages shown in Table 3.2.

Table 3.2: All optical filters purchased from Edmund Optics and ThorLabs for the Sepsis Check prototypes.

FILTER	CHARACTERISTICS	PROTOTYPE	SUPPLIER
84-693	500nm Shortpass OD>4.0	4	Edmund Optics
84-744	525nm Longpass OD>4.0	3, 4	Edmund Optics
FEL0500	500nm Longpass OD>4.0	1, 2	ThorLabs
FL488-3, FL488-10, FL05488-10	488nm Bandpass OD>4.0	2, 3	ThorLabs

The characteristics of interest for the purposes of the Sepsis Check were the optical density, center wavelength, and the cut-on / cut-off wavelength. The optical density of a filter is related exponentially to the transmission percentage at a specific wavelength as demonstrated by the percent transmission Equation 3.2 [18].

$$Percentage\ Transmission = 10^{-Optical\ Density} x100\% \quad (3.2)$$

Typically the optical density is used to describe the transmission percentage in the blocking region of the filter. For example, a longpass filter with an optical density >4.0 will block 99.99% of the light in the blocking region. The 84-744 filter from Edmund optics blocks 99.9998% of the light at $500nm$ in the blocking region as shown below in Figure 3.8.

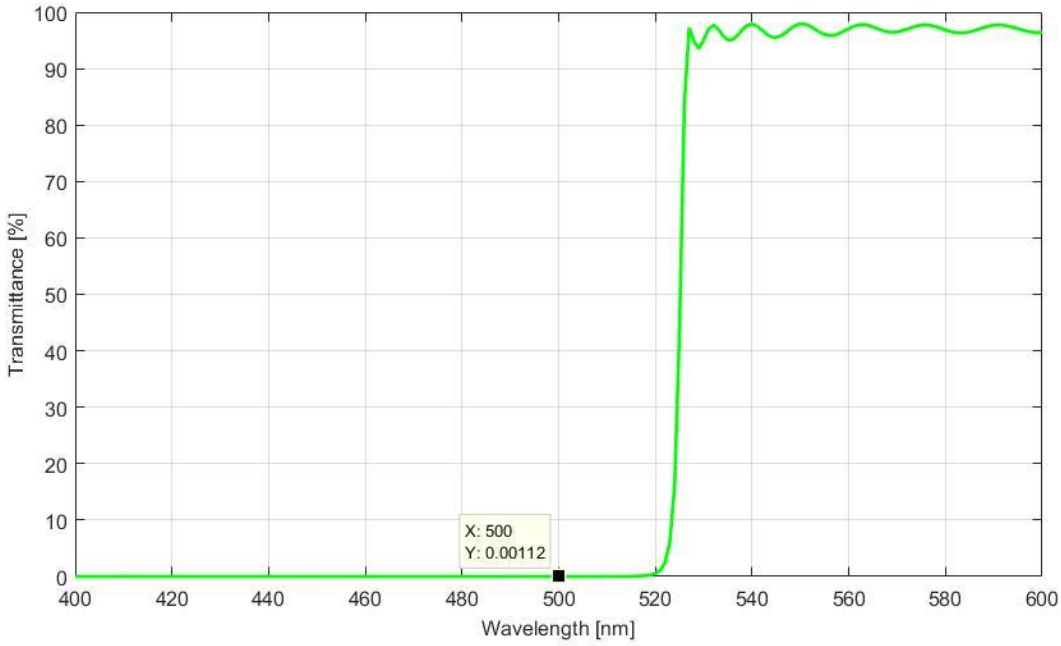

Figure 3.8: The spectrum of the 525nm longpass filter (Part Number: 84-744) from Edmund Optics with an optical density >4.0 shows 0.001% transmission of wavelengths at 500nm which is within the blocking region. Data for this spectrum is provided by [48].

The cut-on wavelength is a characteristic of a longpass filter that denotes the wavelength at which the transmission increases to 50% throughput. Likewise, the cut-off wavelength is the equivalent characteristic of a shortpass filter that denotes the wavelength at which transmission decreases to 50% throughput. The cut-on wavelength for a longpass filter is shown below in Figure 3.9.

The center wavelength is the wavelength in the middle of the FWHM as depicted in Figure 3.10. The FWHM is the width of the spectrum at 50% percentage transmission.

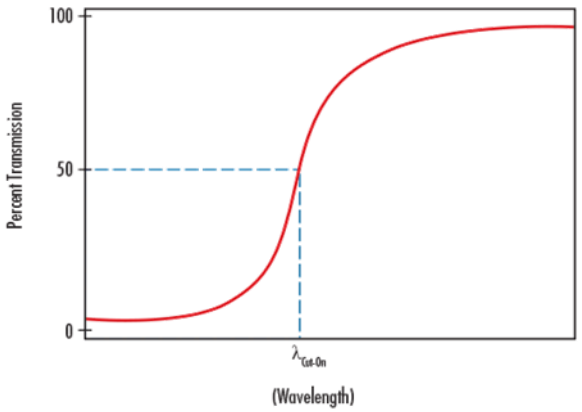

Figure 3.9: Example of a cut-on wavelength for a longpass filter [48]

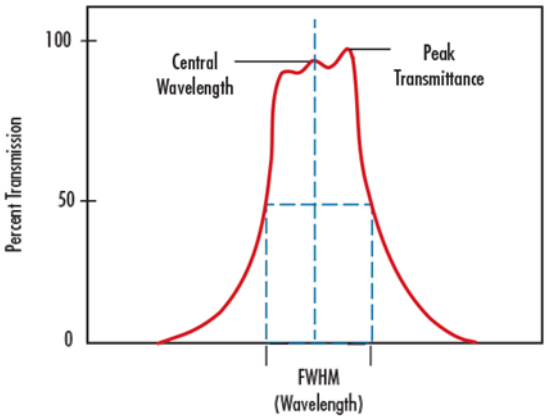

Figure 3.10: Example of the center wavelength and full width at half maximum FWHM of a bandpass filter [48]

The dichroic filters used in the various prototypes had cut-on/off wavelength certainty of $\pm 0.6nm$ or less. However, because of the nature of dichroic mirrors reflecting light based off of their incident wavelength [47], [48], the center wavelength is sensitive to changes in the direction of the incident rays. As a rule of thumb, when the angle of incidence goes from $0°$ to $45°$ the central wavelength shifts down by 10% [48]. Therefore optical lenses are commonly used to collimate the light rays prior to the transmission through the filter which improves accuracy of the center wavelengths.

3.1.4.3 Optical Lenses

In optical fluorescence, lenses are used to collimate diffuse light from point sources, and to focus collimated light onto a point [18]. Elements like LEDs or excited PicoGreen dye are modeled as point sources as they emit light in a conical geometry. This incoming conical geometry can lead to decreased accuracy of the cut-on wavelength for the dichroic filters as discussed earlier [47], [48]. To obtain the strongest signal from the sample, diffusion losses need to be reduced as much as possible. An example of how optical lenses can assist in reducing diffuse light is shown below in Figure 3.11.

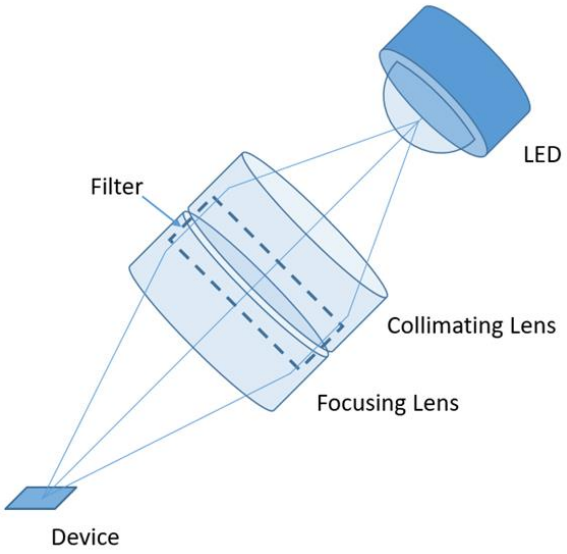

Figure 3.11: Example of how optical lenses can be used to collimate a diffusing ray of light from a point source and subsequently focus that ray of light to a region of interest.

The optical lenses used in the various prototypes are shown below in Table 3.3.

Table 3.3: All optical lenses purchased from ThorLabs for the Sepsis Check prototypes.

LENS	CHARACTERISTICS	PROTOTYPE	SUPPLIER
LA1540-ML	$Focal\ Length = 15.0mm \pm 1\%$	1, 2, 3, 4	Thorlabs
LA1951-A-ML	$Focal\ Length = 25.3mm \pm 1\%$	3, 4	Thorlabs
LA1027-A-ML	$Focal\ Length = 35.0mm \pm 1\%$	4	ThorLabs
LA1560-ML	$Focal\ Length = 25.0mm \pm 1\%$	4	ThorLabs

3.1.4.4 Light Sensitive Photodiodes

A photodiode was used in the emission collection system of the first three prototypes as the functional photodetector to convert light intensity into a measurable electrical signal. A junction photodiode is a light-sensitive device that behaves similarly to an ordinary signal diode. It generates a photocurrent (I_{PD}) that is proportional to the optical intensity (P) absorbed in the depleted region of the junction semiconductor defined as the responsivity of the device [25] Equation 3.3.

$$R(\lambda) = \frac{I_{PD}}{P} \tag{3.3}$$

The photodiode used in the first two prototypes was the FDS100 photodiode provided by *ThorLabs*. It has a responsivity curve as shown below in Figure 3.12.

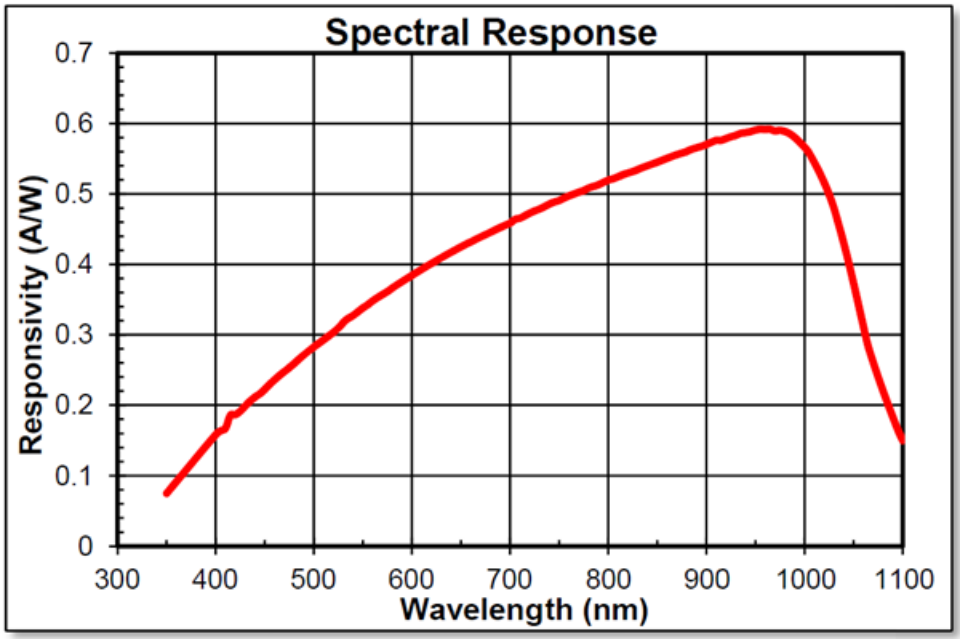

Figure 3.12: Spectral response, or responsivity of the FDS100 photodiode provided by ThorLabs [26]

This basic property was exploited to measure the amount of optical intensity that is emitted by a fluorescent sample.

The third prototype utilized a photodiode from Edmund Optics with a lower dark current. This lowered the theoretical LoD. Photodiodes used in the various Sepsis Check prototypes are outlined in Table 3.4.

Table 3.4: Photodiodes purchased from Thorlabs and Edmund Optics used in the first three prototypes of the Sepsis Check.

PHOTODIODE	CHARACTERISTICS	PROTOTYPE	SUPPLIER
FDS100	$Dark\ Current \leq 2\ nA$	1, 2	Thorlabs
84-612	$Dark\ Current \leq 1\ nA$	3	Edmund Optics

3.1.4.5 Keithley 2410 Source Meter

The dark current is the minimum electrical background noise that is generated by a photodiode. The dark current of the FDS100 photodiode was approximately $2\ nA$ as per the datasheet [26]. This was confirmed with testing conducted with the Keithley 2410 Source Meter which can act as a highly accurate ammeter with a resolution as low as of $50\ pA$ and a limit of detection of $1\ nA$ [49]. This device was used to measure the current from the photodiode to provide preliminary results prior to the design of the electrical amplification system. The photodiode can be directly wired to the Keithley as shown in Figure 3.13.

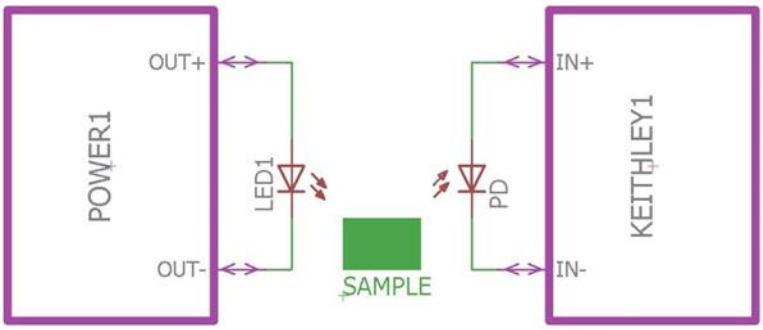

Figure 3.13: A schematic showing the connection of the photodiode to the Keithley 2410 Source Meter.

3.1.4.6 Electrical System

Although the Keithley laboratory equipment was capable of quantifying these small currents it is expensive and bulky. A compact and lower cost handheld device designed for the specific application to quantify low current signals would be better suited for a PoC photodiode design. Therefore a suitable circuit that is capable of measuring nano-ampere currents with high precision was designed.

The Arduino Microcontroller in Figure 3.14 is a cheap electrical input-output analyzing device that is the size of a credit card [46]. This device could read an input electrical signal, perform signal analysis, provide immediate feedback to the user, and allow for control by the user through electrical elements like push buttons.

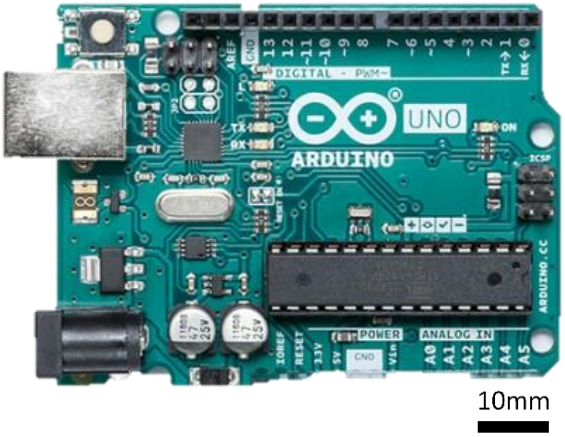

Figure 3.14: Picture of the Arduino Uno used in the prototypes that utilize a photodiode detection method

The Arduino has two types of interfaces, a digital interface allows for I/O readings that are recorded as HIGH or LOW signals. When 5V is applied to a digital input pin, the Arduino recognizes it as a HIGH input and can store that information as a boolean and vise-versa for a 0V or grounded input. The second

interface is the analog interface. Here, the Arduino can detect voltages that range from $0 - 5\ V$ with 8-bit resolution (0-1023) [46]. This results in the Arduino having approximately $0.05\ mV$ resolution. The electrical output of the light sensitive photodiode is between $1 - 20\ nA$. Amplification of this weak current signal to a detectable signal for the Arduino is what the Amplification System does. A schematic of the electrical system is shown below in Figure 3.15.

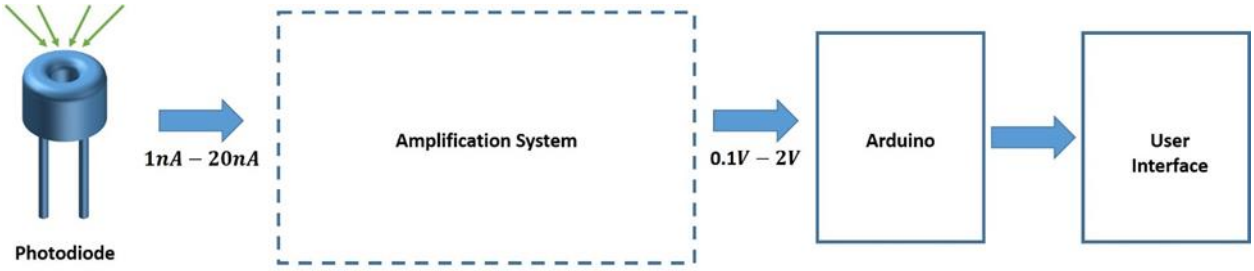

Figure 3.15: Pictogram showing the process of converting the electrical signal from the photodiode detector to the user interface.

3.1.4.6.1 Amplification System

The amplification system needed to convert a dynamic range output from the photodiode that ranged from $1\ nA - 20\ nA$ to a detectable signal in the functional range of the Arduino Microprocessor ($0 - 5\ V$). The amplification system consists of a purchased component called the μCurrent Gold, and a double op-amp and buffer circuit that was built from the functional electrical elements shown in Figure 3.16.

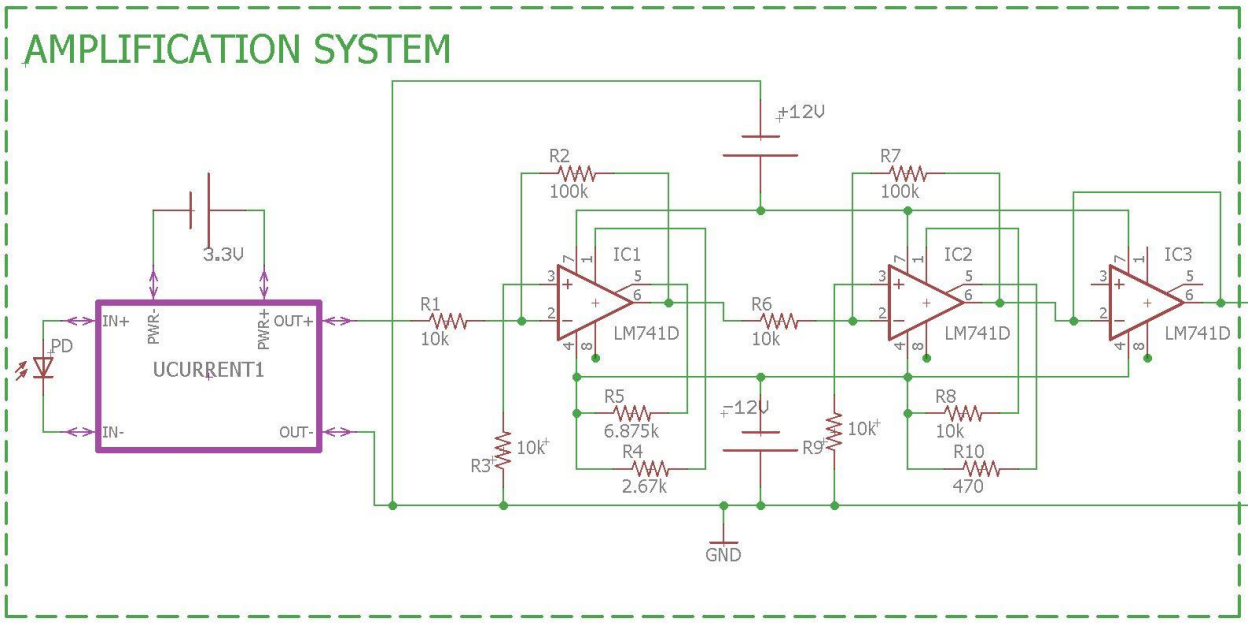

Figure 3.16: Schematic showing how the amplification system takes the photodiode reading and converts it to a measurable signal that can be calibrated with the Arduino Microprocessor. The Amplification system consists of two main components: the µCurrent Gold shown in purple on the left, and the remainder of the circuit which is the voltage amplifier.

The μCurrent Gold is a cheap and readily available current to voltage amplifier. It is capable of converting $1\,nA$ to $1\,mV$ [50]. It uses it's own built in $3.3\,V$ battery to perform the amplification. From there the $1\,mV$ signal goes into the first operational amplifier shown in Figure 3.16 as IC1. This element amplifies the signal from the output of the μCurrent Gold by the ratio of R1 and R2. In IC1 the ratio results in a 10 fold amplification. Likewise for the second operational amplifier (IC2), it amplifies the voltage at R6 by the ratio of R7 to R6 (again 10 fold amplification). This results in a total amplification of 100 fold. These amplification steps require additional voltage supply to power the op-amp. The external voltage supply was $\pm 12V$. The buffer stage (after R7) does not amplify the signal, instead it acts as a buffer. Electrical buffers help to separate elements of a circuit from each other. In this case this buffer removes any current generated from the amplification process, but maintains the voltage (it performs a 1x amplification) therefore protecting the Arduino and removing unnecessary noise generated by the 100x amplification.

3.1.4.6.2 User Interface

The user interface is the combination of a push button with a LCD display. The push button that was used in the LED control system is also used to initiate the process of taking a sample. When the button is pressed the following sequence is initiated:

1. LED turned on
2. Read photodiode measurement
3. Compare photodiode measurement to a moving average of a sample length of 10 samples.
4. If it is within $\pm 10\%$ of the mean of that moving average then display to the LCD screen that a steady state has been reached and the device is confident that it has distinguished the concentration of DNA in the sample.

The total user interface is shown below in Figure 3.17.

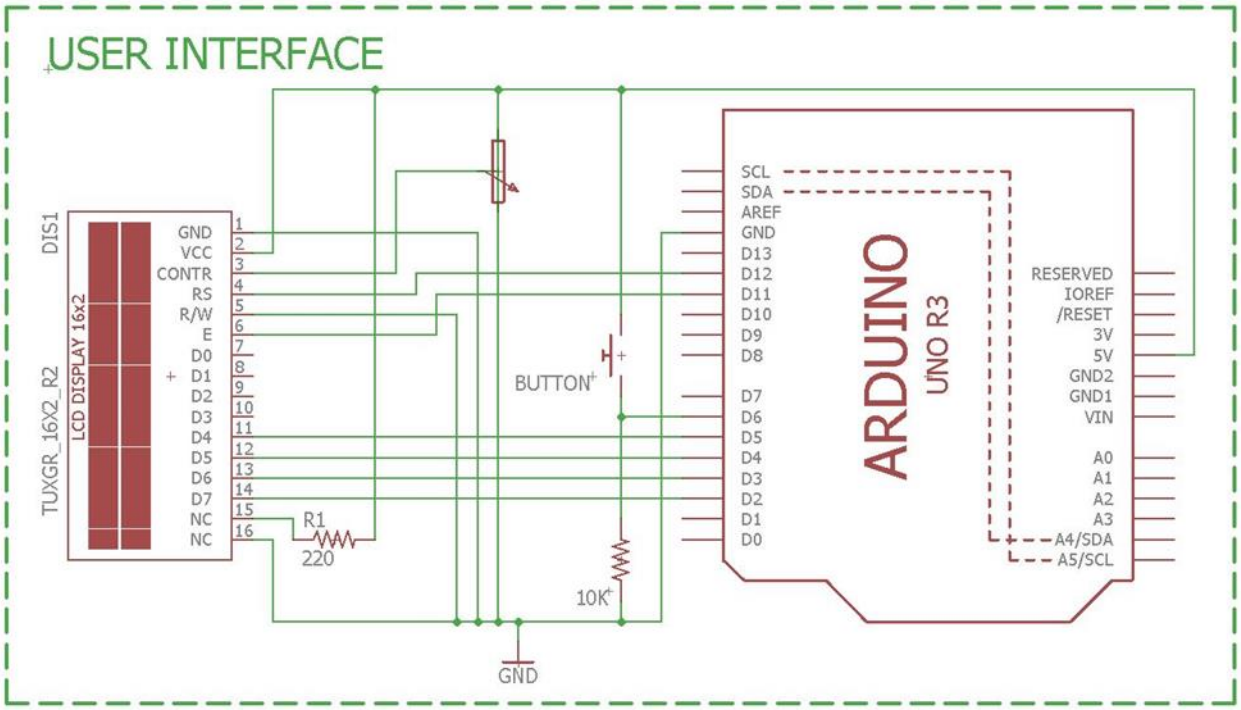

Figure 3.17: Schematic of the User Interface of the Sepsis Check is a combination of a push button and a 16x2 LCD display. Both elements are presented in this circuit diagram.

The push button control system is shown in the middle connected to the $5V$ output of the Arduino. The 16x2 LCD display is shown in its standard connection with the Arduino Microcontroller.

The push button is the functional element of the user interface. Not only does it control the LED control system but it also initiates the data acquisition system and the analysis of the signal that is received from the photodiode. When the push button is pressed it allows for 5V from the Arduino output to go into digital pin D6. This will be detected as a HIGH value. If the switch is left open, digital pin 6 is connected to ground through a $10k\Omega$ pull down resistor thus the Arduino will read this as LOW. The pull down resistor

is another safety factor for the Arduino to ensure that any current coming from ground is nullified and is generally known to be good practice.

3.1.4.7 Imager

The final prototype of the Sepsis Check utilized the cross channel device. For reasons discussed later in the design section, an imaging technique was necessary for the quantification of cfDNA. This is because the quantification of cfDNA in the cross channel devices requires spatial information. The imager used in the final prototype is a miniaturized 8MP camera shown in Figure 3.18 which can take high definition images of the microfluidic devices.

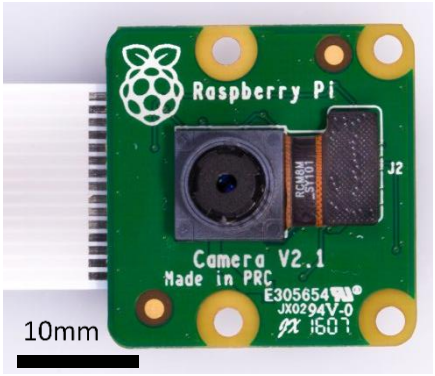

Figure 3.18: Picture of the Raspberry Pi Camera which was used as the imager in the fourth prototype

It is $25mm\ x\ 23mm\ x\ 9mm$ in size and has a focal length set to infinity. In practice this means objects at infinity (further than $1m$ from the lens) are in focus. With the imager design the final product needs to be processed. A specific area of the image can represent the desired changes.

3.1.4.7.1 Image Processing

The imager provides high definition images that need to be analyzed to detect and calibrate dsDNA in solution. This was done using an image processing program called ImageJ. The program is used to measure the average intensity of the reservoir as shown in Figure 3.19.

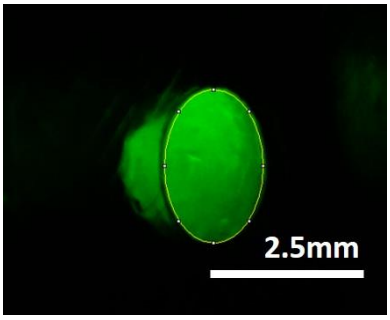

Figure 3.19: ImageJ processing of a $5\mu g/mL$ $\lambda - DNA$ sample in the reservoir device. An area of interest is selected shown as the yellow circle and the average pixel intensity in that area is calculated.

First the image is converted to a greyscale image with 8 bit resolution (0-255), an area of interest (shown as the yellow circle in Figure 3.19) is selected, and the mean intensity of the pixels in that area is recorded.

3.2 The Sepsis Check Designs

The Sepsis Check is the handheld device that consists of an optical exposure and detection system, an electrical readout unit, and appropriate instrument housing. The goal of the system is to be able to accurately quantify cfDNA concentrations from $1\mu g/mL$ to $10\mu g/mL$. In total there was 4 prototype revisions made.

Throughout the prototyping stages the excitation and emission systems were separated with an angle to mimic a combination of the epifluorescence and parallel ray geometries. This separates the excitation beam from the fluorescence and improves the sensitivity of the device to the emitted photons from intercalated PicoGreen. Another aspect of the prototypes that remained unchanged throughout the prototyping journey was the use of the $470nm$ LED. Many LED options were available, however, this option had a significantly higher peak optical power ($170mW$) which maximizes the intensity of the fluorescence emission by PicoGreen. The prototypes varied many other characteristics based on the performance criteria described below.

3.2.1 Performance Criteria

The $470nm$ LED provides $170mW$ of optical power distributed across a range of wavelengths according to the spectrum shown in Figure 3.5. The integral of the spectrum is the optical power of the LED, therefore the sum of the optical power from wavelength A to wavelength B can represent the percentage of optical power emitted in that range. For example, 0.66% of the area underneath the curve of the LED's spectrum is between $523nm$ and $600nm$. That equates to $1.12mW$ of optical power. This can be used to determine the optical energy transmitted through each element of the Sepsis Check prototype. The

performance criteria used to improve the design of the prototypes was the optical strength of the background noise compared to the optical strength of the excited PicoGreen fluorescent dye with a $1\mu g/mL$ dsDNA sample in the reservoir device.

The concentration of PicoGreen in the sample can be calculated by using the bonding ratio of dsDNA to PicoGreen ($1\ ng\ dsDNA : 0.442\ ng\ PG$), the molar mass of PicoGreen, and the following equation.

$$1\mu g/mL * 0.442 * 1ng\ PG/1ng\ dsDNA$$

$$C_{PG} = 0.442\mu g/mL$$

$$C_{PG}[mol/L] = \frac{0.442\mu g/mL}{552.805 g/mol}$$

$$C_{PG}[mol/L] = 8.00x10^{-7} mol/L$$

The molar extinction coefficient is a measure of how strongly a substance absorbs light [37]. The molar extinction coefficient of PicoGreen is $70000 cm^{-1}M^{-1}$ [37]. Compared to other dsDNA fluorophores PicoGreen's extinction coefficient is 1.75 times greater than Hoechst 33258 and 10-fold greater than ethidium bromide [37]. The molar extinction coefficient can be calculated using the Beer-Lambert Law in Equation 3.4 [18] which relates:

$A -$ The amount of light absorbed by the sample for a particular wavelength

$\varepsilon -$ The molar extinction coefficient

$l -$ The distance that the light travels through the solution

$c -$ The concentration of the solution

$$A = \varepsilon lc \tag{3.4}$$

The distance that the light travels can be approximated by the middle of the reservoir which equates to $1mm$ of active distance in which the light can interact with the sample.

$$A = 70000 cm^{-1}[mol/L]^{-1} * 0.1cm * 8.00x10^{-7} mol/L$$

$$A = 0.56\%$$

Therefore the PicoGreen fluorescent tag will absorb approximately 0.56% of the optical power it receives from the excitation system. The quantum yield of a fluorescent dye is the number of times a specific event

occurs per photon absorbed [37] shown below in Equation 3.5 [18]. The number of photons is directly proportional to the optical intensity.

$$\phi = \frac{\#\ Photons\ Emitted}{\#\ Photons\ Absorbed} \tag{3.5}$$

The quantum yield of PicoGreen is 53% when bound to calf thymus dsDNA [37]. This equation can be used to determine the percentage of excitation light that will be re-emitted as fluorescent light from the PicoGreen tag.

Fluorescence emission from PicoGreen is emitted uniformly in all directions. A lens can be utilized to capture and collimate a larger amount of that fluorescence emission by increasing the cone angle. The closer the lens can be to the sample and still collimate the light, the more fluorescence can be captured. The Sepsis Check utilizes an angled checkmark geometry to isolate the excitation and emission light beams. This limits the minimum distance because of the diameters of the lenses that are cheap and readily available for prototyping. Based on experimentation a distance of approximately $25mm$ is the minimum distance from the sample to the emission collection lens. Therefore, to allow for casing around the lens as well as tolerances in the 3D printed housing unit, a lens with a diameter of $25mm$ and a focal length of $35mm$ was utilized and can be used to calculate this loss in optical intensity described below in Figure 3.20 and Figure 3.21.

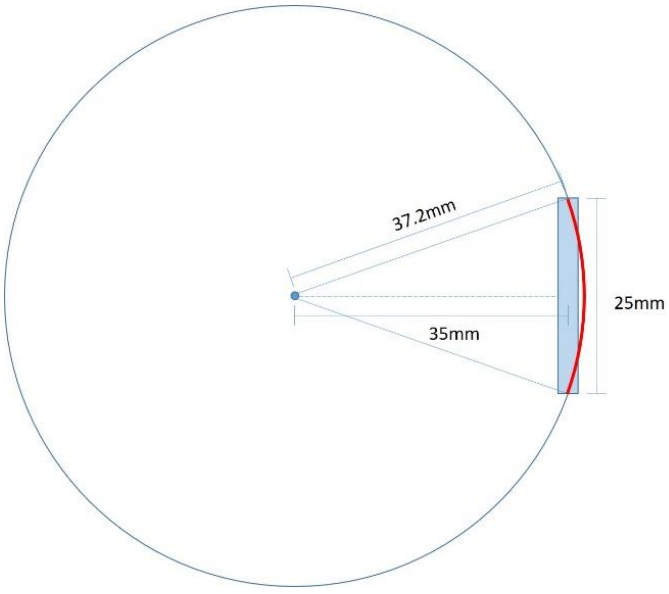

Figure 3.20: Point source of the Fluorescence emission of PicoGreen relative to the lens utilized to capture the optical intensity from the sample

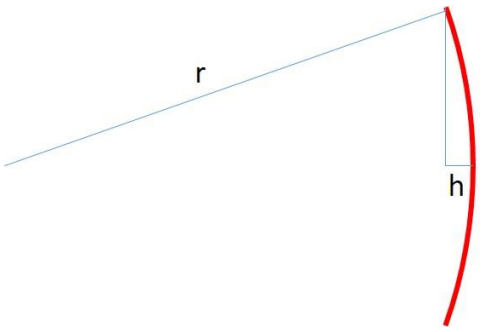

Figure 3.21: Calculating of the cone angle of fluorescence that can be captured by the 25mm diameter collimating lens.

$$r = \sqrt{(12.5)^2 + (35)^2}$$
$$r = 37.17mm$$

$$h = 37.17mm - 35mm$$
$$h = 2.17mm$$

Surface area of a sphere:

$$A = 4\pi r^2$$
$$A = 4\pi(37.2mm)^2$$
$$A = 17361.8mm^2$$

Surface area of the spherical sector:

$$A = 2\pi rh$$
$$A = 2\pi(37.17mm)(2.17mm)$$
$$A = 506.79mm^2$$

Percentage of the optical energy captured by the lens:

$$Capture\ Efficiency = \frac{506.79mm^2}{17361.8mm^2} = 2.92\%$$

Therefore the efficiency of the absorption and emission of the fluorescence sample can be summarized as 0.56% absorbed, 53% converted to fluorescence, and 2.9% captured for a total efficiency of 0.0086%. With these calculations, the optical power from the excited PicoGreen dye in a $1\mu g/mL\ \lambda - DNA$ solution can be calculated and compared against the background noise from the inefficiencies in the optical system.

3.2.2 Light Sensitive Photodiode Design Prototypes

A photodiode was used in the first three prototypes mimicking the design of most μTAS systems as well as personal previous experience designing a pulse oximeter that showed the capability to linearly quantify optical intensity.

3.2.2.1 Prototype 1

The concept behind the design of the first prototype was to start with a maximum amount of excitation optical power. Therefore, as shown in Table 3.5 and the image of the prototype in Figure 3.22 the only optical component of the excitation system was the $470nm$ LED with no filters used. The emission

collection system was designed to provide the specificity to capture emission photons in the range of the PicoGreen emission profile. Components of Prototype 1 are shown below in Table 3.5.

Table 3.5: Optical elements used in Prototype 1

EXCITATION SYSTEM		**EMISSION SYSTEM**	
OPTICAL ELEMENT	SPECIFIC CHARACTERISTIC	OPTICAL ELEMENT	SPECIFIC CHARACTERISTIC
LED470L	$470nm$ Center Wavelength	FEL0500	$500nm$ Longpass Filter
		LA1540-ML	Focusing Lens
		FDS100	Broadband Photodiode

Prototype 1 is shown in Figure 3.22. The prototype was designed with an angle between the excitation and emission system that acted as a method to separate the excitation beam from the fluorescence emission as is done in epifluorescence and parallel ray systems. The actual angle and distance from the sample were based on the diameters of the elements that minimized the distance to the sample. The only other constraint on the geometry was the lens. A lens with a short focal length of $15\ mm$ was utilized to focus collimated light from the sample onto the photodiode. Therefore, the photodiode was $15\ mm$ from the focal plane of the lens. The distance from the sample to the LED and filter were based off of their diameters and the angle.

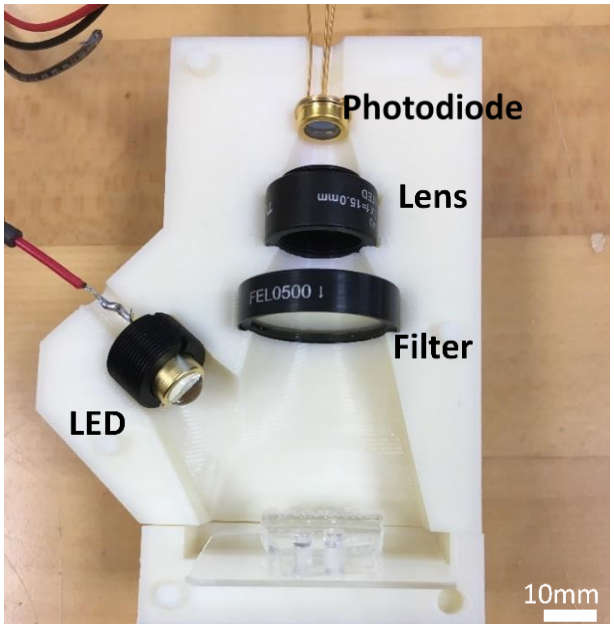

Figure 3.22: Internal picture of Prototype 1 including the optical elements included in the design

The performance of Prototype 1 was analyzed by using the spectra of the optical elements and the known fluorescent characteristics described earlier. Analysis of the performance of Prototype 1 began with the spectrum of the excitation system shown below in Figure 3.23.

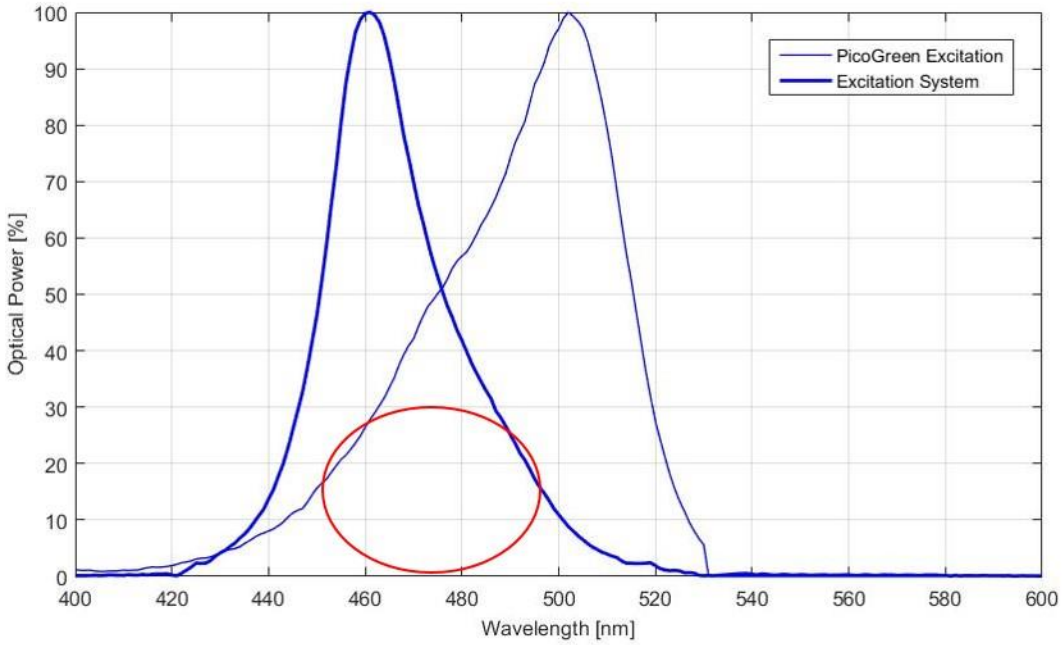

Figure 3.23: Comparison of the Excitation System of Prototype 1 against the PicoGreen absorbance spectrum [45], [34].

The excitation system of Prototype 1 is the raw $470nm$ LED. There are no other optical elements between the LED and the sample. This allows for maximum optical power transmission to the sample. It can be seen that there is a lot of overlap between the spectrum of the excitation system and absorbance spectrum of PicoGreen as shown by the red circle. This means that PicoGreen will be highly excited by this LED.

The emission collection system is comprised of a $500nm$ longpass filter and a focusing lens. The spectrum of these individual elements, as well as their combined spectrum is shown below in Figure 3.24.

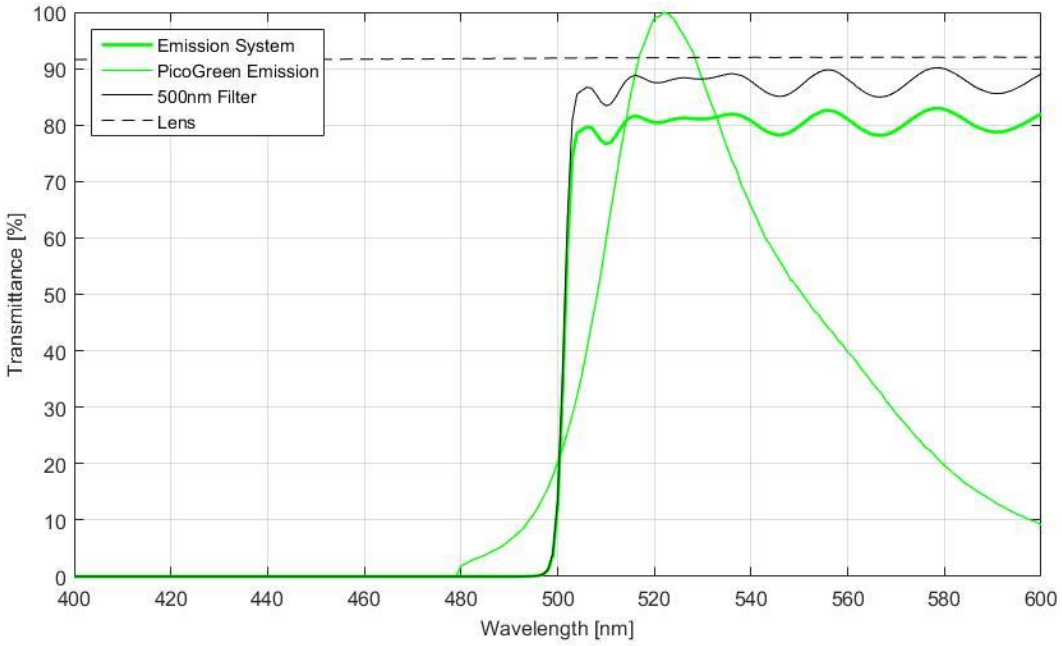

Figure 3.24: Comparison of the Emission System of Prototype 1 against the Emission spectrum of PicoGreen. Raw data courtesy of [47], [51], [34]. *The Emission System (thick green line) is the combination of the* $500nm$ *longpass filter spectrum (solid black line) and the LA1540-ML lens (dashed black line).*

The emission spectrum covers the vast majority of the PicoGreen emission spectrum. In theory this suggests that the system can capture the majority of the released photons from PicoGreen. The emission system also allows for a very high transmittance percentage for wavelengths above $500nm$.

Taking a closer look at the excitation spectrum one could notice that there is a significant amount of optical power supplied to the sample above $500nm$. This is the source of the leakage light which causes a poor signal to noise ratio in this first prototype. In theory, photons above $500nm$ from the LED could reflect off of the surfaces inside the Sepsis Check and be captured by the emission collection system which is highly sensitive to photons above $500nm$. This is known as the leakage noise which has been calculated and shown below in Figure 3.25.

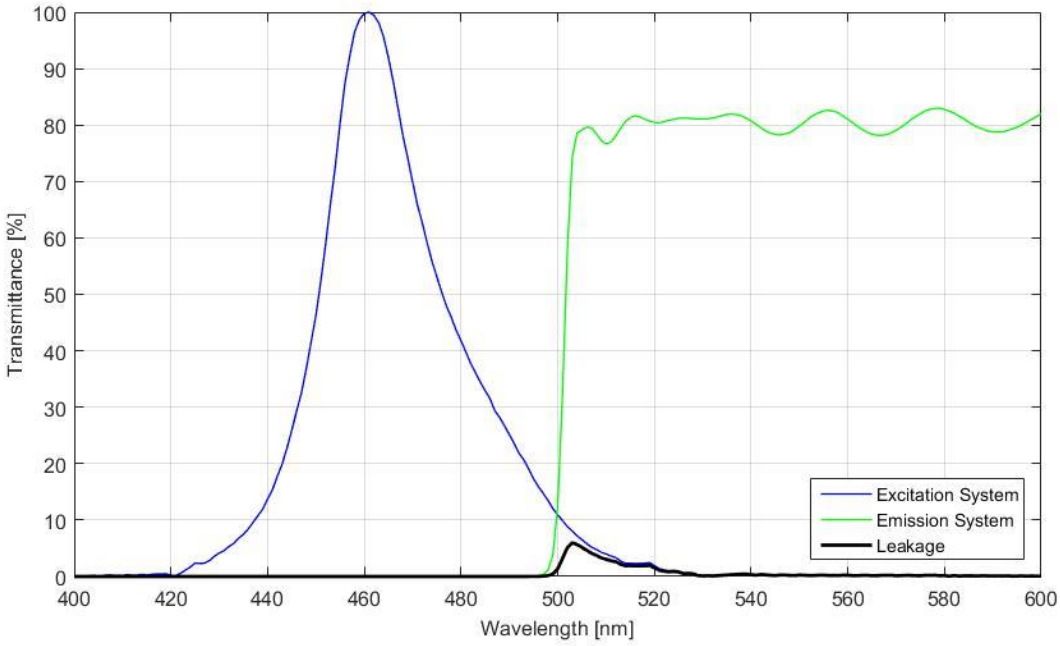

Figure 3.25: Point-wise multiplication of the excitation system and the emission system of Prototype 1 results in the Leakage Noise spectrum (thick black line). The leakage spectrum represents the optical power of the LED that is capable of transmitting through the entire design.

The combination of the $470nm$ LED and the PicoGreen excitation system in Figure 3.23 gives the amount of excitation light that hits the sample also known as the leakage spectrum shown in Figure 3.25. Summation of the leakage spectrum equates to $4.541mW$ of optical power. This can be compared to the optical intensity that reaches the photodiode detector from a $1\mu g/mL$ sample of $\lambda - DNA$ below in Figure 3.26.

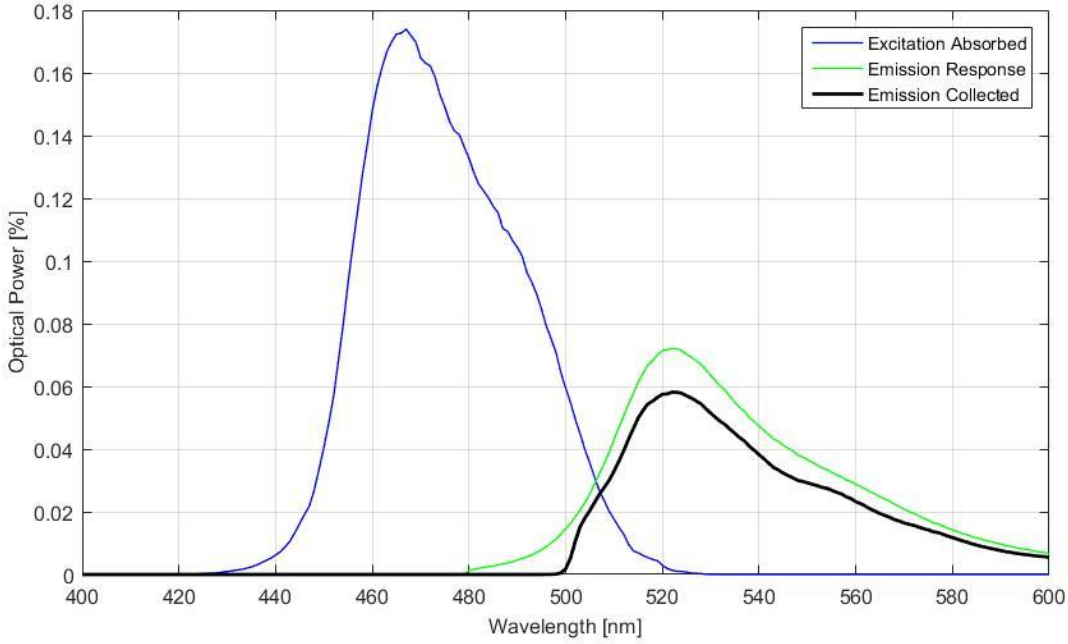

Figure 3.26: The comparison of the optical power that is absorbed by PicoGreen (blue), versus the optical power emitted by PicoGreen (green), and the amount of that emission spectrum that is captured by the emission collection system of Prototype 1 (black) when the reservoir device is filled with a $1\mu g/mL$ sample of λ-DNA.

The optical intensity of the incident light that will be absorbed by the intercalated PicoGreen dye can be calculated from the Beer Lambert Law. Based on the geometry of the reservoir design, a sample with $1\mu g/mL$ of dsDNA (therefore $8.00x10^{-7}\ mol/L$ of PicoGreen) will absorb 0.56% of the incident light. The area under the curve of the Excitation Absorbed line in Figure 3.26 is proportional to the number of photons absorbed by PicoGreen. As a result of the quantum yield of PicoGreen, 53% of that optical energy will be converted into emission photons which is represented by the green Emission Response spectrum in Figure 3.26. The Emission Response can then be captured by the emission collection system resulting in the final Emission Collected spectrum in Figure 3.26.

As a result, the final optical power of a $1\mu g/mL$ sample of $\lambda - DNA$ in a reservoir device is $0.147mW$. It is very clear that the problem is that the LED, although it has a center wavelength of $470nm$ still has relatively high optical power above $500nm$ where the emission system becomes sensitive. This results in a high amount of background noise. This issue was seen and is demonstrated in the results from Prototype 1 and was a major focus of the changes made in Prototype 2.

3.2.2.2 Prototype 2

The primary objective of the second prototype was to reduce the optical intensity of the leakage noise by adding optical elements in the excitation system that reduced the intensity of the excitation light at wavelengths above $500nm$. The changes on this design was the introduction of a focusing lens and a bandpass filter for the excitation system. The optical elements of Prototype 2 are shown below in Table 3.6.

Table 3.6: Optical elements used in Prototype 2

EXCITATION SYSTEM		**EMISSION SYSTEM**	
OPTICAL ELEMENT	SPECIFIC CHARACTERISTIC	OPTICAL ELEMENT	SPECIFIC CHARACTERISTIC
LED470	$470nm$ Center Wavelength	FEL0500	$500nm$ Longpass Filter
LA1540-ML	Focusing Lens	LA1540-ML	Focusing Lens
FL05488-10	$488nm$ Bandpass Filter	FDS100	Broadband Photodiode

Prototype 2 is shown below in Figure 3.27 and Figure 3.28.

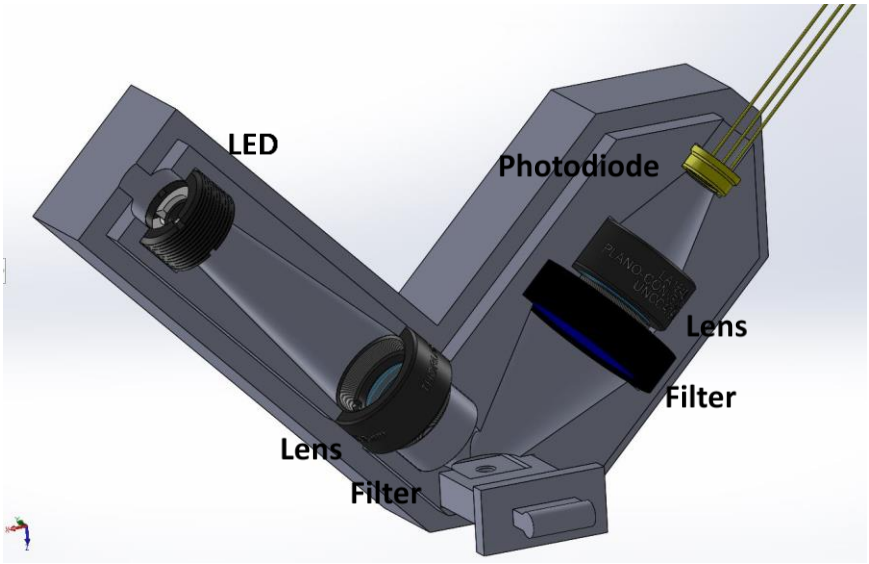

Figure 3.27: Cross section CAD drawing of Prototype 2 showing the internal optical elements

Figure 3.28: Picture of Prototype 2 with drawer designed to hold a reservoir device

The addition of the lens focusing the light from the LED onto the sample improves the ability of the excitation system to excite PicoGreen. With more photons exciting PicoGreen, more photons will be emitted. The addition of the bandpass filter makes the excitation system specific to the excitation of PicoGreen dye. With a center wavelength of $488nm$ and a FWHM of $10nm$, it significantly reduces optical intensities outside of the $478 - 498nm$ range. The combination of a $500nm$ longpass filter that blocks wavelengths below $500nm$ and a bandpass filter that significantly blocks wavelengths above $498nm$ results in a specific excitation and emission system. The caveat to the addition of a bandpass filter is that the total excitation optical power reaching the sample is significantly reduced which is shown below in Figure 3.29.

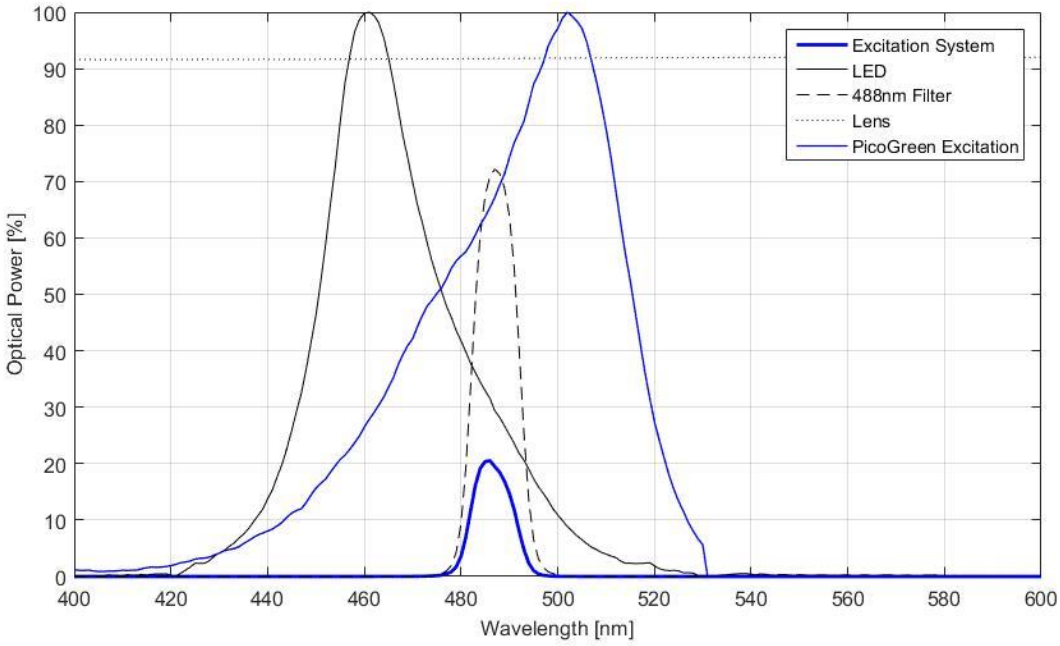

Figure 3.29: Comparison of the excitation system of Prototype 2 versus the absorption spectrum of PicoGreen [45], [34]. *The Excitation System (thick blue line) is the point-wise multiplication product of the LED (thin black line), the 488nm bandpass filter (dashed black line), and the LA1540-ML focusing lens (dotted black line). The PicoGreen absorption spectrum is shown as the thin blue line.*

The area under the Excitation System is $10.64mW$ vs the $170mW$ in Prototype 1. The addition of the lens makes it so that more of the light from the excitation system in Prototype 2 reaches the sample. In Prototype 1 the diffusion angle of the ball lens on the LED (7°) decreased the optical intensity that interacted with the sample. In this design a higher percentage of the photons are directed onto the sample. The addition of the lens assists with exciting PicoGreen, however the biggest improvement over Prototype 1 is the reduction of optical intensities above $500nm$.

The emission system of Prototype 2 is identical to that of Prototype 1 shown in Figure 3.24. The addition of the bandpass filter greatly decreases optical intensities above $498nm$ in the excitation system, therefore this addition significantly reduces the leakage noise as shown below in Figure 3.30.

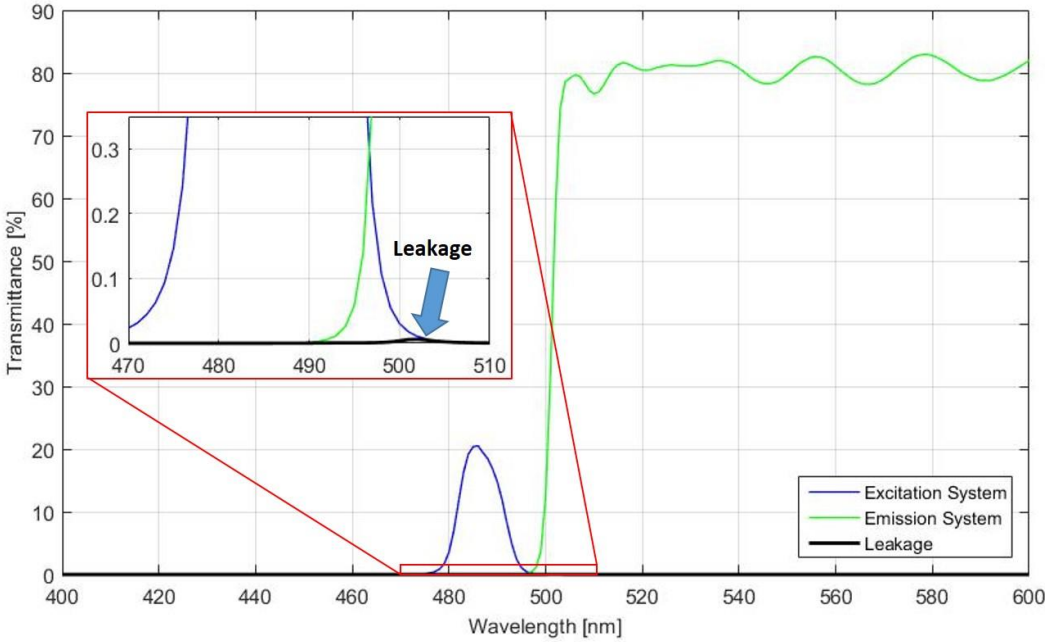

Figure 3.30: Point-wise multiplication of the excitation system (blue line) and the emission system (green line) of Prototype 2 results in the Leakage Noise spectrum (thick black line). The leakage spectrum represents the optical power of the LED that is capable of transmitting through the entire design.

Now that the higher wavelengths of the excitation light hitting the sample have been attenuated, the peak excitation spectrum and the passing region of the emission system are separated. This results in a smaller amount of leakage noise as shown in the magnified spectrum in Figure 3.30. The total optical power of the leakage noise of Prototype 2 is $2.1\mu W$. This is significantly less than the leakage noise in Prototype 1, however, now that the total power of the excitation system is reduced, the optical power of a $1\mu g/mL$ sample is also reduced as shown in Figure 3.31.

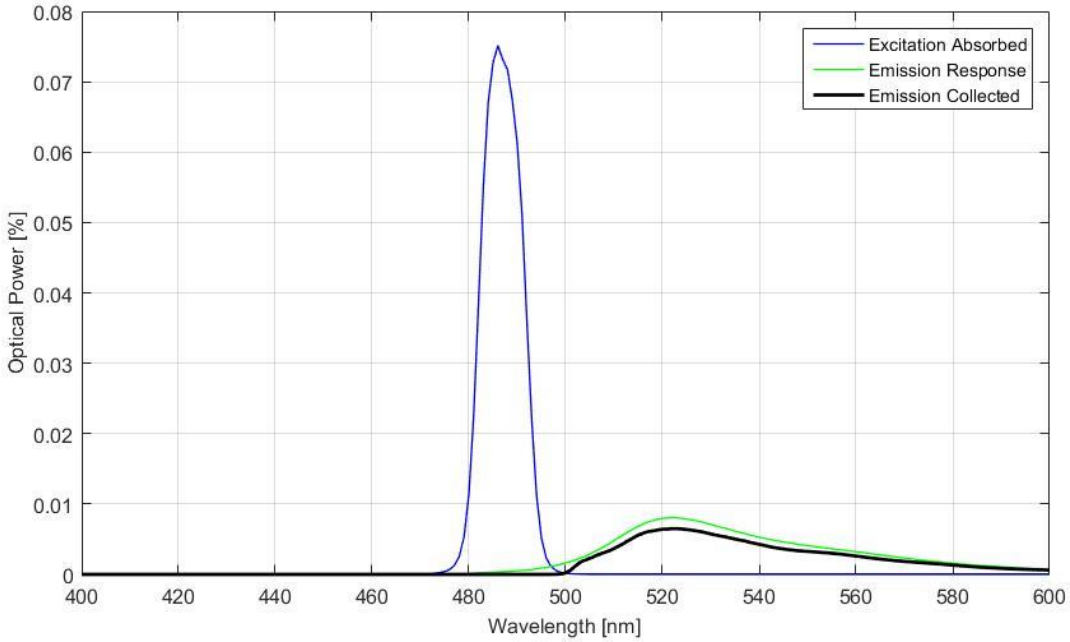

Figure 3.31: The comparison of the optical power that is absorbed by PicoGreen (blue), versus the optical power emitted by PicoGreen (green), and the amount of that emission spectrum that is captured by the emission collection system of Prototype 2 (black) when the reservoir device is filled with a $1\mu g/mL$ sample of λ-DNA.

The optical power of a $1\mu g/mL$ sample in Prototype 2 is $16.4\mu W$. In theory this means that Prototype 2 will be able to differentiate between $1\mu g/mL$ of dsDNA and a blank sample. This improvement was then taken to Prototype 3 where the design changed to allow for the incorporation of a cross channel device. It was important to move towards the cross channel device because the cross channel allows for separation of dsDNA from other materials in whole blood.

3.2.2.3 Prototype 3

The third prototype was necessary to be able to perform detection of dsDNA in the cross channel design. Prototype 3 is shown below in Figure 3.32.

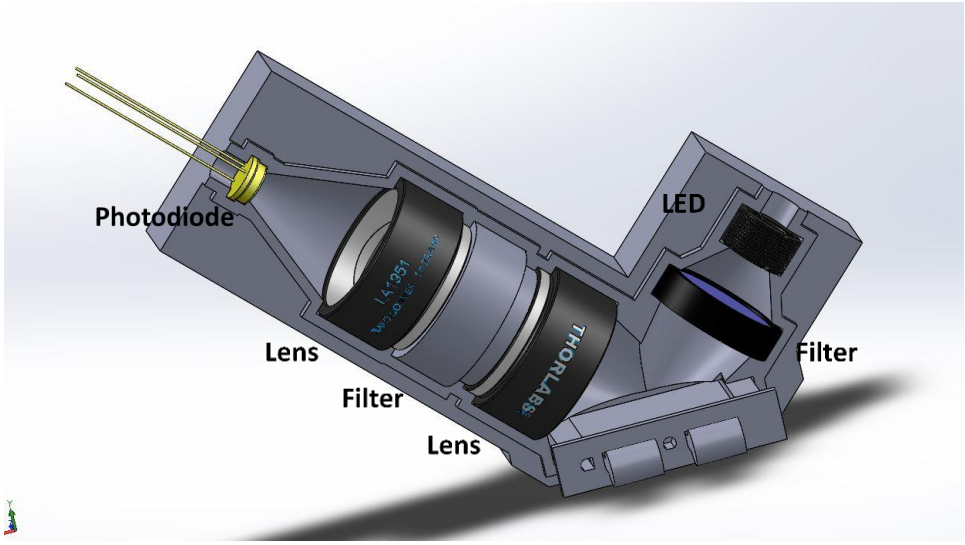

Figure 3.32: Cross sectional CAD diagram of Prototype 3 showing the optical elements incorporated into the design.

Prototype 3 introduced the addition of a second lens in the emission system, a bandpass filter with a FWHM of $\pm 3nm$ in the excitation system, a $525nm$ longpass filter, and a more sensitive broadband photodiode. The geometry of the emission system considers the sample as a point source which emits diffused light. This diffused light is captured by a collimating lens, which improves the accuracy of the cut-on wavelength of the longpass dichroic filter because dichroic filters are sensitive to changes in the angle of incidence as discussed earlier [47], [48]. The narrower bandpass filter decreases the strength of the leakage noise because it nullifies excitation wavelengths above $491nm$ which is further away from the emission system. However, this also decreases the strength of the excitation system that excites PicoGreen, and thus decreases the strength of the emitted photons from PicoGreen. Therefore, a more sensitive broadband photodiode with a better responsivity curve was employed. A high quality $525nm$ longpass filter was also introduced to replace the $500nm$ longpass filter used in Prototype 2. This further separates the excitation and emission profiles. The optical elements of Prototype 3 are shown below in Table 3.7.

Table 3.7: Optical elements used in Prototype 3

EXCITATION SYSTEM		**EMISSION SYSTEM**	
OPTICAL ELEMENTS	SPECIFIC CHARACTERISTICS	OPTICAL ELEMENTS	SPECIFIC CHARACTERISTICS
LED470	$470nm$ Center Wavelength	LA1951-ML	Collimating Lens
FL488-3	$488nm$ Bandpass Filter	84-744	$525nm$ Longpass Filter
		LA1951-ML	Focusing Lens
		84-612	Broadband Photodiode

The combination of the $470nm$ LED as well as the $488nm$ bandpass filter gives the excitation system spectrum shown below in Figure 3.33.

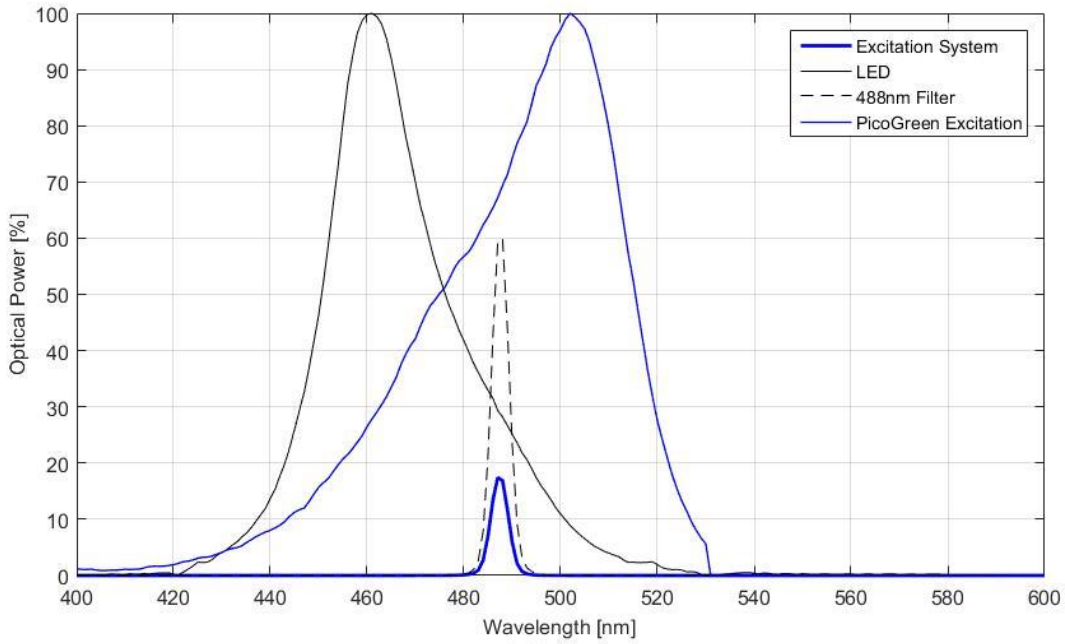

Figure 3.33: Comparison of the excitation system of Prototype 3 versus the absorption spectrum of PicoGreen [45], [34]. *The Excitation System (thick blue line) is the point-wise multiplication product of the LED (thin black line) and the 488nm bandpass filter (dashed black line). The PicoGreen absorption spectrum is shown as the thin blue line.*

The longpass filter and the two lenses which are used to collimate the light from the PicoGreen sample, pass it through the $525nm$ filter, and focus it on the photodiode all combine to make the cumulative emission system spectrum shown below in Figure 3.34.

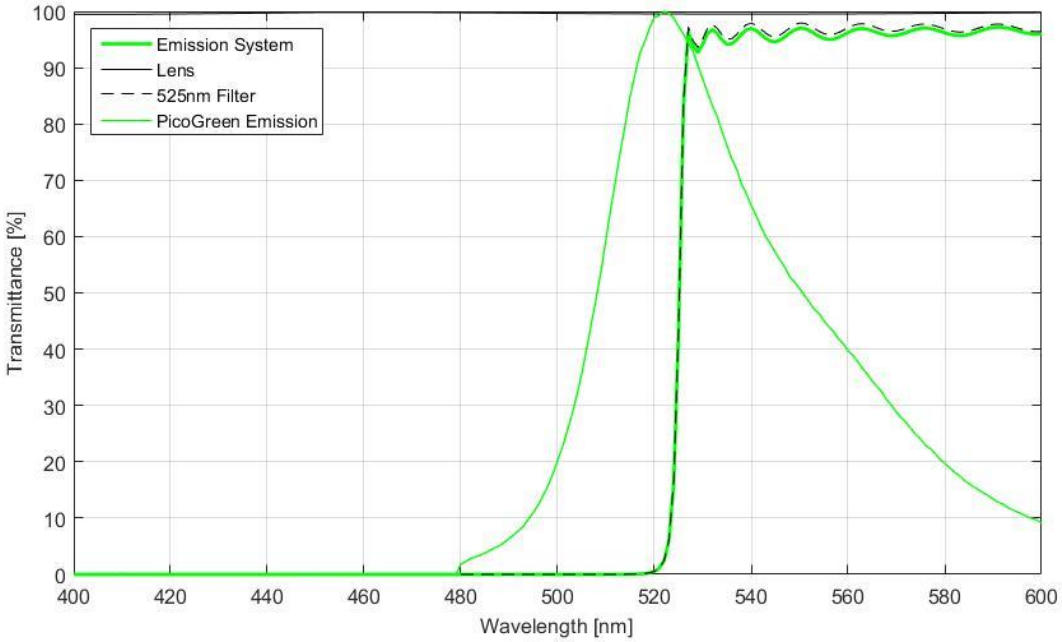

Figure 3.34: Comparison of the emission system of Prototype 3 against the Emission spectrum of PicoGreen [47], [34]. *The Emission System (thick green line) is the combination of the* $525nm$ *longpass filter spectrum (dashed black line) and the LA1540-ML lens (solid black line).*

Pushing the cut-on wavelength of the longpass filter to $525nm$ from $500nm$ separates the spectrum of the excitation and emission systems as shown in the Leakage Noise figure below. This decreases the leakage noise in Figure 3.35.

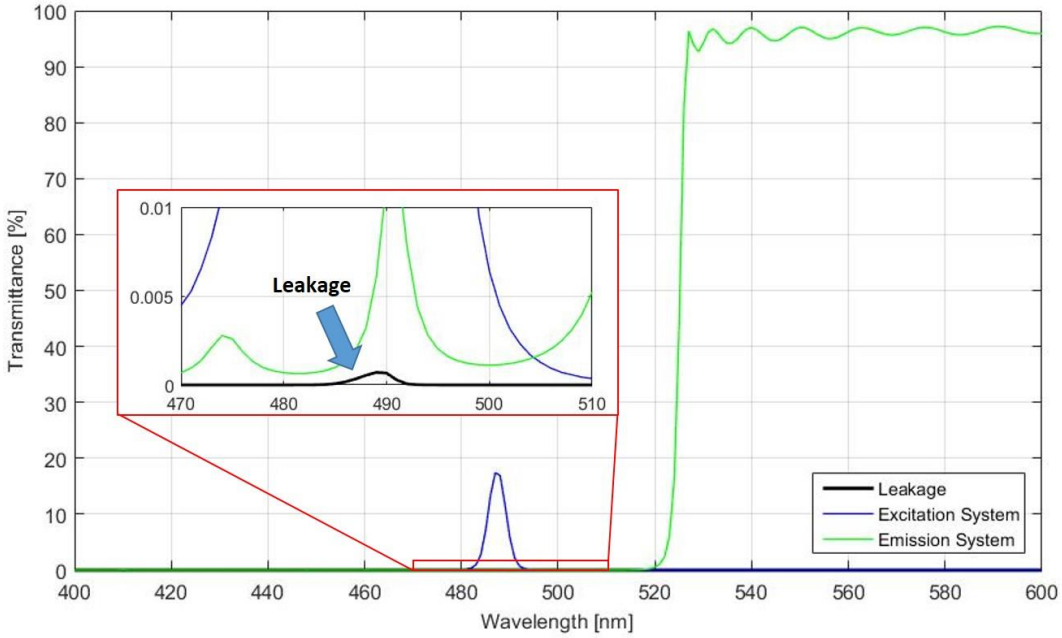

Figure 3.35: Point-wise multiplication of the excitation system and the emission system of Prototype 3 results in the Leakage Noise spectrum (thick black line). The leakage spectrum represents the optical power of the LED that is capable of transmitting through the entire design.

The optical power of the leakage noise is now $0.16\mu W$. Also, note that the majority of the spectrum in the leakage noise is well within the excitation spectrum (less than $500nm$) and far from the emission spectrum of PicoGreen. This means that the optics of the prototype are optimized to the best of what is readily available in the market. Comparing this to the optical power of a $1\mu g/mL$ sample of dsDNA in Figure 3.36 the following conclusions can be made about the design of Prototype 3.

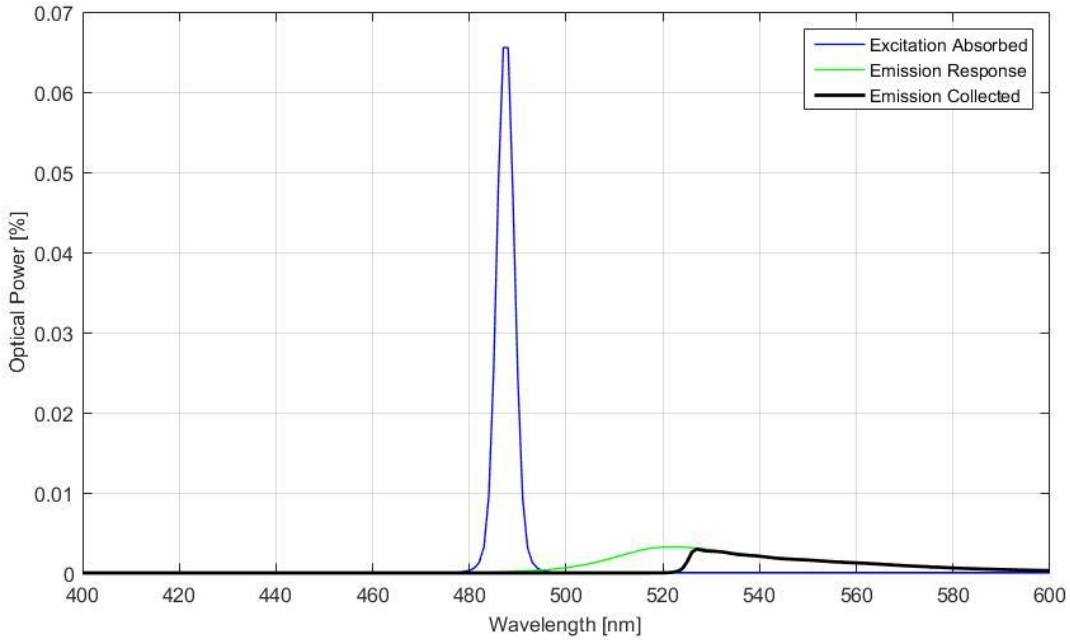

Figure 3.36: The comparison of the optical power that is absorbed by PicoGreen (blue), versus the optical power emitted by PicoGreen (green), and the amount of that emission spectrum that is captured by the emission collection system of Prototype 3 (black). When the reservoir device is filled with a $1\mu g/mL$ sample of λ-DNA.

The optical power of the emission collected spectrum in Figure 3.36 is $5.2\mu W$. The location of the emission spectrum captured by a $1\mu g/mL$ is above $520nm$ whereas the peak of the leakage noise spectrum is around $490nm$. This is significant because it gives the design confidence that any photon received above $520nm$ is almost certainly from excited PicoGreen and is not from the leakage noise. For the detection and calibration of dsDNA in the reservoir device shown in Figure 3.37, Figure 3.38, Prototype 3 was a highly optimized design.

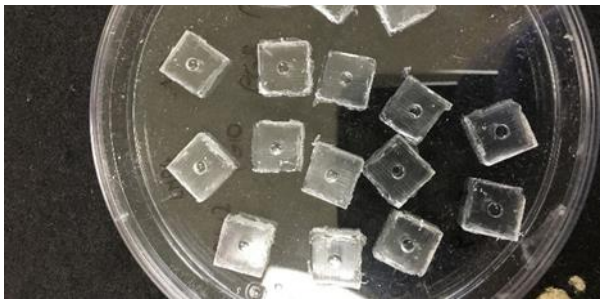

Figure 3.37: Micro-reservoir devices made of PDMS that were used to characterize the photodiode prototypes and the Sepsis Check

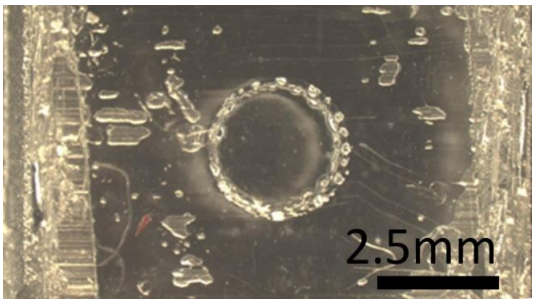

Figure 3.38: Micro-reservoir device made of PDMS

Moving forward the goal of the Sepsis Check was to provide a real time quantification of cfDNA in whole blood. An important aspect to this is the isolation of cfDNA from contaminants in whole blood by using

the cross channel device. The design of the photoresist and thus the design of the cross channel device was based off of Jun Yang's preliminary work on this project [6] shown below in Figure 3.39 and Figure 3.40.

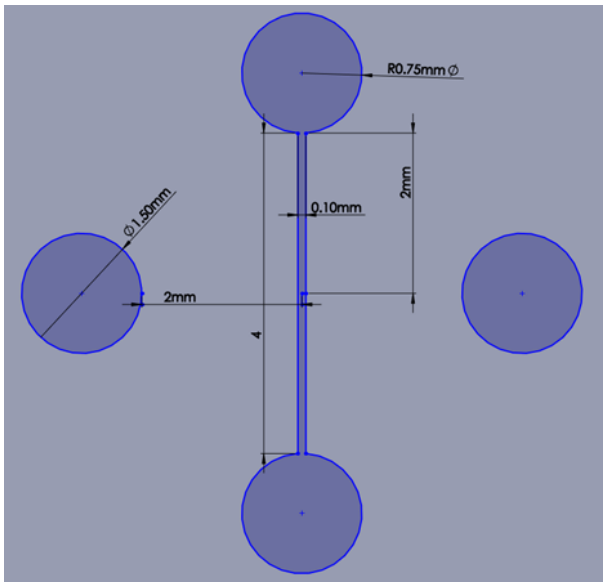

Figure 3.39: Dimensions of the sample channel in the microfluidic cross channel device. This layer was 60μm deep

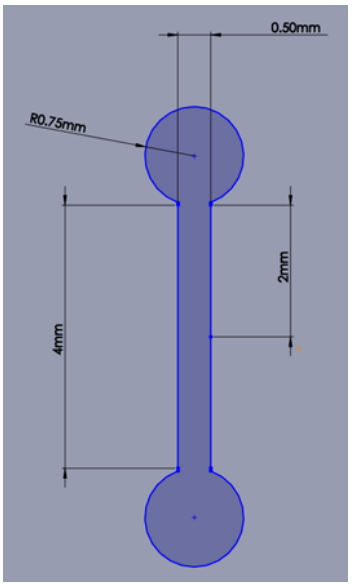

Figure 3.40: Dimensions of the accumulation channel in the microfluidic cross channel device. This layer was 160μm deep.

Prototype 3 was capable of accepting the cross channel device however preliminary experiments showed that a photodiode detection method was not well suited for detection of dsDNA accumulation in the intersection of the cross channels. The photodiode takes a singular optical intensity measurement of the entire area which causes a problem because some fluorescent PicoGreen will remain in the sample channel and not accumulate in the intersection. This will give a false signal to the photodiode that it cannot distinguish from a positive sample of accumulated dsDNA in the accumulation channel. Therefore, a final prototype revision was necessary to provide information to the user regarding the spatial information of the fluorescence. This final prototype utilized an imager system to solve this problem.

3.2.3 Imager Prototype

The Raspberry Pi camera used in conjunction with the image analysis software ImageJ provided the necessary spatial information to the user to define a region of interest to measure optical intensity. The final prototype is shown below in Figure 3.41.

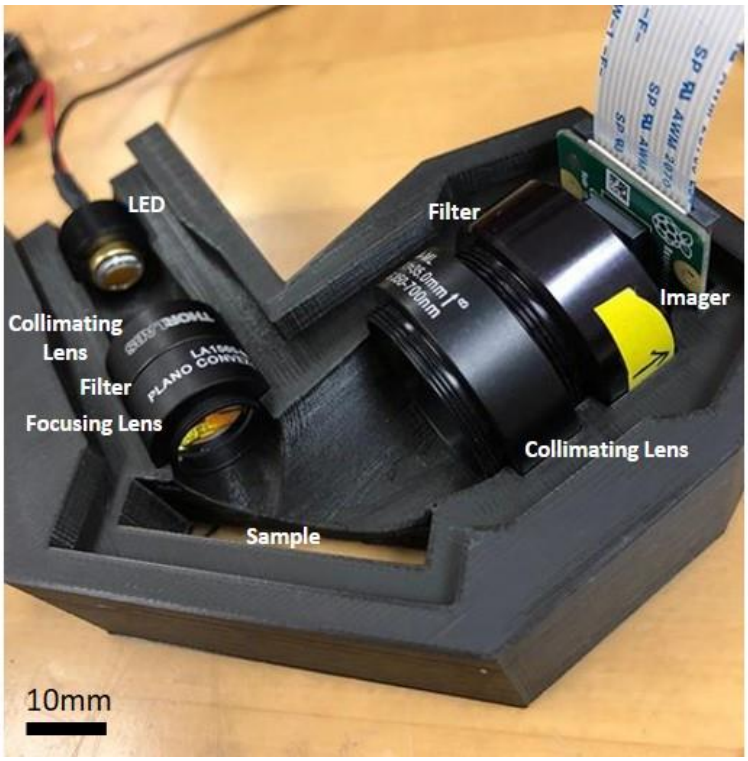

Figure 3.41: Cross section picture of the final Prototype of the Sepsis Check with a Raspberry Pi camera.

Changes in the final prototype allowed for incorporation of a Raspberry Pi camera imaging system. After adding the imager, it was noticed that the ball lens on the LED was non-uniformly diffusing the light across the device. Therefore a collimating lens was used to direct the light through the filter and then a focusing lens was used to focus the light on the cross channel. The second change was that the focusing lens for the emission collection system was removed. This is because the Raspberry Pi Camera has a focal length of infinity, therefore the camera will be in focus when collimated light hits the detector. To accomplish this, a single lens was used to collimate the light emitting from the excited PicoGreen sample. The list of optical components used in Prototype 4 are described below in Table 3.8. Finally the cost of the optical components of the final Prototype 4 were listed and summated to provide a total cost of the prototype in Table 3.9.

Table 3.8: Optical elements used in Prototype 4

EXCITATION SYSTEM		**EMISSION SYSTEM**	
OPTICAL ELEMENT	SPECIFIC CHARACTERISTIC	OPTICAL ELEMENT	SPECIFIC CHARACTERISTIC
LED470	$470nm$ Center Wavelength	LA1027-ML	Collimating Lens
LA1540-ML	Collimating Lens	84-744	$525nm$ Longpass Filter
FL05488-3	$488nm$ Bandpass Filter	Raspberry Pi Camera	Imager
LA1560-ML	Focusing Lens		

Table 3.9: All components of Prototype 4 including provider and cost

Component	**Specific Characteristic**	**Provider**	**Cost**
LED470	$470nm$ Center Wavelength	Thorlabs	$58.14
LA1540-ML	Collimating Lens	Thorlabs	$35.45
FL05488-10	Bandpass Excitation System Filter	Thorlabs	$48.20
LA1560-ML	Focusing Lens	Thorlabs	$33.66
LA1027-ML	Collimating Lens	ThorLabs	$46.41
84-744	$525nm$ Longpass Filter	Edmund Optics	$215.00
Raspberry Pi Camera	Imager	Amazon	$32.99
Raspberry Pi	Microcontroller	Amazon	$36.70
		Total:	$506.55

The combination of these optical elements maintains the optimization of the optical power in Prototype 3 but allows for the use of an imaging detection system. The combination of the elements in the excitation system make the spectrum shown in Figure 3.42.

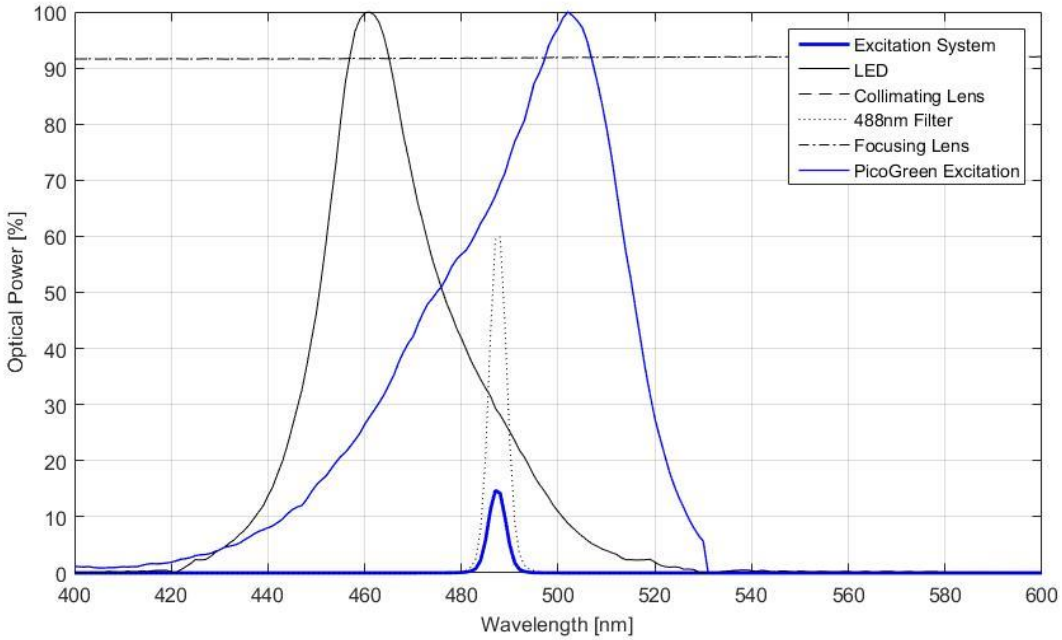

Figure 3.42: Comparison of the excitation system of Prototype 4 versus the absorption spectrum of PicoGreen [45], [34]. *The Excitation System (thick blue line) is the point-wise multiplication product of the LED (thin black line), the 488nm bandpass filter (dotted black line), and the two LA1540-ML lenses (dashed and dash-dot black lines). The PicoGreen absorption spectrum is shown as the thin blue line.*

Similar to Prototype 3, the excitation system blocks a significant amount of the optical power above $491nm$. The elements in the emission system of Prototype 4 combine to make the emission system in Figure 3.43.

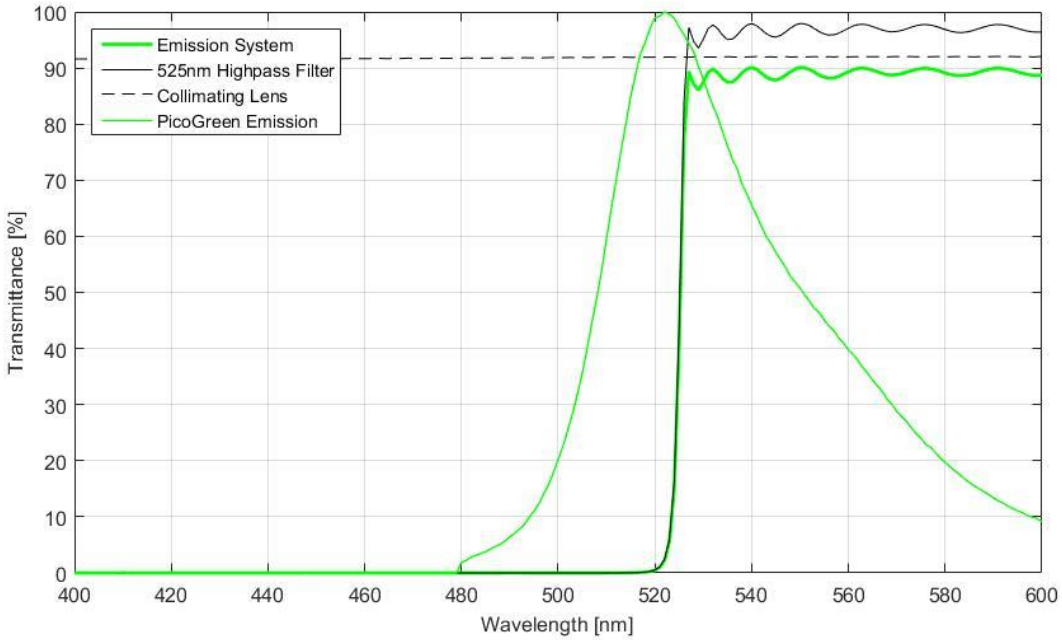

Figure 3.43: Comparison of the Emission System of Prototype 4 against the Emission spectrum of PicoGreen [47], [34]*. The Emission System (thick green line) is the combination of the* $525nm$ *longpass filter spectrum (black line) and the LA1540-ML lens (dashed black line).*

The leakage light from the excitation system that can transmit through the emission system is shown below in Figure 3.44.

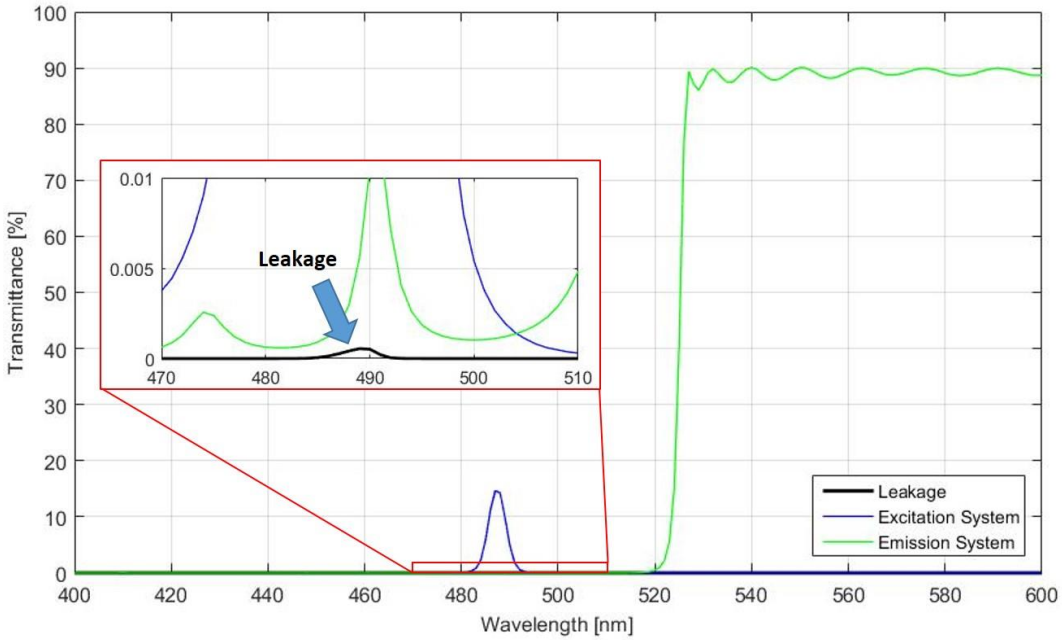

Figure 3.44: Point-wise multiplication of the excitation system and the emission system of Prototype 4 results in the Leakage Noise spectrum (thick black line). The leakage spectrum represents the optical power of the LED that is capable of transmitting through the entire design.

Prototype 4 does an excellent job at minimizing the leakage background signal from the excitation system. The optical power of the leakage noise of Prototype 4 is $0.127\mu W$. Just like Prototype 3, very little optical intensity from the excitation system can make it through the emission system. Comparing this to a $1\mu g/mL$ sample of dsDNA in the reservoir device in Figure 3.45.

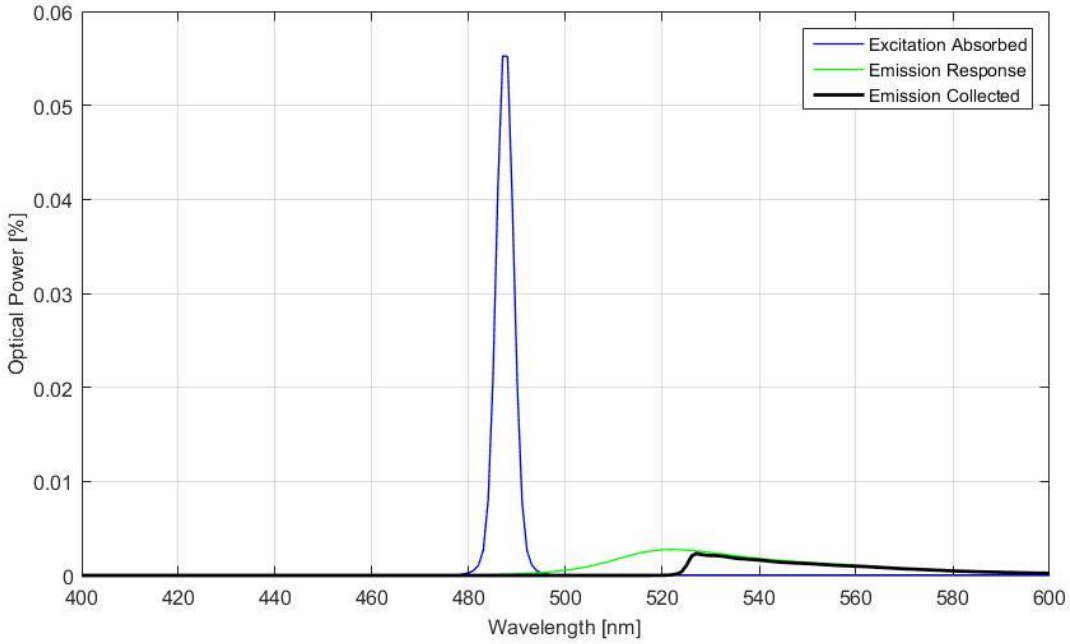

Figure 3.45: The comparison of the optical power that is absorbed by PicoGreen (blue), versus the optical power emitted by PicoGreen (green), and the amount of that emission spectrum that is captured by the emission collection system of Prototype 3 (black). When the reservoir device is filled with a $1\mu g/mL$ sample of $\lambda - DNA$.

3.2.4 Summary of the Sepsis Check Prototypes

Prototype 4 is the optimal design for the performance criteria chosen to model the design of the Sepsis Check. It is an ideal design for the excitation of PicoGreen dye and, in theory, shows that a sample with $1\mu g/mL$ is over 30x the optical intensity of any background noise that could be picked up by the detector. The summary of these theoretical calculations is shown below in Table 3.10.

Table 3.10: Comparison of the four Sepsis Check prototypes

PROTOTYPE	DEFINING IMPROVEMENT	LEAKAGE NOISE	$1\mu g/mL$ SAMPLE STRENGTH	SIGNAL TO NOISE RATIO
PROTOTYPE 1	Only LED in excitation	$4.54mW$	$0.15mW$	0.03
PROTOTYPE 2	Bandpass filter added to excitation system	$2.1\mu W$	$0.16\mu W$	7.81
PROTOTYPE 3	Longpass filter cut-on wavelength changed from $500nm$ to $525nm$	$0.16\mu W$	$5.2\mu W$	32.5
PROTOTYPE 4	Incorporation of imaging system	$0.13\mu W$	$4.1\mu W$	32.3

In total, the signal to noise ratio of Prototype 4 is very high in comparison with Prototypes 1 and 2. Prototype 3 also had a very high signal to noise ratio, however Prototype 4 is superior because it allows for the implementation of the cross channel devices that is necessary for separation of cfDNA from other materials in the blood. Therefore, in theory Prototype 4 will provided the optimal result for the performance criteria that was set for the design of the Sepsis Check. This improvement in the signal to noise ratio was also shown in the results from the various designs.

Chapter 4.

4 Results and Discussion

The design criteria stated in Chapter 3 provided a framework for the development of the prototypes. In this chapter, the development of successive generations of prototypes (as shown in Figure 4.1) that progressively meet the design criteria is presented.

First, experiments conducted with Prototype 2 are presented demonstrating the detection of a $20\mu g/mL\ \lambda - DNA$ sample in TE buffer in the reservoir devices. Next, Prototype 3 was characterized, where the $\lambda - DNA$ to PicoGreen mass ratio was optimized. The fluorescent response of the $\lambda - DNA$ sample in Prototype 3 was measured and found to be linear in the range of $1 - 20\mu g/mL$. Prototype 3 was also characterized using $\lambda - DNA$ spiked in healthy patient blood plasma and the response was also found to be linear. Finally, the accumulation and detection of $\lambda - DNA$ was shown in the cross channel device using Prototype 4.

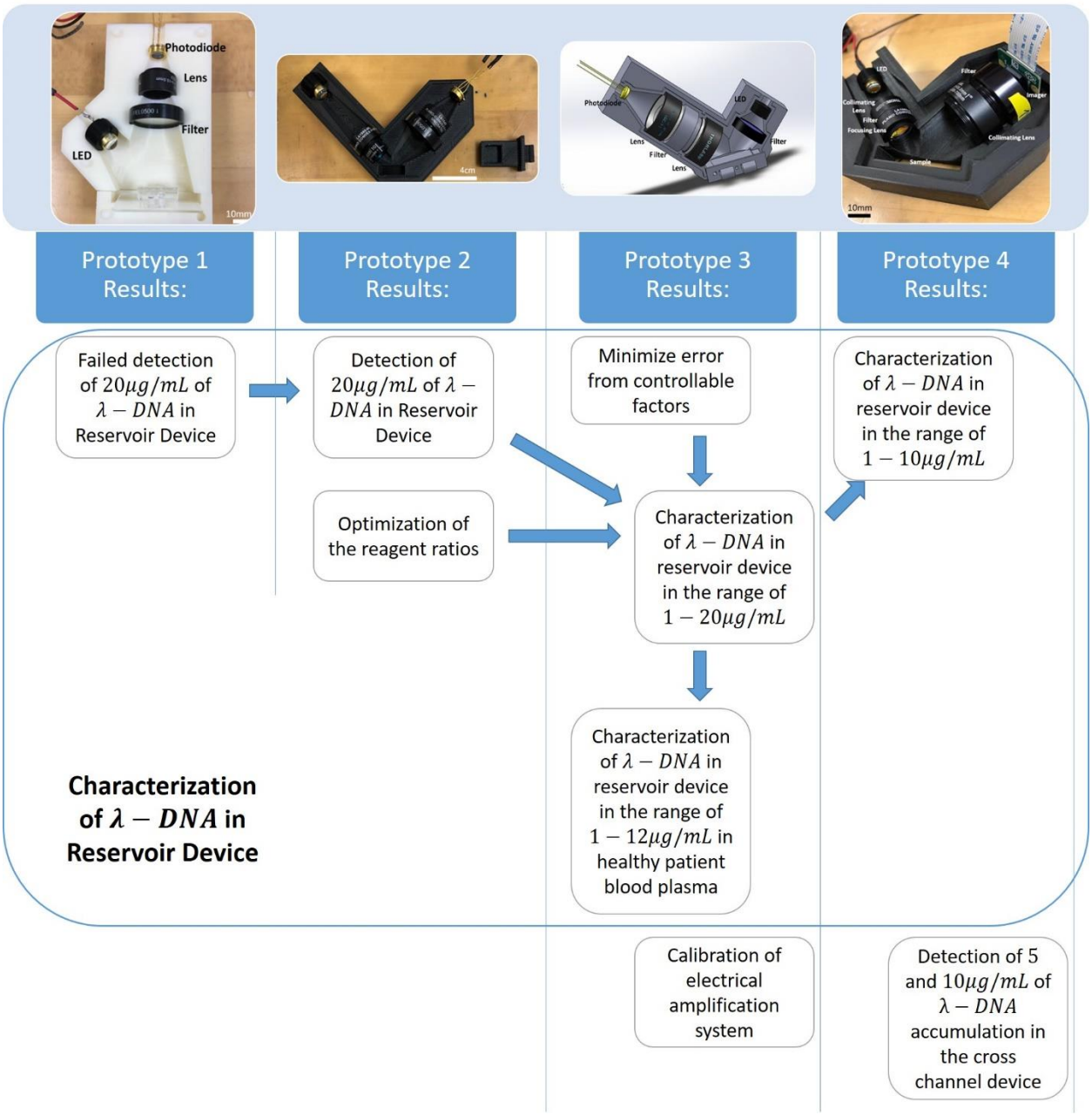

Figure 4.1: Development of the Sepsis Check prototypes and the results that were obtained with each prototype. Sequential arrows show the progress from a failed detection of $20\mu g/mL$ to characterization of $1 - 10\mu g/mL$ of $\lambda - DNA$ in Prototype 4 in the reservoir device as well as characterization of $1 - 12\mu g/mL$ of $\lambda - DNA$ in healthy patient blood plasma. Additional results were shown including the calibration of the electrical amplification system and the detection of accumulation of $5\mu g/mL$ and $10\mu g/mL$ of $\lambda - DNA$ in the cross channel device.

The goal of the Sepsis Check was to quantify cfDNA in whole blood with the cross channel dsDNA separating microfluidic device in a handheld PoC system. The reservoir devices were used in order to control the mass of DNA present in each measurement so that linear calibration of DNA concentration

could be performed. Initial characterization and testing was performed on $20\mu g/mL$ of $\lambda - DNA$ in TE buffer because $20\mu g/mL$ was the maximum concentration of cfDNA measured in severely septic patients [5].

4.1 Prototype 1 Results

In order to characterize the concentration of DNA in the reservoir devices for sample solutions were prepared. Three of which contained $5\mu L$ of $\lambda - DNA$ at a concentration of $20\mu g/mL$ and one of them was a control with no $\lambda - DNA$. All four samples contained $5\mu L$ of 200x diluted PicoGreen dye as per the specification sheet instructions. The goal of this experiment was to detect $20\mu g/mL$ of $\lambda - DNA$ in the reservoir device as a preliminary result before attempting to characterize the fluorescence intensity with the concentration of $\lambda - DNA$. The results are shown in Figure 4.2.

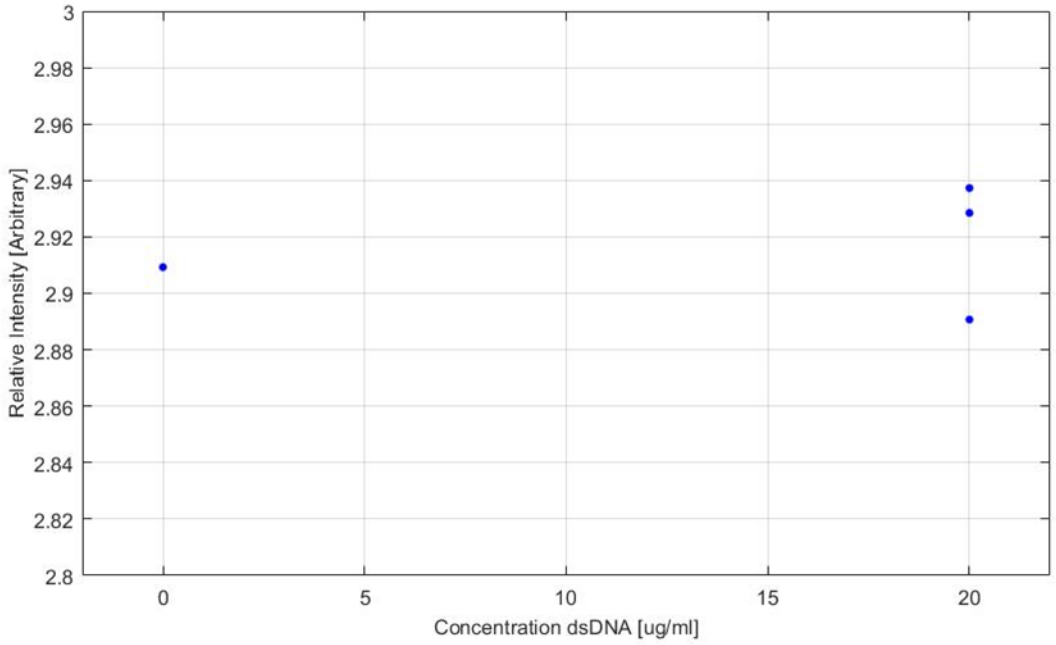

Figure 4.2: Comparison of the optical intensity from three $20\mu g/mL$ of $\lambda - DNA$ samples in the reservoir devices against a background sample that contained no $\lambda - DNA$. All samples contained the same concentration of PicoGreen dye.

The results show that there was no statistical difference between the $20\mu g/mL$ $\lambda - DNA$ samples and the background sample. The 3D printed housing was printed out of off-white ABS which is partially transparent. Light from the LED was visible from the outside of the device during testing. This suggested that light from the LED and even the lights in the ceiling could transmit through the housing unit to the photodiode. The spectrum of light from the ceiling is broad and includes wavelengths in the sensitive range of the emission collection system. Similarly, the LED emits photons across a spectrum of

wavelengths with a FWHM of $22nm$. With this range there was a significant amount of optical power with wavelengths longer than $500nm$ that transmitted through the emission collection system to the photodiode causing a high background signal.

4.1.1 Reducing Background

Prototype 1 used a photodiode as the sensor which inherently has a dark current associated with the spontaneous generation of charge carriers. The dark current which serves as the limit of detection can be measured as the current output of the photodiode when there is zero optical power contacting the junction. The dark current of the FDS100 photodiode was tested to be about $1nA$. The goal of this experiment was to decrease the background noise to as close to the dark current as possible.

To test the hypothesis that light from the environment was leaking through the optical housing unit and contacting the photodiode junction the 3D printed ABS was covered with opaque tape. This blocked light from transmitting through and reaching the photodiode. The experiment was conducted with reservoir devices. The results from this experiment are shown below in Figure 4.3.

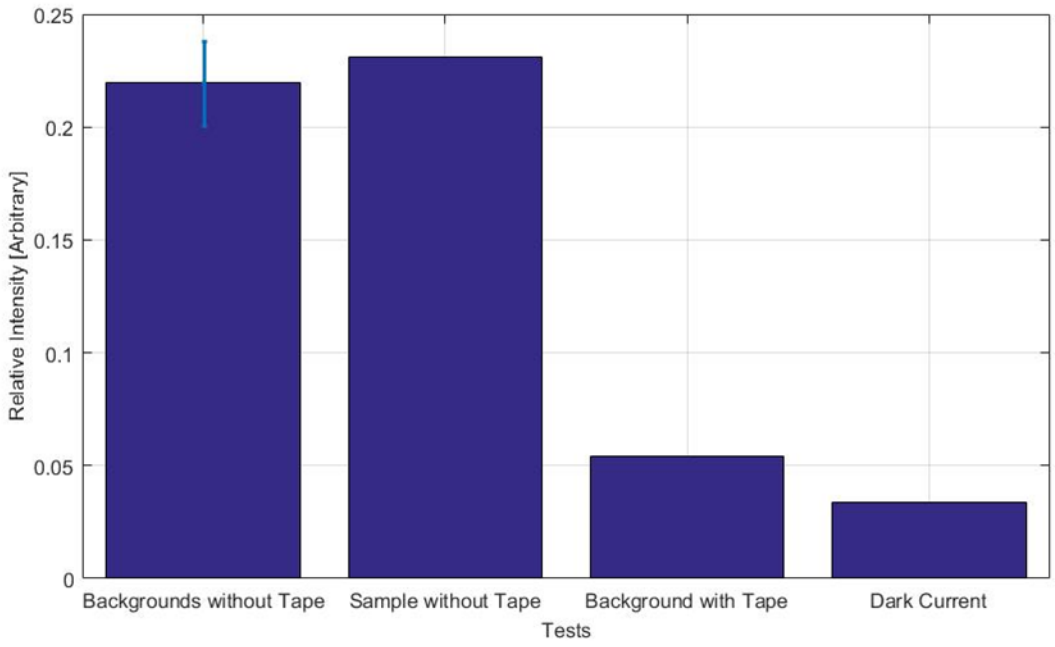

Figure 4.3: Results showing that the original Prototype 1 could not differentiate between a blank sample (Backgrounds without Tape) and a $20\mu g/mL$ sample (Sample without Tape). When Prototype 1 was modified by covering it with opaque tape the background (Background with Tape) was reduced close to the dark current (Dark Current).

When a sample was measured with a transparent Prototype 1 housing unit, both the background sample and the sample with $\lambda - DNA$ was over 4x the strength of the dark current of the FDS100 photodiode.

Furthermore, when tape was not used, a $20\mu g/mL$ sample of $\lambda - DNA$ was not statistically different from the background samples ($p\ value = 0.2676$). The effect of making the housing unit of Prototype 1 opaque decreased the background signal by approximately 3x near the strength of the dark current. This change was implemented in the design of Prototype 2 by using black 3D printed ABS material which replaced the original off-white ABS.

4.2 Prototype 2 Results

Prototype 2 was made with black 3D printed ABS to reduce stray light and its impact on the background noise. A $488nm$ bandpass filter with a $10nm$ FWHM and a focusing lens were added in the excitation system to reduce the intensity of the excitation system above $500nm$. The bandpass filter was designed to greatly reduce optical power of the LED above $493nm$ from transmitting through to the photodiode. A focusing lens was also added to the excitation system to focus the light from the LED onto the sample.

4.2.1 Characterization of $\lambda - DNA$ in TE Buffer in Reservoir Devices

The response of Prototype 2 was characterized using samples with various DNA concentrations in order to develop a calibration curve that could be used to estimate the concentration of DNA in an unknown sample. Serial dilutions of DNA were prepared between $0.08\mu g/mL$ and $50\mu g/mL$. Each sample contained $5\mu L$ of $\lambda - DNA$ and $5\mu L$ of PicoGreen diluted as per the standard sample preparation procedure described in Chapter 3. Three samples at each DNA concentration were sequentially loaded into the reservoir devices and measured with Prototype 2. The resultant characterization plot is shown below in Figure 4.4.

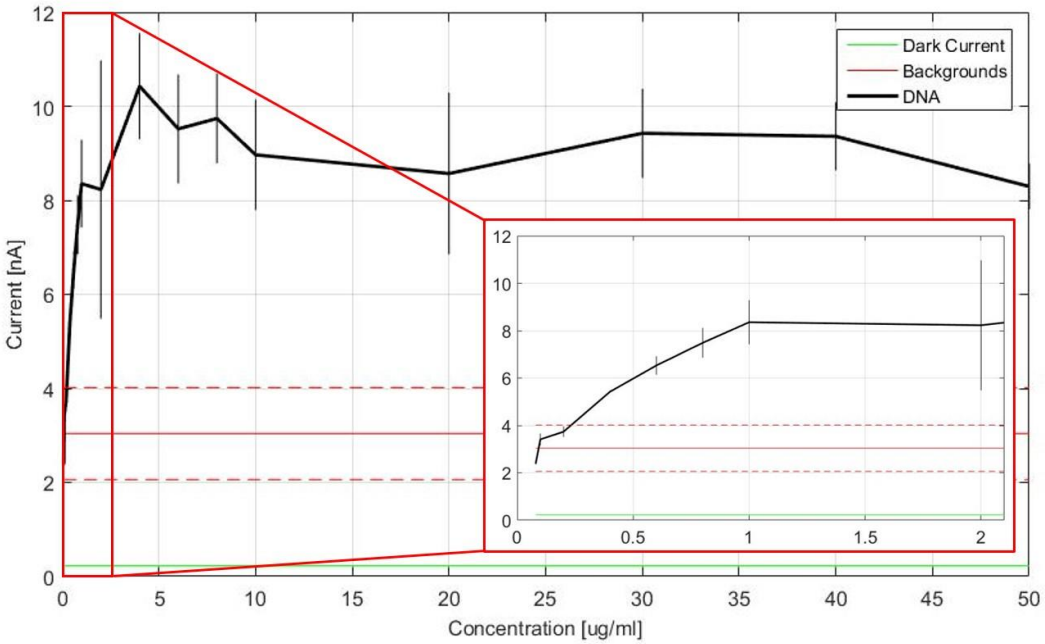

Figure 4.4: Characterization from $0.08\mu g/mL$ to $50\mu g/mL$ in Prototype 2. Error bars represent standard deviation. Sample size n=3.

From the insert of the graph in Figure 4.4 a linear relationship between the concentration of DNA and the current output of the photodiode can be seen at lower concentrations. However, the measured signal saturates at higher concentration above $1\mu g/mL$. These results were compared against the same characterization conducted with the reservoir devices in the fluorescence microscope available in the lab in Figure 4.5.

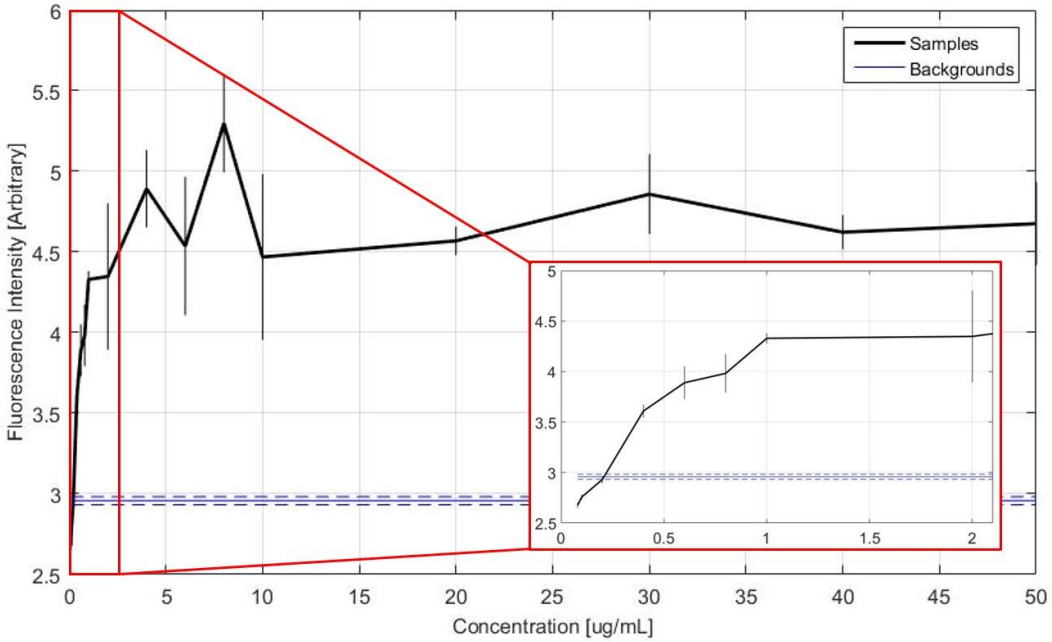

Figure 4.5: Characterization of $\lambda - DNA$ from $0.08\mu g/mL$ to $50\mu g/mL$ in the reservoir device with the fluorescence microscope. Error bars represent standard deviation. Sample size $n = 3$.

The results from the characterization experiment show a relatively linear relationship between $\lambda - DNA$ and the fluorescence intensity from 0 to $1\mu g/mL$ in both Prototype 2 and the fluorescence microscope. However, above $1\mu g/mL$ the fluorescence intensity appeared to saturate. The saturation of the signal could be a result of an unoptimized combination of the PicoGreen dye with the DNA present in the solution. Therefore, various ratios of these mixtures were tested to determine the appropriate concentration of the dye for the intended application.

4.2.2 Variable PicoGreen Dilutions

Since the concentration of DNA in the sample varies from below $1\mu g/mL$ to $10\mu g/mL$, it is important to identify a suitable concentration of PicoGreen dye to be added to the reservoir to ensure that 1) the DNA is clearly visible and 2) that the mass ratio of DNA to PicoGreen does not affect the quantification process. Therefore, various concentrations of PicoGreen were tested. The standard PicoGreen dilution ratio according to the specification sheet should be 200x, therefore PicoGreen dilutions of 200x, 20x, and 2x were prepared. Samples with $25\mu g/mL$ and $50\mu g/mL$ of $\lambda - DNA$ were mixed with the various PicoGreen concentrations for comparison. The fluorescence intensity was captured with both the Sepsis Check and fluorescence microscope and the results are shown below in Figure 4.6 and Figure 4.7.

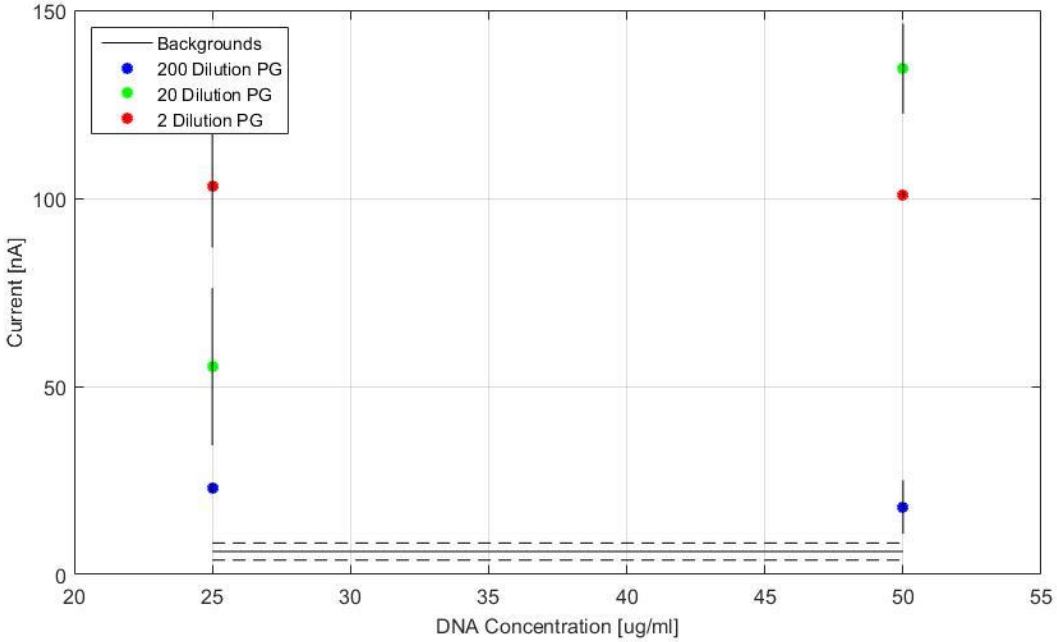

Figure 4.6: Effect of changing PicoGreen concentration on the fluorescence intensity of a $25\mu g/mL$ and $50\mu g/mL$ sample in the Sepsis Check. Error bars represent standard deviation. Sample size $n = 3$.

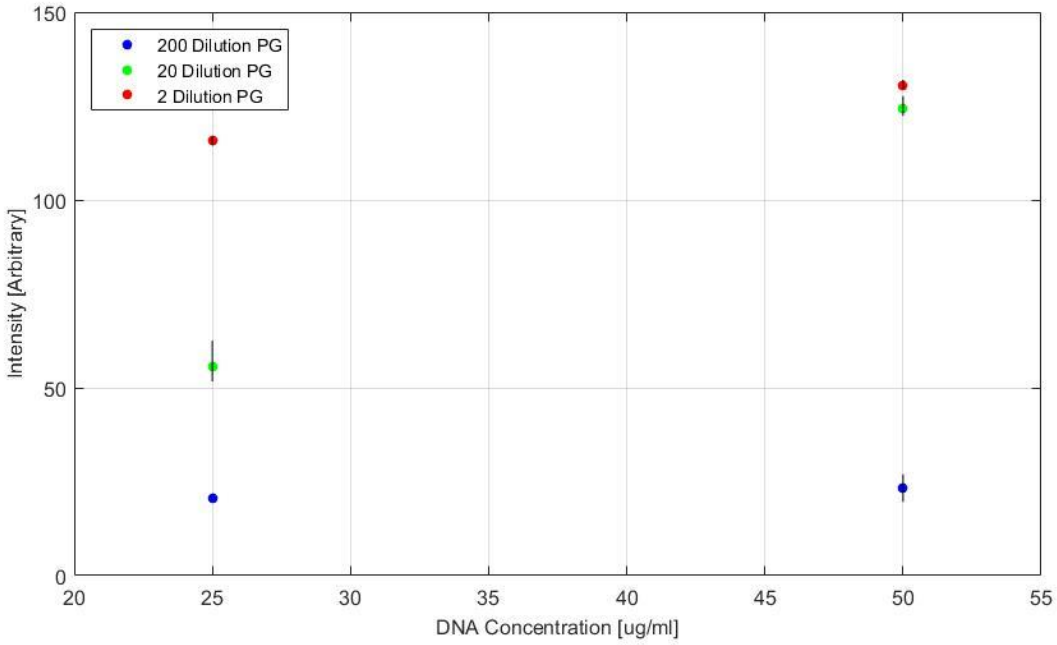

Figure 4.7: Effect of changing PicoGreen concentration on the fluorescence intensity of a $25\mu g/mL$ and $50\mu g/mL$ sample in the reservoir devices with the fluorescence microscope. Error bars represent standard deviation. Sample size $n = 3$.

Changing the PicoGreen concentration had a significant effect on the fluorescence intensity in the reservoir devices. The 200x and 2x diluted PicoGreen showed no significant difference in fluorescence

intensity between $25\mu g/mL$ and $50\mu g/mL$. However, the 20x diluted PicoGreen showed a much higher signal from the sample containing $\lambda - DNA$ at a concentration of $50\mu g/mL$ compared with the sample containing $\lambda - DNA$ at a concentration of $25\mu g/mL$. This shows that the concentration of the PicoGreen dye could have been the causative reason for the saturation of signal at concentrations of DNA above $1\mu g/mL$ in the characterization experiment in Prototype 2 and as such a PicoGreen dilution of 20x should be used instead of 200x.

Although a linear response was not obtained during the experiment with Prototype 2 in Figure 4.5, it was still able to detect $\lambda - DNA$ in concentrations as low as $0.6\mu g/mL$. These results provide confidence to suggest that Prototype 2 was in fact capable of characterizing the DNA concentrations with signal output from the photodiode, so experimentation on the third prototype was initiated.

4.3 Prototype 3 Results

Based on the measurements and observations from Prototype 2, a new Prototype 3 was developed which incorporated improved optics with an additional lens, narrower excitation bandpass filter, more sensitive photodiode, and a longpass filter with a cut-on wavelength of $525nm$ instead of $500nm$. In addition, it could be used to measure intensity using both the reservoir and cross channel devices. In total the changes allowed Prototype 3 to perform characterization of fluorescence intensity in the reservoir device and DNA accumulation in the cross channel device with higher sensitivity in order to meet the design criteria described in Chapter 3.

The first experiment conducted using Prototype 3 was the characterization experiment to determine whether the response of the system was linear and proportional to the concentration of $\lambda - DNA$ in the sample. With prototype 1, this was not possible due to high background noise. Prototype 2, showed the potential, however the experimental procedure was flawed and the ratio of PicoGreen to DNA was found to be insufficient. In addition, the standard deviation of each concentration was found to be significantly large. Prototype 3 and the experimental procedure were both refined to provide higher sensitivity and decreased error. The experimental procedure was conducted as follows: $5\mu L$ of $\lambda - DNA$ at concentrations that varied from $1\mu g/mL$ to $20\mu g/mL$ were loaded into the reservoir devices with $5\mu L$ of 20x diluted PicoGreen dye. The dye was mixed well with the DNA and allowed to intercalate before the reservoir was loaded into Prototype 3. The resultant electrical signal from the photodiode was recorded and is displayed against the DNA concentration in Figure 4.8.

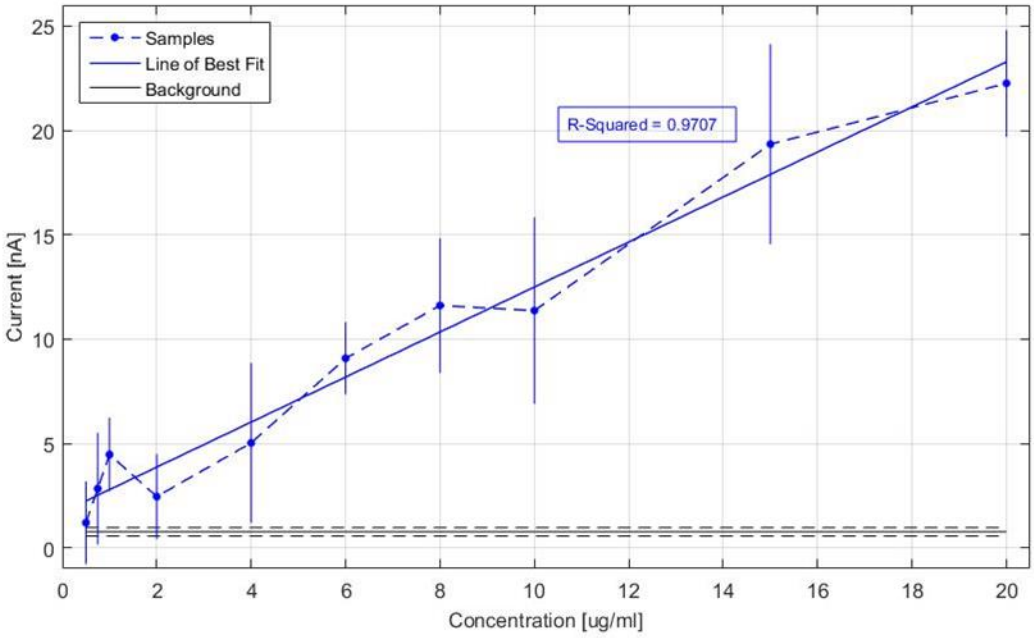

Figure 4.8: Characterization of Prototype 3 from less than $1\mu g/mL$ to $20\mu g/mL$. Error bars represent standard deviation. Sample size of $n = 6$.

Prototype 3 showed a linear relationship between the concentration of $\lambda - DNA$ in TE buffer and the current output of the photodiode from less than $1\mu g/mL$ to $20\mu g/mL$ with a R^2 value of 0.97. This relationship was then tested in blood plasma from healthy patients.

4.3.1 Characterization of Prototype 3 using Spiked Plasma

The Sepsis Check was characterized using blood plasma as an intermediate step towards testing in whole blood. Plasma introduces additional complications such as the presence of proteins and electrolytes that could interfere with the measurement. For instance, the plasma is yellow and partially opaque which could block some of the fluorescence intensity from excited PicoGreen that is deep in the sample. The plasma samples were provided by another research project: DNA as a Prognostic Marker in ICU Patients Study, Clinical Trials (DYNAMICS, government identifier: NCT01355042). In that study, plasma and clinical data was collected from septic and non-septic critically ill patients at nine study sites. For each of the patients, data on cfDNA levels and clinical outcomes were available. The results of this experiment are presented below in Figure 4.9 in comparison with the characterization experiment conducted in TE buffer.

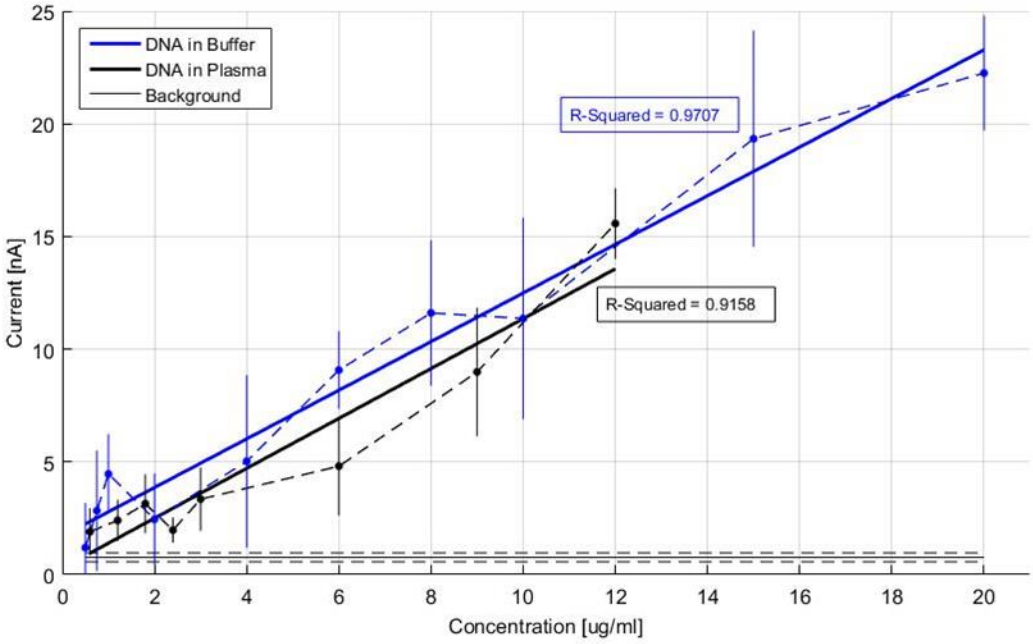

Figure 4.9: Characterization experiment of $\lambda - DNA$ in healthy patient plasma vs $\lambda - DNA$ in TE buffer. Error bars represent standard deviation. Sample size $n = 6$.

The characterization in healthy blood plasma showed a linear relationship with the same slope as the characterization in TE buffer. The linear correlation is still high ($R^2 = 0.92$) and the statistical difference of a sample at a concentration of $1\mu g/mL$ from the background noise is significant ($p\ value < 0.001$). Comparing the two linear fits, the optical intensity obtained from plasma is approximately $1.25nA$ lower than in TE buffer regardless of the concentration of DNA. This means that the decrease in optical intensity was caused by a factor that is independent of the DNA concentration. Each plasma sample contained $3\mu L$ of plasma, regardless of the DNA concentration. The protein contents in the plasma could have absorbed a portion of the excitation and emission photons thus causing a relatively constant reduction in response. This hypothesis requires further testing and validation in future experiments.

Further experiments with septic patient samples need to also be pursued using plasma or isolated DNA samples. The $\lambda - DNA$ utilized for characterization in buffer or spiked in plasma in the previous results consists of dsDNA with a base pair length from $125bps$ to $23.1kbps$ [34]. The cfDNA produced by NETosis in septic patients is primarily between $150bps$ to $300bps$. While this difference in strand length does not change the concentration of DNA in terms of mass per volume, it has been shown that intercalation of a dye into a DNA duplex substantially increases the DNA inter-base pair distance and thus the total DNA length [52]. When dealing with short strands of dsDNA this increase in strand length can be negligible, but

in much longer strands nearly 100 fold longer in length, the increased strand length could lead to a higher PicoGreen to DNA mass bonding ratio and thus a stronger fluorescence for the same concentration of DNA [52]. This could theoretically limit the accuracy of a characterization plot of $\lambda - DNA$ when comparing against cfDNA. To test this limitation, $\lambda - DNA$ could be cut to shorter lengths prior to characterization to better simulate cfDNA in whole blood.

Another characteristic of the plasma characterization experiment was that the error bars (that represent the standard deviation) for each concentration were large and had a clear impact on the sensitivity. Therefore a test was conducted to see if this was from experimental variations introduced due to handling of the samples, or if it is inherent to the measurement setup itself.

4.3.2 Repeatability Test

A repeatability test was conducted with ten samples at a concentration of $2.5\mu g/mL$ and ten samples at $10\mu g/mL$. The purpose of this was to determine if the error was correlated with DNA concentration and thus an inherent error. The results are shown below in Figure 4.10.

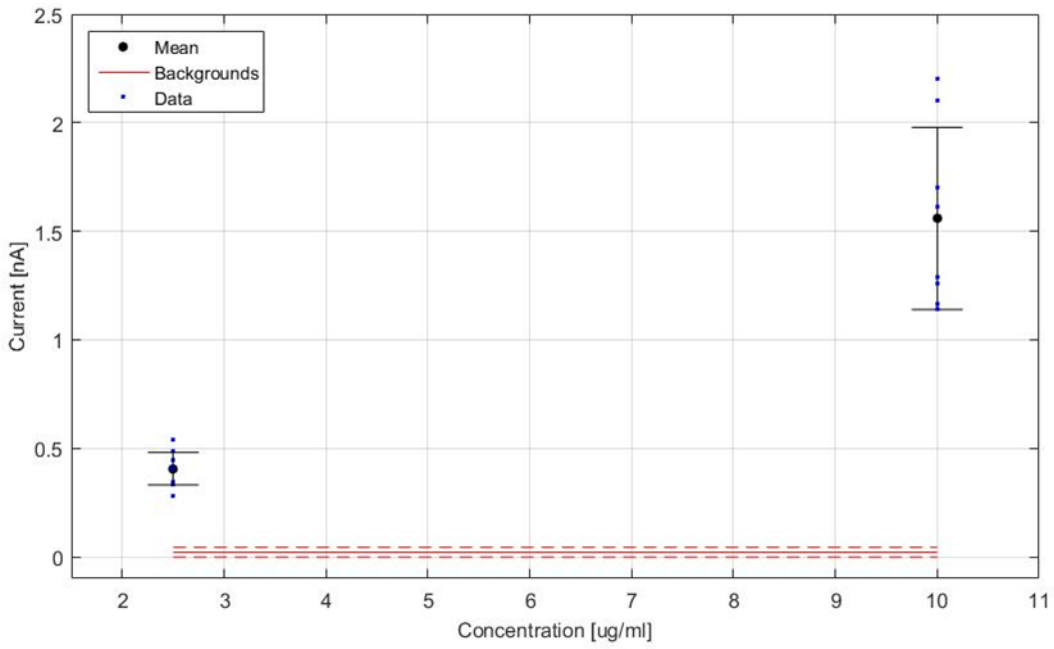

Figure 4.10: Reliability experiment where 10 samples at $2.5\mu g/mL$ are compared against 10 samples at $10\mu g/mL$ in Prototype 3 in the reservoir devices. Error bars represent standard deviation. Sample size $n = 10$.

The results show that the variation in the data is correlated to the concentration of DNA in the sample. Therefore the cause of the variation must come from the sample preparation. If the volume pipetted was off by $\pm 0.1\mu L$ then it would cause a greater change in the mass of DNA at higher concentrations. This

explanation fits with the increasing error and thus could be the source. Furthermore, this shows that the characterization experiment in Prototype 3 could still be improved by tightening up the experimental protocol and decreasing the error in the lower concentration samples.

Nevertheless, these results confirm that the optical system is robust enough to measure the difference in DNA levels within the range of interest in realistic samples. With these results the next step of the Sepsis Check prototype design process was to ensure that these small electrical signals that are being detected using the Keithley 2410 source meter can be detected in a PoC handheld device. Therefore the amplification circuit was calibrated to be able to convert the nA current signals to a voltage signal that can be detected by the microcontroller.

4.3.3 Characterization of the Electrical System

The amplification circuit was an integral component of the photodiode prototypes. The amplification circuit was necessary because the current output of the FDS100 and 84-612 photodiodes were in the range of $1 - 30nA$. This current range was measurable during preliminary testing because the Keithley 2410 source meter that was used is a highly accurate instrument with a LoD of $50pA$ [49]. Since this was also expensive, a circuit was designed to replace the Keithley and serve as a low cost handheld device specific for the quantification of low current signals. This nano-amp measurement circuit was calibrated by generating a source signal in the range of $1 - 100nA$ using the Keithley 2410. This current (signal) was amplified using a commercially available current to voltage amplifier (μCurrent Gold) which is capable of converting $1nA$ to $1mV$. The transformed voltage signal was provided to a two stage op-amp circuit with a buffer circuit to amplify the signal by two orders of magnitude (from $1mV$ to $100mV$). The characterization results comparing the input ($1 - 100nA$ current signal) to the output ($0.1V$ to $10V$) of the nano-amp circuit is shown below in Figure 4.11.

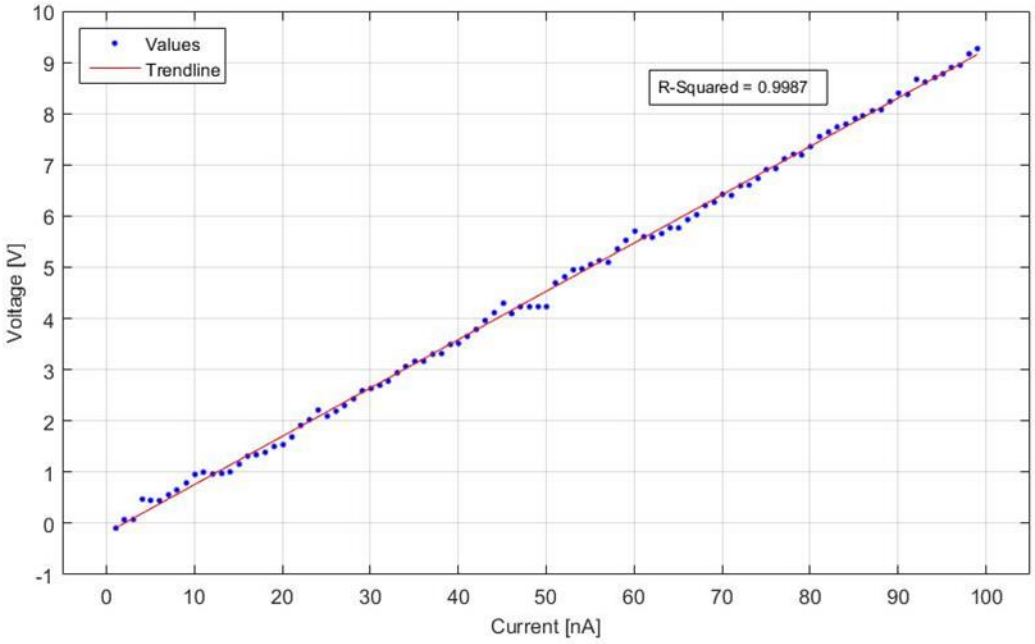

Figure 4.11: Amplification of $1-100nA$ to $0.1-10V$ by the electrical amplification system

This result show a highly linear relationship between the current input and the voltage output of the device with an $R^2 > 0.99$. In practice the amplification system is capable of amplifying the photodiode output which ranges from $1-30nA$ to a voltage signal from $0.1-3V$. The Arduino microprocessor has an analog range of $0-5V$ with 8-bit resolution. This correlates to a resolution of $0.005V$ which correlates to a current resolution of $0.05nA$ or $50pA$ similar to the Keithley 2410 source meter.

These results demonstrate that the optical system designed with a photodiode as the detector works well for the reservoir devices. It can quantify the concentration of DNA with optical intensity received by a photodiode. However the optical intensity received by the photodiode is actually correlated to the total mass of excited PicoGreen inside the reservoir. Since the volume of the sample is constant in the reservoir device, its fluorescence intensity can be correlated to the concentration of the sample. This is not the case with the Cross Channel devices.

4.3.4 Cross Channel Detection of $\lambda - DNA$

Detection of $\lambda - DNA$ in the cross channel is more difficult because PicoGreen is distributed non-uniformly throughout the cross channels. In the cross channel device, the correlating factor between DNA concentration and optical intensity is the accumulation of DNA in the agarose gel at the intersection of

the channels. The intersection of the cross channel is the area of interest and is labelled in Figure 4.12 b) below.

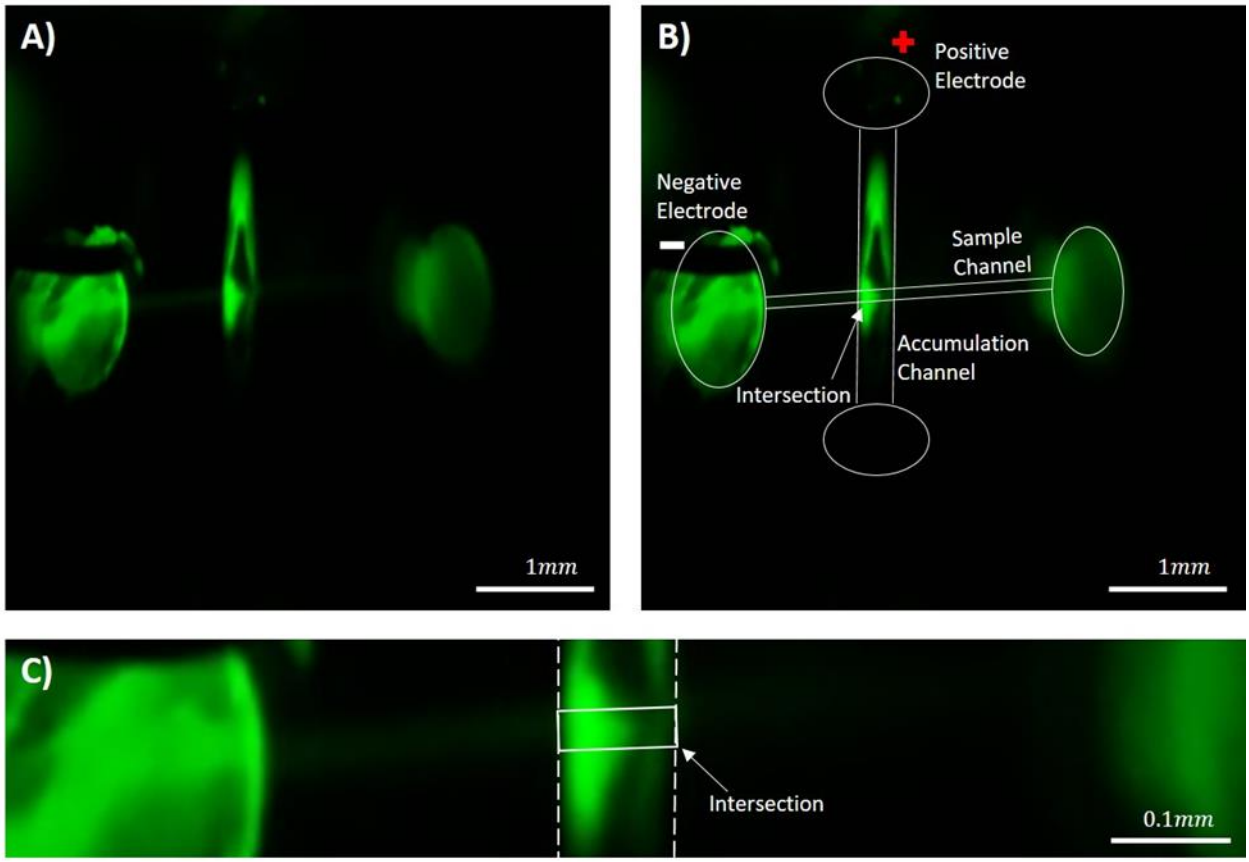

Figure 4.12: The accumulation of $5\mu g/mL$ of $\lambda - DNA$ at the channel intersection. A) An unlabeled picture of the cross channel device after 5 minutes of $5\mu g/mL$ of $\lambda - DNA$ accumulating at the intersection showing the presence of DNA in the sample channel reservoirs which were used to load the DNA into the device as well as the accumulation channel. B) A labelled version of the same picture showing the reservoirs and the geometry of the cross channel device. C) Magnified picture showing the area of interest: the intersection of the accumulation and sample channels. The optical intensity in the intersection is correlated to the concentration of DNA.

The concentration of DNA in the sample channel is correlated to the optical intensity perceived at the intersection of the channels as a result of gel electrophoresis. With this in mind, the use of a photodiode for detection of accumulation may not be suitable as the signal generated is a summation of the fluorescence intensity from the entire device which remains constant throughout the gel electrophoresis procedure. The significance of this is demonstrated below in Figure 4.13.

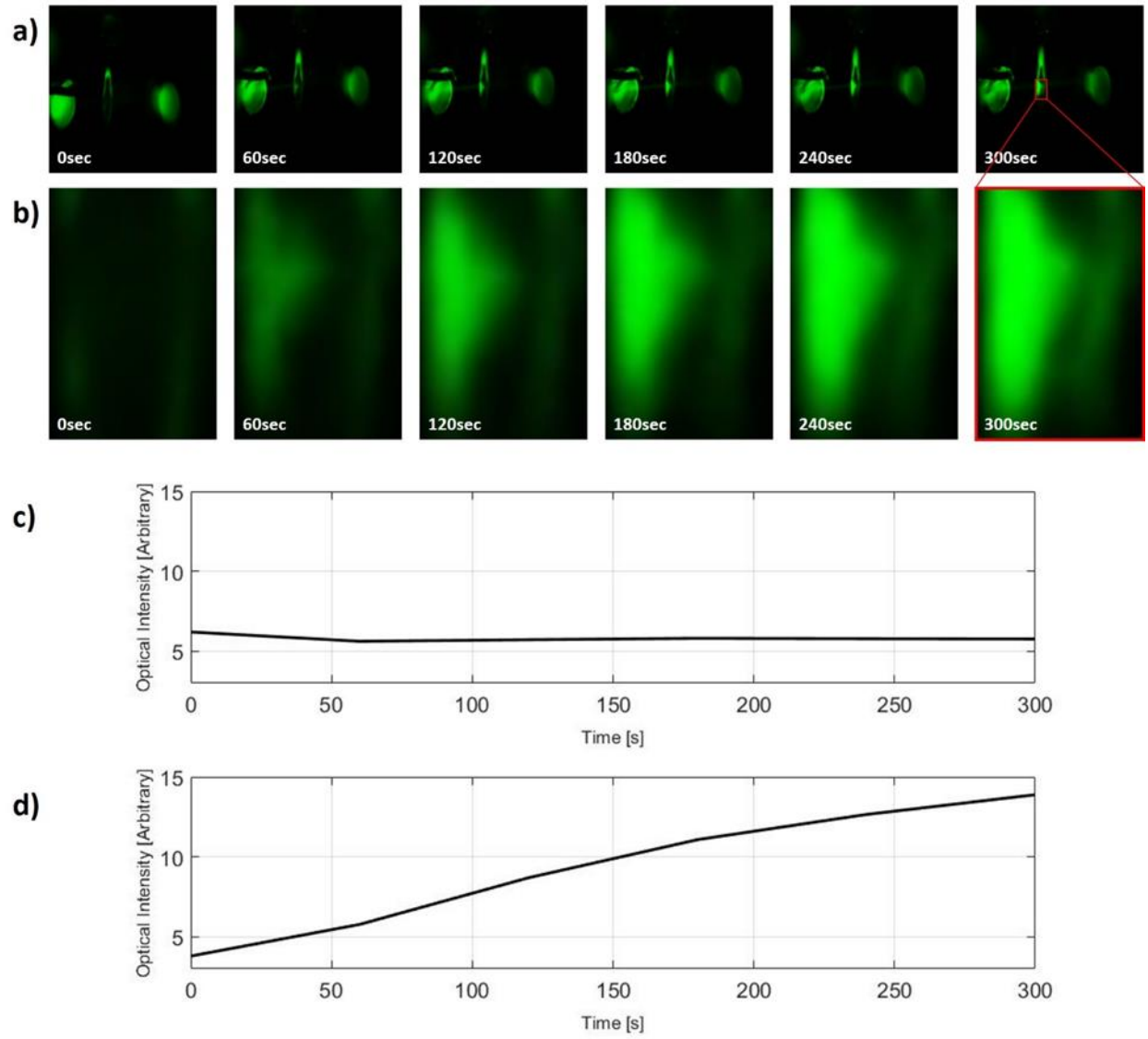

Figure 4.13: Demonstration of the importance of the imager design and why the photodiode design does not work with the cross channel devices. In A) accumulation of $5\mu g/mL$ of $\lambda - DNA$ on the intersection of the cross channels is demonstrated in a wide field of view. B) Shows a magnified image of the intersection of the channels which is the area of interest. C) Shows a plot of the average intensity of the images in A) over five minutes of gel electrophoresis. D) Shows the average optical intensity of the images in B) at the intersection of the channel over five minutes.

The accumulation of dsDNA at the intersection of the cross channel can be seen in Figure 4.13 A) and magnified in Figure 4.13 B). Initially (at $t = 0$) the vertical accumulation channel was absent of dsDNA and after one minute of gel electrophoresis with 9V dsDNA can clearly be seen accumulating in the agarose gel at the intersection of the channels. The photodiode in Prototype 3 measures the optical intensity of the entire device including: the inlet and outlet of the sample channel, the sample channel itself, the intersection of the channels, and the accumulation channel. As a result the measurement taken by Prototype 3 does not change over the five minute accumulation as shown in Figure 4.13 C). This is because

DNA is migrating from the sample channel into the accumulation channel and thus the total mass of DNA is not changing over time. By combining the photodetector imaging system with an image processing program an area of interest can be selected similar to how the intersection was magnified in Figure 4.13 B). An example of the selection of the area of interest is shown in Figure 3.19. The result is that accumulation of dsDNA at the intersection of the cross channels can be detected and measured. The result of the average intensity of the intersection is shown in Figure 4.13 D). This result shows the limitations of the photodiode in Prototype 3 and was the reason for moving to a fourth prototype that used an imaging detector.

4.4 Prototype 4 Results

In Prototype 4, the photodiode was replaced by a photo-imager. The settings for the imaging prototype removed the automatic white balancing, had a shutter speed of $50ms$, and custom sharpness, brightness, and saturation settings which are described in further detail in the Appendix.

The purpose of this prototype was to demonstrate that fluorescent intensity at specific locations of the device can be measured. Initial characterization was performed in the reservoir devices and then in cross channel devices.

4.4.1 Characterization of $\lambda - DNA$ in the Reservoir Devices

The purpose of this experiment was to demonstrate that the fourth prototype was able to linearly characterize the optical intensity from $\lambda - DNA$ in TE buffer as was done with Prototypes 1, 2, and 3. Again $5\mu L$ of $\lambda - DNA$ at various concentrations and $5\mu L$ of PicoGreen at a dilution ratio of 20x were loaded and mixed thoroughly in the reservoir devices. Each concentration was repeated three times. A single sample of each concentration is shown below in Figure 4.14.

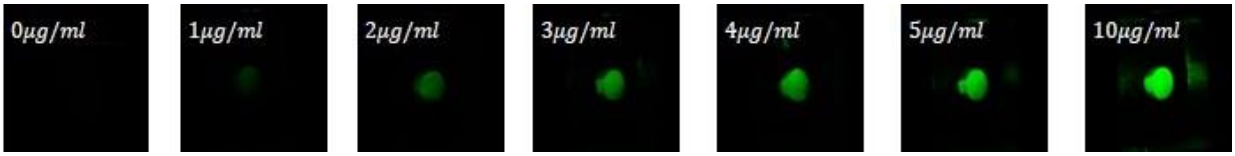

Figure 4.14: Experiment demonstrating $\lambda - DNA$ characterization in Prototype 4 with the imaging prototype. Samples were loaded in the reservoir devices with increasing concentrations of $\lambda - DNA$ to show the capability of the Sepsis Check to linearly characterize between $\lambda - DNA$ concentration and optical intensity.

Figure 4.14 shows that Prototype 4 was capable of detecting down to $1\mu g/mL$ of $\lambda - DNA$ in the reservoir device. The average intensity of the reservoirs were calculated using ImageJ as shown earlier in Figure 3.19. The averages were plotted to produce the characterization chart shown below in Figure 4.15.

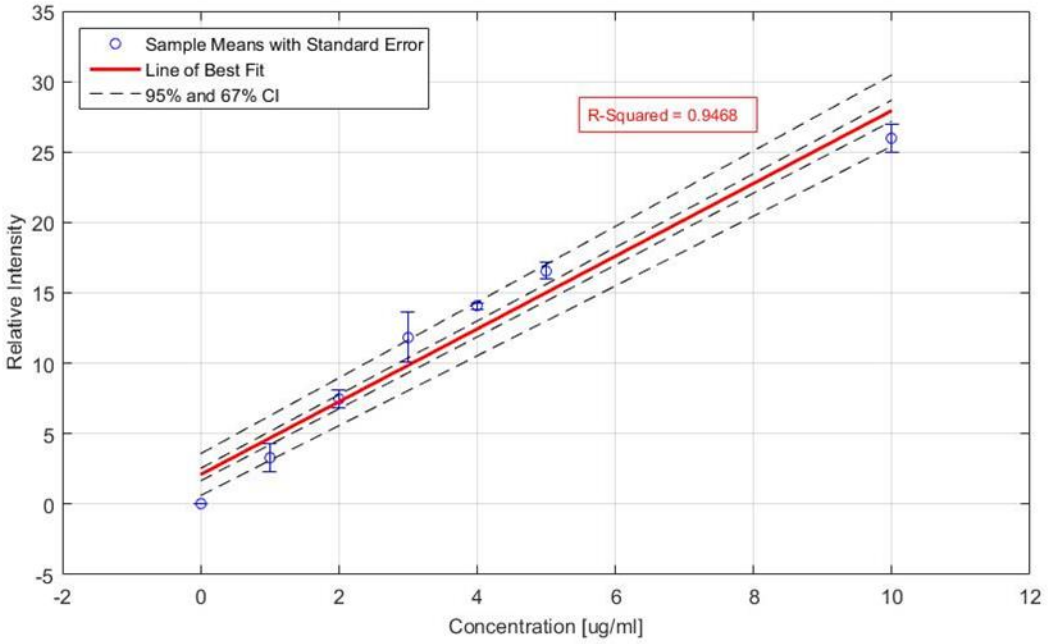

Figure 4.15: Characterization of the imager prototype. The relative intensity of fluorescence in the selected area corresponded to the DNA concentration in the sample. Error bars show standard deviation. Sample size $n = 3$. Note: the confidence intervals are shown to assist with easy comparison of the intensities

The linearity of the characterization with the confidence intervals showed a strong correlation between $\lambda - DNA$ concentration and optical intensity. Figure 4.16 below shows the comparison of the relative intensity of a $1\mu g/mL$ sample and a $5\mu g/mL$ sample.

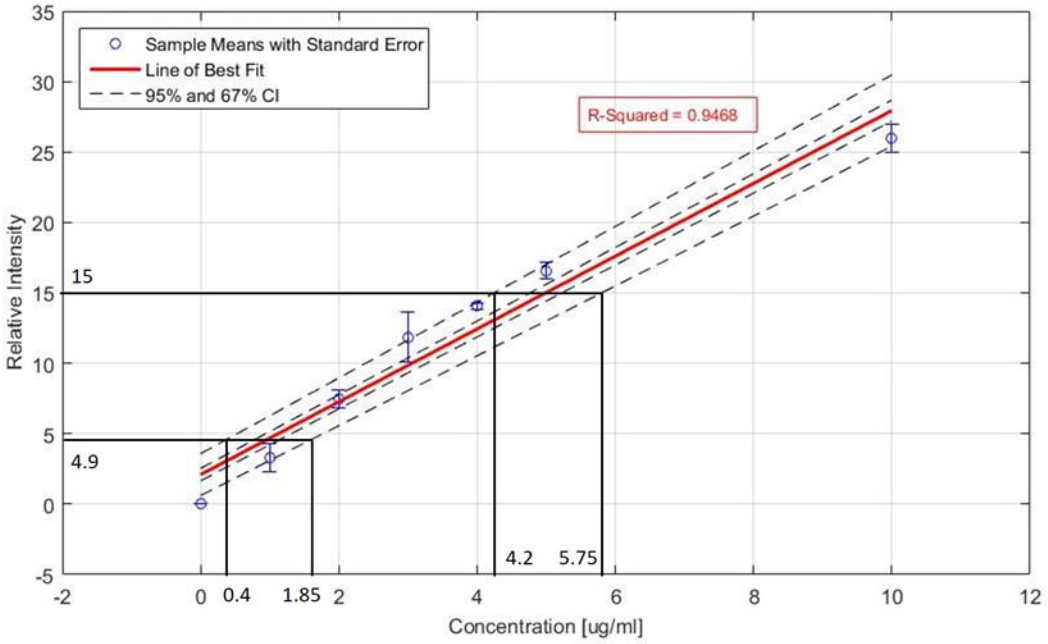

Figure 4.16: Demonstration of the reverse analysis of the Prototype 4 characterization chart to determine DNA concentration from a relative intensity reading from the Sepsis Check. Error bars show standard deviation. Sample size $n = 3$.

The characterization of Prototype 4 showed that it was capable of distinguishing the differences between 1 and $5\mu g/mL$ of DNA in the reservoir devices. For instance, it allowed the user to say with 95% confidence that a relative intensity value of 4.9 correlated to a dsDNA concentration between $0.4\mu g/mL$ and $1.85\mu g/mL$ and a relative intensity of 15 correlated to a dsDNA concentration between $4.2\mu g/mL$ and $5.75\mu g/mL$.

4.4.2 Detection in the Cross Channel Devices

After demonstration of the efficacy of the measurement device in reservoir devices, the imager design was also tested using cross channel devices. The cross channel device configuration facilitates 1) the use of lower volume of blood, 2) provides a way to separate DNA from the other components of the blood that could potentially interfere with the measurement, and 3) accumulates DNA to provide greater sensitivity. Similar to the characterization of the detector, these experiments required a dilution of $\lambda - DNA$, PicoGreen, and TE buffer solution.

Once the reagents were mixed, a $2\mu L$ droplet of $\lambda - DNA$ and PicoGreen mixture was placed on the sample channel inlet and aspirated through to fill the sample channel the same way the accumulation channel was filled with gel. The device was placed in the Sepsis Check loading drawer, the electrodes were connected to the reservoirs, and the device was pushed into the Sepsis Check ready for analysis as shown in Figure 4.17.

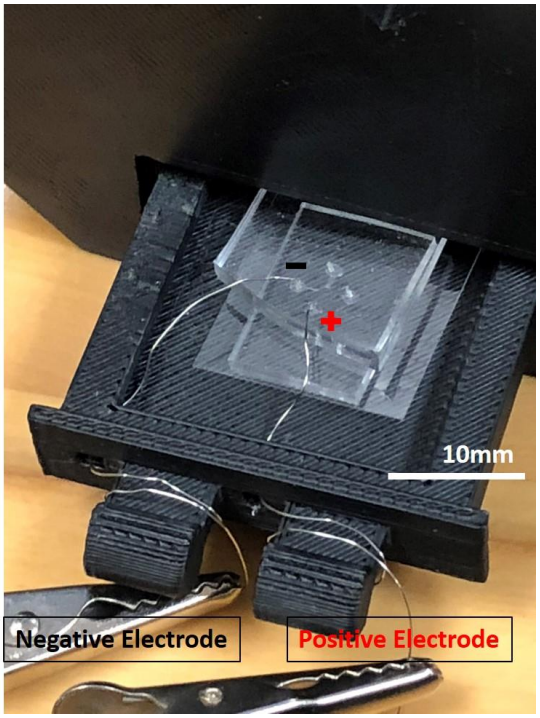

Figure 4.17: Cross channel loaded with a sample prepared for analysis in the Sepsis Check Prototype 4

The shutter speed of the Raspberry Pi Camera was set to $10ms$ for the characterization of the reservoir devices, however, for the cross channel devices, there was less total mass of fluorescent PicoGreen and only a percentage of the sample accumulates at the intersection of the channels. Therefore the shutter speed was lengthened to $50ms$. The first picture was taken for a sample at the zeroth time point. The positive electrode of the gel electrophoresis power supply was connected to the accumulation reservoir and the negative electrode was connected to the sample reservoir. This transported the negatively charged DNA towards the positive electrode and caused accumulation of DNA at the intersection of the channels. The power supply provided $9V$ to perform the gel electrophoresis. The current provided by this power supply was verified to ensure a completed circuit through the gel and sample. A current less than $2\mu A$ would mean there was a problem with the electrical connection. The DNA was loaded into the sample channel as described earlier. In Figure 4.18 A) the sample channel was the horizontal channel and the accumulation channel was the vertical channel. The accumulation channel was filled with 1% agarose gel

prior to DNA loading. A picture was taken every $30s$ for five minutes. The resultant accumulation at the intersecting region between the sample and the accumulation channel was quantified and plotted in Figure 4.18 B).

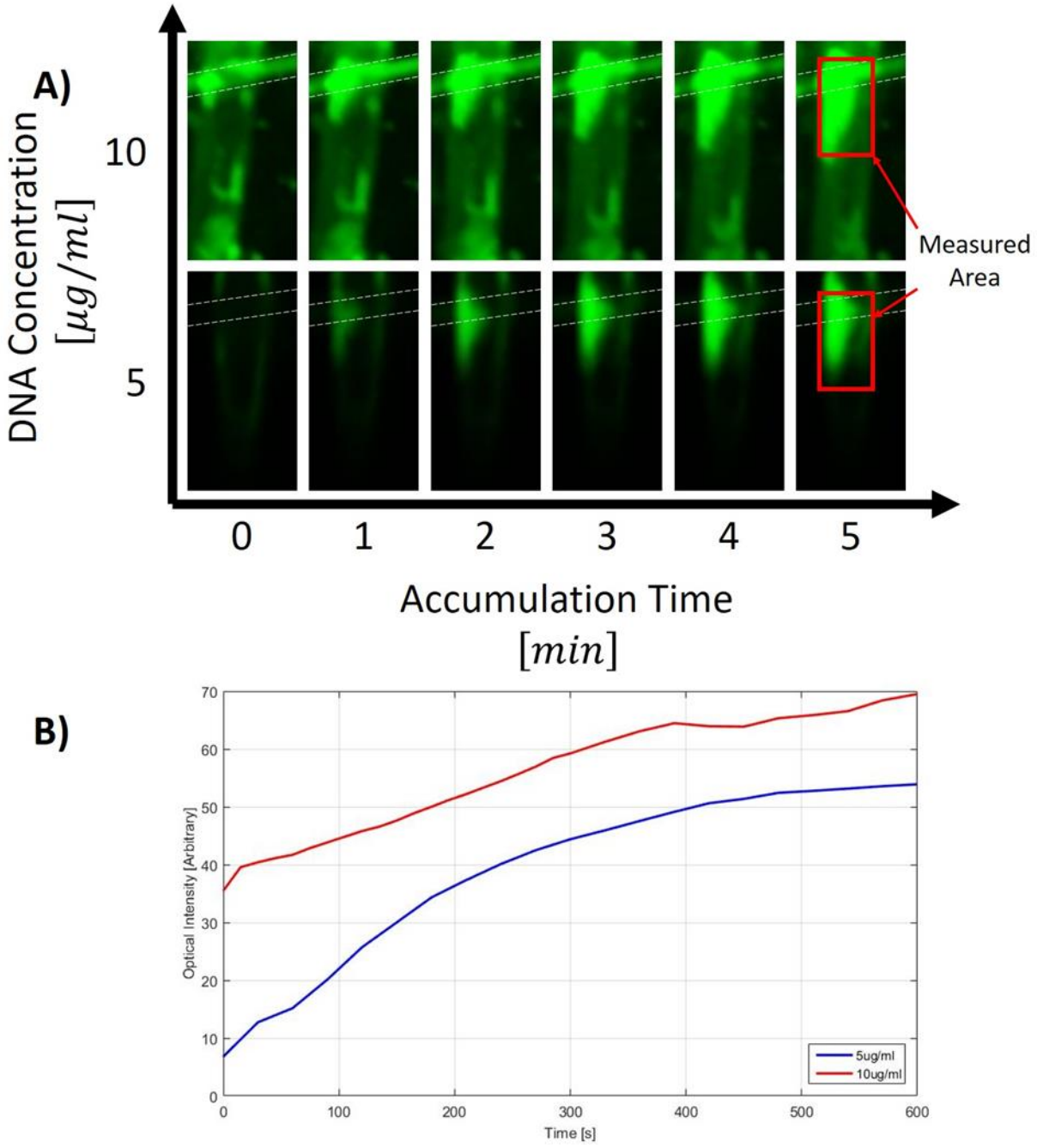

Figure 4.18: Comparison of $10\mu g/mL$ and $5\mu g/mL$ samples in the cross channel device. In both scenarios, the average intensity value of the intersection was measured over 5 minutes to give the data shown in B).

Multiple results can be concluded from the increase in optical intensity captured by Prototype 4 in Figure 4.18 B). Firstly, DNA accumulation at the intersection was clearly present and measured with Prototype 4. Gel electrophoresis caused the fluorescently tagged dsDNA to migrate and accumulate at the intersection of the cross channel device. Secondly, the optical intensity of the $10\mu g/mL$ sample was higher than the intensity of the $5\mu g/mL$ sample throughout the accumulation procedure which supports the fact that DNA concentration is correlated to optical intensity at the intersection of the cross channel.

Another observation was that the initial reading of the $10\mu g/mL$ was 5x the intensity of the $5\mu g/mL$ sample when in theory it should be 2x the intensity. Figure 4.18 A) shows that there appears to be DNA accumulating at the intersection of the $10\mu g/mL$ sample before the gel electrophoresis procedure was initiated. This could be due to osmotic forces pulling the DNA into a weak gel or contamination of the gel with DNA during the loading step. The reason for this difference in initial intensity needs to be investigated further. Another question that this result presented was why the optical intensity of the $5\mu g/mL$ sample increased more rapidly and by a greater factor than the $10\mu g/mL$ sample. Potentially these questions could be from experimental error or an unknown factor. Regardless, further experimentation and an increased sample size needs to be pursued. In summary, Prototype 4 showed the capability of detecting DNA accumulation at the intersection of the cross channel device, however the quantification of DNA with optical intensity at the intersection of the cross channels still requires work. With further experiments this system could provide discriminative powers and assist with sepsis prognostication.

Chapter 5.

5 Conclusion and Future Work

Sepsis, particularly in severe cases, has a very high mortality rate and places a significant load on the ICU in most hospitals due to long stay times and resource consumption [8], [2]. Current solutions to identify severe sepsis include severity scoring systems and biomarkers. Severity scoring systems suffer from interpretation error, non-specificity to sepsis prognostication, and an uncomprehensive evaluation of the patient's condition. A multitude of biomarkers have been proposed in the field of sepsis prognostication [9]. However, a single biomarker to provide prognostic capability for sepsis evaluation is unlikely due to the fact that sepsis is a very complex pathophysiological process that involves coagulation, contact system activation, inflammation, apoptosis, and other physiological mechanisms [9]. This limits the viability of biomarkers for sepsis prognostication.

Recently circulating cfDNA has been found to be a reliable indicator for predicting mortality in ICU patients. Current cfDNA quantification methods include laboratory grade UV and fluorescence spectroscopy units, or micro total analysis systems (μTAS's). Despite the reliable and impressive LoD of laboratory equipment, it is not at the PoC and requires additional time consuming steps such as dsDNA isolation and centrifugation to quantify the concentration of cfDNA. Although many μTAS's have been designed for analyzing DNA on chip such as in sequencing or amplification, a simple handheld device for accurate and reliable quantification of dsDNA in whole blood or plasma has not been pursued. Finally, miniaturized fluorescence systems have been proposed for such applications, however the combination of high sensitivity, wide field of view image acquisition, and independence from laboratory equipment has not been developed.

This thesis is focused on the development of a handheld fluorescence analysis tool called the Sepsis Check that measures dsDNA concentration in realistic samples such as in plasma. It is capable of quantifying DNA in a reservoir (chamber type) device as well as detect DNA accumulation on a cross channel device at concentrations relevant to sepsis prognostication.

The Sepsis Check used a disposable cartridge device to hold the sample. The reservoir devices provides consistent sample volume to allow for correlation to dsDNA concentration and the cross channel device separates dsDNA from other materials in blood. The dsDNA concentration was quantified / detected using a dsDNA specific fluorophore PicoGreen. A portable and reusable optical excitation and emission system was designed with a photo-imaging analysis system to linearly characterize $\lambda - DNA$ in the reservoir devices in TE buffer and detect $\lambda - DNA$ accumulation in the cross channel device.

5.1 Results from the Contribution

5.1.1 Linear Characterization of $\lambda - DNA$ in Reservoir Devices in TE Buffer

Sepsis severity can be diagnosed by accurately measuring the concentration of cfDNA. Therefore, linear characterization between $\lambda - DNA$ concentration in the reservoir devices in TE buffer and the optical intensity measured with the imager design is important for sepsis prognostication. A $\lambda - DNA$ concentration from $1\mu g/mL$ to $10\mu g/mL$ was mapped to an optical intensity reading on the imager design with an R^2 value of 0.97. This proves that the design can allow the user to confidently discriminate between potential survivors and potential non-survivors of sepsis.

5.1.2 Optimization of the PicoGreen and $\lambda - DNA$ Mass Bonding Ratio

PicoGreen is typically used to quantify dsDNA concentrations less than $1\mu g/mL$ in larger volumes [37], [34]. For concentrations this low the suggested dilution factor was 200x dilution. Characterization experiments with the first two prototypes showed a linear relationship between $0.4\mu g/mL$ and $1\mu g/mL$ however from $1\mu g/mL$ to $50\mu g/mL$ there was no change in optical intensity. The concentration of PicoGreen was increased from a dilution of 200x to a dilution of 20x and the result was a linear calibration from $0.4\mu g/mL$ to $20\mu g/mL$.

5.1.3 Linear Characterization of Healthy Plasma Spiked with $\lambda - DNA$

Quantification of cfDNA concentration in whole blood is more difficult than quantification in TE buffer because it introduces contaminants that block fluorescence emissions from the fluorescently tagged dsDNA in the sample [37]. Therefore, as an intermediate step $\lambda - DNA$ concentration was linearly characterized when spiked in healthy patient plasma in the reservoir device. The result was that $\lambda - DNA$ was linearly characterized in healthy patient plasma with an R^2 value of 0.92. As shown in Figure 4.9 the slope of the linear characterization in plasma had the same slope as the linear characterization in TE buffer. The difference between the two relationships was that characterization in TE buffer had a lower LoD, being able to distinguish between a $0.5\mu g/mL$ $\lambda - DNA$ sample and the background noise whereas

the characterization in plasma could only detect as low as $1\mu g/mL$. The similarity of the slopes of the linear fit gives additional confidence to the result because the only difference between the healthy patient samples and the spiked plasma samples was the addition of $3\mu L$ of blood plasma which could be causing the increase in LoD due to its opacity.

5.1.4 Detection of $\lambda - DNA$ Accumulation at the Cross Channel Intersection

In order to accurately quantify cfDNA concentration in whole blood the dsDNA can be separated from the contaminants using gel electrophoresis in the cross channel device. Detection of $\lambda - DNA$ accumulating in the intersection of the cross channel device was done with $10\mu g/mL$ and $5\mu g/mL$ with the fourth imager prototype. This is a necessary step towards quantification of $\lambda - DNA$ in the cross channel device. This theoretically gives the design the ability to detect cfDNA in whole blood as the cross channel devices are capable of separating dsDNA for other contaminants in a whole blood sample.

5.2 Future Work

Although the design and the results presented show the value of Prototype 4, future improvements on the design and further experiments could improve the characterization of dsDNA concentration and detection of dsDNA in the cross channel device. The experiment conducted with the cross channel device needs further experimentation and repetition.

An increased sample size and experiments conducted with $1\mu g/mL$ in the cross channel device will provide further confidence regarding the fluorescent intensity of the intersection as well as confidence intervals that could support the definition for a threshold to identify between $1\mu g/mL$ and $5\mu g/mL$.

The major design change would be to change the mounted filters to thin film surface coating filters that have been implemented in other μTAS systems [29]. The checkmark geometry of the four Sepsis Check prototypes was designed to: 1) avoid excitation light leaking through to the photodetector and 2) integrate both an excitation and emission filter as shown in Figure 5.1.

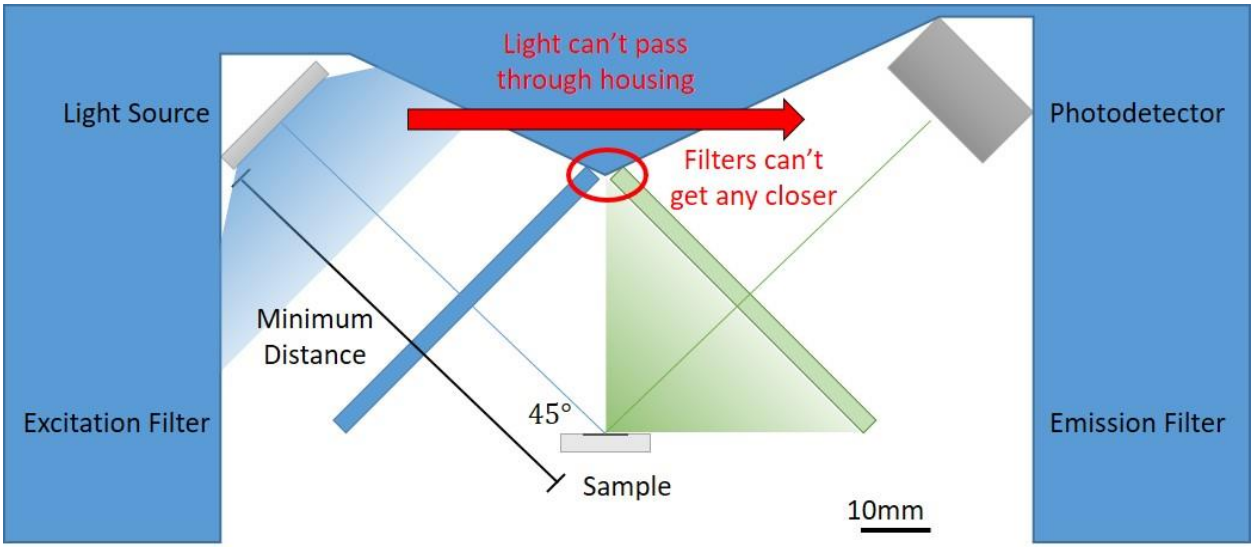

Figure 5.1: Pictogram to show why the $45°$ angle between the excitation system and emission system was necessary for the minimization of background noise. The sample and filters are to scale to show the limits on how close the excitation and emission systems can get to the sample.

This design allowed for the light source and photodiode to be as close to the sample as possible while using the opaque housing unit to block direct light from the light source onto the photodetector. This design greatly reduced the background noise that would be caused by the light from the source being detected by the photodetector. A smaller angle could be used to move the light source and photodetector closer to the sample but then the photodetector would be directly in the line of sight of the light source. Oppositely, the angle could be increased but the filters would need to be moved further from the sample to maintain alignment. This geometrical optimization was decided when moving from the first prototype to the second and was maintained through to the fourth prototype.

The design of the next prototype would utilize a linear reflection system that uses a surface mounted circular array of LED's and a central photodetector. Both elements would be covered with thin film filters that give it the spectral specificity of the original, no excitation leakage, and a much smaller overall design with uniform excitation intensity distributed across the sample. The new design would have an excitation filter with a cut-off frequency of $500nm$ and an optical density > 4.0 and an emission filter with a cut-on frequency of $525nm$ and an optical density > 4.0. The next prototype would be designed as shown in Figure 5.2.

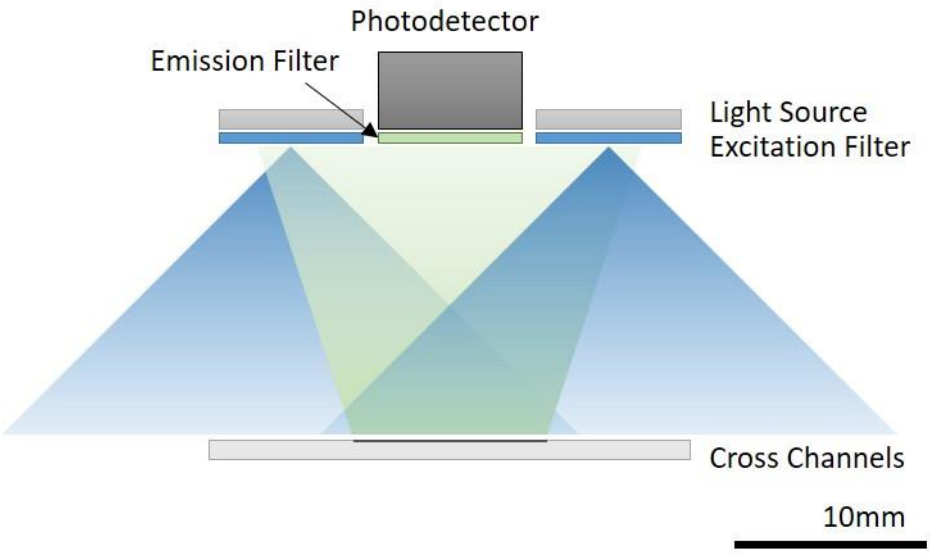

Figure 5.2: Future design of the Sepsis Check

This would allow for consistent and cheaper manufacturing of the optical filters which were the most cost inefficient aspect of the previous four designs. The thin film filters also greatly miniaturizes the design. The geometry of the design will now be limited by the photodetector and LED light sources. The linear and circular design of the excitation and emission systems allowed for a uniform excitation area on the cross channel device.

Additional experiments would also be conducted with the design to improve two major results that were presented in this thesis. The experiments using healthy patient blood plasma could be expanded to determine a proper correlation factor between the characterization in TE buffer and blood plasma. Additionally an experiment using healthy patient blood plasma needs to be conducted with the final prototype. Potentially this could help provide insight into the inferior LoD. A correlation between the plasma concentration and optical intensity received needs to be established.

Detection of $\lambda - DNA$ accumulating at the intersection of the cross channels could also be improved by simply running more experiments and increasing the sample size. Following this, a characterization of the accumulation of $\lambda - DNA$ in the cross channel can be conducted. Characterization would allow for the definition of an intensity value that correlates to the severity of sepsis in a sample. In theory a high DNA concentration equates to more DNA mass accumulating at the intersection. This metric could be used to discriminate between potential survivors and potential non-survivors.

References

[1] M. Singer *et al.*, "The Third International Consensus Definitions for Sepsis and Septic Shock (Sepsis-3)," *JAMA*, vol. 315, no. 8, pp. 801–810, 2016.

[2] L. Husak *et al.*, "National analysis of sepsis hospitalizations and factors contributing to sepsis in-hospital mortality in Canada.," *Healthc. Q.*, vol. 13, no. September, pp. 35–41, 2010.

[3] K. Strand and H. Flaatten, "Severity scoring in the ICU: a review," *Acta Anaesthesiol. Scand. Found.*, vol. 52, pp. 467–478, 2008.

[4] T. Chan and F. Gu, "Early diagnosis of Sepsis Using Serum Biomarkers," *Mol. Diagnosis*, vol. 11, no. 5, pp. 487–496, 2011.

[5] D. J. Dwivedi *et al.*, "Prognostic utility and characterization of cell-free DNA in patients with severe sepsis," *Crit. Care*, vol. 16, no. 4, p. R151, 2012.

[6] J. Yang *et al.*, "A microfluidic device for rapid quantification of cell-free DNA in patients with severe sepsis," *Lab Chip*, vol. 15, no. 19, pp. 3925–3933, 2015.

[7] A. Lever and I. Mackenzie, "Sepsis: definition, epidemiology, and diagnosis.," *BMJ*, vol. 335, no. 7625, pp. 879–883, 2007.

[8] R. A. Balk and R. C. Bone, "Definitions for Sepsis and Organ Failure and Guidelines for the Use of Innovative Therapies In Sepsis," *Crit. Care*, vol. 5, pp. 1–8, 1989.

[9] C. Pierrakos and J.-L. Vincent, "Sepsis biomarkers: a review," *Crit. Care*, vol. 14, pp. 1–18, 2010.

[10] R. Knob *et al.*, "Sequence-specific sepsis-related DNA capture and fluorescent labeling in monoliths prepared by single-step photopolymerization in microfluidic devices," *J. Chromatogr. A*, vol. 1562, pp. 12–18, 2018.

[11] T. Beiter *et al.*, "Neutrophils release extracellular DNA traps in response to exercise," *J Appl Physiol*, vol. 117, pp. 325–333, 2014.

[12] Y. Zhang *et al.*, "Detection of sepsis in patient blood samples using CD64 expression in a microfluidic cell separation device," *Analyst*, vol. 143, no. 1, pp. 241–249, 2018.

[13] M. M. Aeinehvand, R. F. Martins Fernandes, M. F. Jiménez Moreno, V. J. Lara Díaz, M. Madou, and S. O. Martinez-Chapa, "Aluminium valving and magneto-balloon mixing for rapid prediction of septic shock on centrifugal microfluidic platforms," *Sensors Actuators, B Chem.*, vol. 276, no. August, pp. 429–436, 2018.

[14] T. J. Gould *et al.*, "Cell-Free DNA Modulates Clot Structure and Impairs Fibrinolysis in Sepsis," *Arterioscler. Thromb. Vasc. Biol.*, vol. 35, no. 12, pp. 2544–2553, 2015.

[15] H. Schwarzenbach, D. S. B. Hoon, and K. Pantel, "Cell-free nucleic acids as biomarkers in cancer patients," *Nat. Rev. Cancer*, vol. 11, no. 6, pp. 426–437, 2011.

[16] K. Jung, M. Fleischhacker, and A. Rabien, "Cell-free DNA in the blood as a solid tumor biomarker—A critical appraisal of the literature," *Clin. Chim. Acta*, vol. 411, no. 0009, pp. 1611–1624, 2010.

[17] A. Rhodes, S. J. Wort, H. Thomas, P. Collinson, and E. D. David, "Plasma DNA concentration as a predictor of mortality and sepsis in critically ill patients," *Crit. Care*, vol. 10, no. 2, pp. 1–7, 2006.

[18] P. McPhie and J. R. Lakowicz, *Principles of Fluorescence Spectroscopy*, Third. Baltimore: Springer, 2000.

[19] Promega Corporation, "DNA Purification - The basics of DNA isolation, plasmid growth and DNA quantitation," *Protocols and Applications Guide*, 2018. [Online]. Available: https://www.promega.ca/resources/product-guides-and-selectors/protocols-and-applications-guide/dna-purification/. [Accessed: 28-Sep-2018].

[20] S. Yu, Y. Wang, X. Li, F. Yu, and W. Li, "The factors affecting the reproducibility of micro-volume DNA mass quantification in Nanodrop 2000 spectrophotometer," *Optik (Stuttg).*, vol. 145, pp. 555–560, 2017.

[21] K. Nielsen, H. S. Mogensen, J. Hedman, H. Niederstatter, W. Parson, and N. Morling, "Comparison of Five DNA Quantification Methods," *Forensic Sci. Int.*, vol. 2, pp. 226–230, 2008.

[22] K. H. Wong and K. L. Campbell, "Factors That Affect Use of Intercalating Dyes Such as PicoGreen, SYBR Green I, Syto-13 and Syto-82 in DNA Assays," *Biol. Reprod.*, vol. 85, no. Suppl_1, p. 725, 2011.

[23] Y. Nakayama, H. Yamaguchi, N. Einaga, and M. Esumi, "Pitfalls of DNA quantification using dnabinding fluorescent dyes and suggested solutions," *PLoS One*, vol. 11, no. 3, pp. 1–12, 2016.

[24] M. Dandin, P. Abshire, and E. Smela, "Optical filtering technologies for integrated fluorescence sensors," *Lab Chip*, vol. 7, no. 8, pp. 955–977, 2007.

[25] ThorLabs, "Photodiodes," *Photodiodes & Photoconductors*, 2018. [Online]. Available: https://www.thorlabs.com/newgrouppage9.cfm?objectgroup_id=285&pn=FDS100. [Accessed: 02-Jun-2018].

[26] ThorLabs, "Si Photodiode 350 - 1100 nm - Specification Sheet." pp. 1–3, 2013.

[27] J. R. Webster, M. A. Burns, D. T. Burke, and C. H. Mastrangelo, "Monolithic capillary electrophoresis device with integrated fluorescence detector," *Anal. Chem.*, vol. 73, no. 7, pp. 1622–1626, 2001.

[28] M. A. Burns *et al.*, "An integrated nanoliter DNA analysis device," *Science (80-.).*, vol. 282, no. 5388, pp. 484–487, 1998.

[29] V. Namasivayam *et al.*, "Advances in on-chip photodetection for applications in miniaturized genetic analysis systems," *J. Micromechanics Microengineering*, vol. 14, no. 1, pp. 81–90, 2004.

[30] C. Wong, M. E. Pawlowski, A. Forcucci, C. E. Majors, R. Richards-Kortum, and T. S. Tkaczyk, "Development of a universal, tunable, miniature fluorescence microscope for use at the point of care," *Biomed. Opt. Express*, vol. 9, no. 3, p. 1041, 2018.

[31] B. Kim, Y. J. Lee, J. G. Park, D. Yoo, Y. K. Hahn, and S. Choi, "A portable somatic cell counter based on a multi-functional counting chamber and a miniaturized fluorescence microscope," *Talanta*, vol. 170, no. February, pp. 238–243, 2017.

[32] K. K. Ghosh *et al.*, "Miniaturized Integration of a Fluorescence Microscope," *Nat. Methods*, vol. 8, no. 10, pp. 871–878, 2013.

[33] F. Helmchen, "Miniaturization of fluorescence microscopes using fibre optics," *Exp. Physiol.*, no. June 2001, 2008.

[34] Invitrogen, "Quant-iT ™ PicoGreen ® dsDNA Reagent and Kits," 2008.

[35] Invitrogen, “Comparison of Quant-iT and Qubit DNA quantitation assays for accuracy and precision.” ThermoFisher Scientific, p. 4, 2016.

[36] A. C. Daniels, D.L., Forster, “λ DNA-HindIII Digest | NEB Product Information,” *New England BioLabs*, 2018. [Online]. Available: https://www.neb.com/products/n3012-dna-hindiii-digest#Product Information. [Accessed: 24-Jun-2018].

[37] V. L. Singer, L. J. Jones, S. T. Yue, and R. P. Haugland, “Characterization of PicoGreen Reagent and Development of a Fluorescence-Based Solution Assay for Double-Stranded DNA Quantitation,” *Anal. Biochem.*, vol. 249, no. 0003, pp. 228–238, 1997.

[38] N. Yagi, K. Satonaka, M. Horio, H. Shimogaki, Y. Tokuda, and S. Maeda, “The Role of DNase and EDTA on DNA Degradation in Formaldehyde Fixed Tissues,” *Biotech. Histochem.*, vol. 71, no. 3, pp. 123–129, 1996.

[39] R. Pomfret, K. Sillay, and G. Miranpuri, “Investigation of the electrical properties of agarose gel : - characterization of concentration using nyquist plot phase angle and the - implications of a more comprehensive in vitro model of the brain,” *Ann. Neurosci.*, vol. 20, no. 3, pp. 99–107, 2013.

[40] J. C. McDonald *et al.*, “Fabrication of microfluidic systems in poly(dimethylsiloxane),” *Electrophoresis*, vol. 21, no. 1, pp. 27–40, 2000.

[41] J. C. Lötters, W. Olthuis, P. H. Veltink, and P. Bergveld, “The Mechanical Properties of the Rubber Elastic Polymer Polydimethilsiloxane for Sensor Applications,” *J. Micromech. Microeng*, vol. 7, no. 97, pp. 145–147, 1997.

[42] Dow Corning Corporation, “Information about Dow Corning ® Brand Silicone Encapsulants.” Dow Corning Corporation, USA, pp. 1–10, 2008.

[43] L. Yu, F. E. H. Tay, G. Xu, B. Chen, M. Avram, and C. Iliescu, “Adhesive Bonding with SU-8 at Wafer Level for Microfluidic Devices,” *J. Phys.*, vol. 34, pp. 776–781, 2006.

[44] Microchem Corp, “SU-8 2000 Permanent Epoxy Negative Photoresist PROCESSING GUIDELINES FOR.” Microchem, Newton, pp. 1–5, 2000.

[45] ThorLabs, “LED 470L with Ball Lens.” Thorlabs, Newton, pp. 1–3, 2011.

[46] Arduino Corporation, “Arduino Uno Rev3,” *Tech Specs*, 2018. [Online]. Available: https://store.arduino.cc/usa/arduino-uno-rev3. [Accessed: 15-Jul-2018].

[47] ThorLabs, “Edgepass Filters: Longpass and Shortpass,” *Thorlabs Spectral Filters*, 2018. [Online]. Available: https://www.thorlabs.com/newgrouppage9.cfm?objectgroup_id=918&pn=FEL0500#3246. [Accessed: 02-Jun-2018].

[48] Edmund Optics, “Optical Filters | Edmund Optics,” 2017. [Online]. Available: https://www.edmundoptics.com/resources/application-notes/optics/optical-filters/. [Accessed: 29-Jun-2018].

[49] SourceMeter and I. Keithley Instruments, “2410 and 2410-C SourceMeter ® Specifications.” pp. 3–5, 2003.

[50] D. L. Jones, “The uCurrent Specification Sheet.” pp. 1–19, 2010.

[51] ThorLabs, “Mounted N-BK7 Plano-Convex Lenses (AR Coating: 350 - 700 nm),” *Mounted N-BK7 Plano-Convex Lenses (AR Coating: 350 - 700 nm)*, 2018. [Online]. Available: https://www.thorlabs.com/newgrouppage9.cfm?objectgroup_id=6277&pn=LA1027-A-ML. [Accessed: 26-Jul-2018].

[52] A. I. Dragan, J. R. Casas-Finet, E. S. Bishop, R. J. Strouse, M. A. Schenerman, and C. D. Geddes, “Characterization of PicoGreen interaction with dsDNA and the origin of its fluorescence enhancement upon binding,” *Biophys. J.*, vol. 99, no. 9, pp. 3010–3019, 2010.

Appendix A.

Standard Operating Procedure for Characterization of $\lambda - DNA$ in Reservoir Devices

1. Manufacture a sufficient quantity of reservoir devices by filling the reservoir molds with PDMS from the Slygard 184 Elastomer Kit in a 10:1 weight ratio of the base to curing agent and placing them in the oven at 80℃ for 30 minutes.
2. Take the highest concentration you wish to simulate (for example: $20\mu g/mL$) and multiply it by 2 from which the standard dilutions will be conducted from.

$$\frac{20\mu g}{mL} * 2 = \frac{40\mu g}{mL}$$

3. The reservoir devices each hold $10\mu L$ of fluid. $5\mu L$ of which is always PicoGreen diluted 20x. Therefore the $20\mu g/mL$ sample contains:
   $2.5uL$ of $40\mu g/mL\ \lambda - DNA$

   $2.5\mu L$ of TE buffer

   $5\mu L$ of 20x PicoGreen dye
4. Pipette the total $10\mu L$ mixture into a reservoir and mix thoroughly by re-pumping 5 to 8 times.
5. Load the filled reservoir device into the Sepsis Check
6. Press the capture button (for the photodiode prototypes) or run the image capture command (for the imager device)
7. Remove the reservoir device from the Sepsis Check, repeat the $20\mu g/mL$ sample 2 more times for a total of 3 quality measurements with $20\mu g/mL$. Then move onto the next concentration (in this case $15\mu g/mL$)
8. Prepare a $15\mu g/mL$ sample as follows:
   $1.88\mu L$ of $40\mu g/mL\ \lambda - DNA$

   $3.12\mu L$ of TE buffer

   $5\mu L$ of 20x PicoGreen dye

Standard Operating Procedure for Detection of $\lambda - DNA$ in the Cross Channel Devices

1. Manufacture an appropriate number of cross channel devices as per the instructions in Chapter 3.1.2.2.3 Fabrication of the Cross Channel Device.
2. Fill the accumulation channel of the cross channel device with 1% Agarose gel as per the instructions in Chapter 3.1.2.2.4 Filling of the Cross Channel Device.
3. Take the highest concentration and multiply it by 2 from which the standard dilutions will be conducted from.

$$\frac{10\mu g}{mL} * 2 = \frac{20\mu g}{mL}$$

4. Prepare the first sample at $10\mu g/mL$ in a separate vial that contains the reagents in the following ratio:

$0.5\mu L$ of $20\mu g/mL\ \lambda - DNA$

$0.5\mu L$ of TE buffer

$1\mu L$ of 20x PicoGreen dye

5. Mix the samples by re-pumping the pipette 5 to 8 times in the vial then load the sample into the sample channel as shown in Chapter 3.1.2.2.4 Filling of the Cross Channel Device.
6. Ensure proper connection with the electrodes by applying a small voltage with the Keithley 2410 power supply and measure a current of at least $2\mu A$ across the electrodes.
7. Turn on the LED
8. Run the image capture program:
   raspistill -n -hf -vf -awb off -ss 10000 -ISO 100 -sh 50 -br 50 -sa 75 –o home/pi/PDMS_Well/July4Experiments/xxx_1.jpg
9. Remove the cross channel device and repeat for as many samples as desired.

Appendix B.

There is two versions of the code for the Sepsis Check, the code run by the Arduino microcontroller and the code run for the Raspberry Pi camera.

Explanation of the Arduino Code for the Photodiode Designs

The Arduino code is used in conjunction with the photodiode designs. This general responsibility of this code is to control when a measurement is ready to be taken and analyze the data received from the photodiode. In basic format, when a push button is pressed the LED is turned on and measurements are recorded to an SD card as well as displayed to a LCD display.

First the necessary Arduino libraries need to be included. Libraries provide extra functionality for use in sketches to manipulate data.

```
// Library for the LCD
#include <LiquidCrystal.h>
// Library for Keypad
#include <Keypad.h>
// Libraries for the Data Logger
#include <SPI.h>
#include <SD.h>
#include <Wire.h>
#include "RTClib.h"
```

Variables need to be defined for the LED Driver which was based off of the Motorized Pinwheel example in the Arduino beginner's book.

```
//***************//Variables for the LED Driver//***************//
const int switchPin = 6;        // Button Pin
const int LEDPin = 7;           // LED Pin
int switchState = 0;            // State of the button
boolean state = false;          // Variable to represent if the button has been pressed for the LED to turn on
//***************//
```

The 'switchPin' represents the pin that the push button is connected to. The 'LEDPin' is the pin that is connected to the transistor which turns the LED on and off. The 'switchState' is a variable which is changed when the push button is pressed (it turns a button into a switch). Finally, the 'state' is the state of the button.

The photodiode output (after amplification) will be read by an analog input (pin A0). This reading will range from 0-1023. The data is filtered and a steady state calculation is performed which is displayed to the user on the LCD screen and recorded in the SD card.

```
//***************//Variables for the Photodiode Measurement and
Mathematics//***************//
const int PD = A0;              // Photodiode pin
const int numReadings = 10;
const int numAverages = 10;

int readIndex = 0;              // the index of the current reading
int averageIndex = 0;           // the index of the current average
int readings[numReadings];      // the readings from the analog input
double total = 0;               // the running total

float averages[numAverages];    // the number of equal averages it takes to get a final reading
float lowerSteadyState = 0;     // lower boundary for the steady state check condition for the averages
float upperSteadyState = 0;     // upper boundary for the steady state check condition for the averages
float sumAverages = 0;          // The sum of the averages to compare to the boundaries for steady state
condition
float average = 0;              // the average
//***************//
```

In order to understand the method by which the data is filtered and compared against a steady state value, the variables need to be well defined. The 'numReadings' variable defines the length of the 'readings[numReadings]' list. Likewise the 'numAverages' variable defines the length of the 'averages[numAverages]' list. The variables 'readIndex' and 'averageIndex' increases by 1 each loop iteration until they reach the 'numReadings' or 'numAverages' maximum. These indices define the point at which the current measurement from analog pin 'A0' will be stored in the 'readings' and 'averages' lists. These lists are utilized to filter the data and check for steady state. The 'total' and 'sumAverages' variables are the sum of the 10 previous readings and 10 previous averages respectively. The 'lowerSteadyState' and 'upperSteadyState' are variables that will be utilized to define the steady state condition. If the measurement is between these limits it is said to be at steady state. Confidence that the measurement is not changing (i.e. at steady state) is important for measurement of fluorescence intensity in the reservoir devices because PicoGreen requires mixing and time to fully intercalate with the $\lambda - DNA$ in the sample.

A numerical keypad can be added to the system for further user input, however this was not fully utilized in the basic format utilized for this design.

```
//***************//Variables for the Keypad//***************//
const byte ROWS = 4;            //four rows
const byte COLS = 3;            //three columns
char keys[ROWS][COLS] = {
 {'1', '2', '3'},
 {'4', '5', '6'},
 {'7', '8', '9'},
 {'#', '0', '*'}
};
byte rowPins[ROWS] = {
 42, 40, 38, 36
};             //Connect to the row pinouts of the keypad
byte colPins[COLS] = {
 34, 32, 30
};                //Connect to the column pinouts of the keypad
//***************//
```

A SD data logger was utilized called the “Arduino Ethernet Shield”. This required many definitions and variables to transfer the data to an SD card properly.

```
//***************//Variables for the Data Logger//***************//
// A simple data logger for the Arduino analog pins

// for the data logging shield, we use digital pin 10 for the SD cs line
const int chipSelect = 10;
uint32_t syncTime = 0;      // time of last sync()

// how many milliseconds between grabbing data and logging it. 1000 ms is once a second
#define LOG_INTERVAL  1000  // mills between entries (reduce to take more/faster data)

// how many milliseconds before writing the logged data permanently to disk
// set it to the LOG_INTERVAL to write each time (safest)
// set it to 10*LOG_INTERVAL to write all data every 10 data reads, you could lose up to
// the last 10 reads if power is lost but it uses less power and is much faster!
#define SYNC_INTERVAL 1000  // mills between calls to flush() - to write data to the card

#define ECHO_TO_SERIAL   1  // echo data to serial port
#define WAIT_TO_START    0  // Wait for serial input in setup()

// the digital pins that connect to the LEDs
#define redLEDpin 8
#define greenLEDpin 9

// The analog pins that connect to the sensors
#define BANDGAPREF 14           // special indicator that we want to measure the bandgap

#define aref_voltage 3.3        // we tie 3.3V to ARef and measure it with a multimeter!
```

```
#define bandgap_voltage 1.1      // this is not super guaranteed but its not -too- off

RTC_DS1307 RTC; // define the Real Time Clock object

// the logging file
File logfile;
//***************//
```

The LCD and keypad libraries need to be initiated.

```
// initialize the library by associating any needed LCD interface pin
// with the arduino pin number it is connected to
LiquidCrystal lcd(12, 11, 5, 4, 3, 2); //Initialize the library with the numbers of the interface pins
Keypad keypad = Keypad( makeKeymap(keys), rowPins, colPins, ROWS, COLS );
```

The SD data logger requires an error check to be conducted before writing to the SD card. If the SD card is not present or if the shield was wired incorrectly, an error would be written to the serial log and printed to the LCD display.

```
//***************//Void for when the SD Card is not working//***************//
void error(char *str)
{
 Serial.print("error: ");
 Serial.println(str);

 // red LED indicates error
 digitalWrite(redLEDpin, HIGH);

 while(1);
}
//***************//
```

The setup of the code is now ready to be initiated. The setup component of the Arduino code is run once in preparation for the loop. In the setup there are a number of items which need to be clarified.

```
void setup(void) {
 //***************//Generic Setup//***************//
 // initializing LCD communications
 lcd.begin(16, 2);
 lcd.clear();
 // initializing Serial communications
 Serial.begin(9600);
 Serial.println();
 //***************//

 //***************//Setup for the LED Driver//***************//
```

```
  //Selecting as an input and output the switch and the LED
  pinMode(switchPin, INPUT);
  pinMode(LEDPin, OUTPUT);
//  // Start the LED off
//  digitalWrite(LEDPin, LOW);
  //***************//

  //***************//Setup for the Photodiode Measurement and Mathematics//***************//
  pinMode(PD, INPUT);
  for (int thisReading = 0; thisReading < numReadings; thisReading++) {
    readings[thisReading] = 0;
  }
  for (int thisAverage = 0; thisAverage < numAverages; thisAverage++) {
    averages[thisAverage] = 0;
  }
  //***************//
```

With Arduino programming, the monitors (LCD and Serial) need to be initiated, and the pins utilized need to be defined as either input or output. The 'switchPin' is connected to the push button and the 'LEDPin' is connected to the transistor which allows current to flow from the battery through the LED. The 'readings[thisReading]' and 'averages[thisAverage]' variables are lists which need to be initially set to zero. If they are not set to zero the standard procedure for the Arduino is to set them to a value of 'NaN' which cannot be utilized in mathematical equations in the loop.

```
//***************//Setup for the Data Logger//***************//
  // use debugging LEDs
  pinMode(redLEDpin, OUTPUT);
  pinMode(greenLEDpin, OUTPUT);

#if WAIT_TO_START
  Serial.println("Type any character to start");
  while (!Serial.available());
#endif //WAIT_TO_START

  // initialize the SD card
  Serial.print("Initializing SD card...");
  // make sure that the default chip select pin is set to
  // output, even if you don't use it:
  pinMode(chipSelect, OUTPUT);

  // see if the card is present and can be initialized:
  if (!SD.begin(chipSelect)) {
    error("Card failed, or not present");
  }
  Serial.println("card initialized.");
```

```
 // create a new file
 char filename[] = "LOGGER00.CSV";
 for (uint8_t i = 0; i < 100; i++) {
  filename[6] = i/10 + '0';
  filename[7] = i%10 + '0';
  if (! SD.exists(filename)) {
   // only open a new file if it doesn't exist
   logfile = SD.open(filename, FILE_WRITE);
   break;  // leave the loop!
  }
 }

 if (! logfile) {
  error("couldnt create file");
 }

 Serial.print("Logging to: ");
 Serial.println(filename);

 // connect to RTC
 Wire.begin();
 if (!RTC.begin()) {
  logfile.println("RTC failed");
#if ECHO_TO_SERIAL
  Serial.println("RTC failed");
#endif  //ECHO_TO_SERIAL
 }


 logfile.println("millis,reading,average,vcc");
#if ECHO_TO_SERIAL
 Serial.println("millis, reading, average, vcc");
#endif //ECHO_TO_SERIAL

//  // If you want to set the aref to something other than 5v
//  analogReference(EXTERNAL);
 //***************//
}
```

The setup for the data logger includes a few characteristics, identification of the pin modes, definition of the filename and file format, and an overarching if statement that checks if the SD card is present, the output is prepared, the RTC library is working properly, and connects the data written to the logger to the serial monitor. This concludes the setup of the Arduino. From here the program is prepared to begin the loop which is run continuously.

```
void loop(void) {
 //***************//Generic Loop Information//***************//
 DateTime now;

 // delay for the amount of time we want between readings
 delay((LOG_INTERVAL -1) - (millis() % LOG_INTERVAL));
 //***************//
```

The loop is initiated with the definition of the date and the delay between measured samples. The delay between samples is very important for the computer processing because the steady state calculation and writing to the SD card takes processing power and time.

```
 //***************//Loop for the LED Driver//***************//
 //Reading if the switch has been pushed
 switchState = digitalRead(switchPin);

 if (state == false) {
  //If the switch has been pushed turn on the LED
  digitalWrite(LEDPin, LOW);
 }
 else {
  //If the switch hasn't been pushed don't turn on the LED
  digitalWrite(LEDPin, HIGH);
 }
 if (switchState == 1) {
  state = !state;
 }
 //***************//
```

The push button pin is read. If the push button is pressed it will change ‘switchState’ from 0 to 1. If switch state equals 1 then the boolean variable ‘state’ is switched from false to true and thus turn the LED on.

```
 //***************//Loop for the Photodiode Measurement and Mathematics//***************//
 // subtract the reading in the current index:
 total = total - readings[readIndex];
 // read from the sensor:
 readings[readIndex] = analogRead(PD);
 delay(10);
 // add the reading to the total:
 total = total + readings[readIndex];
 delay(10);
```

At the start of the Arduino code the variable ‘numReadings’ is set to 10 and thus the ‘readings’ list has dimensions of 1x10. The ‘total’ is the summation of the 10 previous readings. In the setup of the code the first 10 readings are set to 0. The total should always equal to the sum of the 10 previous readings and so

before reading the 11th measurement, the reading in the current index (the first reading) needs to be removed from the sum. The photodiode signal is recorded in the readings list at that index and the total is re-evaluated.

```
lcd.setCursor(0, 0);
lcd.print(readings[readIndex]);

Serial.print(readings[readIndex]);
Serial.print("    ");
Serial.print(total);
Serial.print("    ");
```

The reading is presented to the user on the LCD to provide immediate feedback and is printed to the serial which will be mirrored to the SD writer for logging of the data point later in the loop.

```
// advance to the next position in the array:
readIndex = readIndex + 1;
// if we're at the end of the array...
if (readIndex >= numReadings) {
  // ...wrap around to the beginning:
  readIndex = 0;
}
```

The index of the readings list is advanced after the measurement is taken in preparation for the next measurement. The 'readIndex' variable ranges from 0 – 9 because it is limited by the 'numReadings' variable. This is how the 'numReadings' variable controls the length of the 'readings' list.

```
// calculate the average and add the average to the list of averages
averages[averageIndex] = total / numReadings;

Serial.println(averages[averageIndex]);

// advance to the next position in the average array:
averageIndex = averageIndex + 1;
```

The average of the 'readings[readIndex]' is calculated by dividing the total by the number of readings. This is displayed for the user to see the filtered measurement with a window size of 10. This is the number which will be utilized to define and compare against the steady state condition.

```
// if we're at the end of the average array
if (averageIndex >= numAverages) {
  // Check to see if we have reached steady state
  //1. Create the lower and upper conditions for the steady state
  // This is a check to see if all of the averages are within +-1 of the first value
```

```
  lowerSteadyState = averages[0] * 10 - 9;
  upperSteadyState = averages[0] * 10 + 9;
  //2. Create the sum of the averages to compare against boundary conditions
  sumAverages = averages[0] + averages[1] + averages[2] + averages[3] + averages[4] +
  averages[5] + averages[6] + averages[7] + averages[8] + averages[9];
  // Compare sum vs boundaries
  if ((sumAverages > lowerSteadyState) && (sumAverages < upperSteadyState)) {
   lcd.setCursor(0, 1);
   lcd.print("SS: ");
   lcd.setCursor(4, 1);
   lcd.print(averages[0]);
  }
  else {
   lcd.clear();
  }
  // wrap around to the beginning:
  averageIndex = 0;
 }
 delay(10);
 //***************//
```

Once every 10 samples the steady state condition is checked. This is initiated when the index of the averages list reaches the end (I.e. 'averageIndex >= 'numAverages'). First the lower and upper limits of the steady state condition are defined according to the average that was calculated 9 samples ago. If the current average is within these limits then the average has remained constant for 10 readings and thus the device is considered at steady state. Steady state has been defined as a range of ± 9 which equates to a range of $\pm 0.5nA$. The 10 previous averages are summated and compared against the upper and lower states. If the system is within this $1nA$ range then the LCD will display the fact that it is at steady state by denoting the value with a 'SS:' character before the measurement displayed. If the system is not at steady state just the average is displayed. At the end of this procedure the index value of the average list is returned to 0.

Now that the raw data and filtered data have been calculated and measured, the data is written to the SD card.

```
 //***************//Loop for the Data Logger//***************//
 // log milliseconds since starting
 uint32_t m = millis();
 logfile.print(m);           // milliseconds since start
 logfile.print(", ");
#if ECHO_TO_SERIAL
 Serial.print(m);           // milliseconds since start
```

```
  Serial.print(", ");
#endif

  logfile.print(readings[readIndex]);
  logfile.print(", ");
  logfile.print(averages[averageIndex]);
#if ECHO_TO_SERIAL
  Serial.print(readings[readIndex]);
  Serial.print(", ");
  Serial.print(averages[averageIndex]);
#endif //ECHO_TO_SERIAL

  // Log the estimated 'VCC' voltage by measuring the internal 1.1v ref
  analogRead(BANDGAPREF);
  delay(10);
  int refReading = analogRead(BANDGAPREF);
  float supplyvoltage = (bandgap_voltage * 1024) / refReading;

  logfile.print(", ");
  logfile.print(supplyvoltage);
#if ECHO_TO_SERIAL
  Serial.print(", ");
  Serial.print(supplyvoltage);
#endif // ECHO_TO_SERIAL

  logfile.println();
#if ECHO_TO_SERIAL
  Serial.println();
#endif // ECHO_TO_SERIAL

  digitalWrite(greenLEDpin, LOW);

  // Now we write data to disk! Don't sync too often - requires 2048 bytes of I/O to SD card
  // which uses a bunch of power and takes time
  if ((millis() - syncTime) < SYNC_INTERVAL) return;
  syncTime = millis();

  // blink LED to show we are syncing data to the card & updating FAT!
  digitalWrite(redLEDpin, HIGH);
  logfile.flush();
  digitalWrite(redLEDpin, LOW);

  //***************//
}
```

The data is printed to the serial monitor from which the data logger can easily echo to the SD card. This requires some syncing time and provides feedback with on-board red and green LED's.

Raspberry Pi Command for the Imager Design

The Raspberry Pi does not require as sophisticated code and analysis of the signal because it provides an image. The optimized Raspberry Pi camera code is:

raspistill -n -hf -vf -awb off -ss 10000 -ISO 100 -sh 50 -br 50 -sa 75 –o home/pi/PDMS_Well/July4Experiments/xxx_1.jpg

raspistill takes a still image. Hf and vf perform horizontal and vertical flips on the image to align it for consistency. Awb off removes the auto white balancing function that is usually on for a typical image. Ss 10000 is the shutter speed in micro seconds. ISO 100 is a mixture of the color contrast. Sh 50 is the sharpness. Br 50 is the brightness. Sa is the saturation. O home/pi/PDMS_Well/July4Experiments/xxx_1.jpg is the location on the raspberry pi where the image is saved.